HYPERBOLIC NETWORKS IN BIOMEDICINE

Suncica Canic
Department of Mathematics
Center for Mathematical Biosciences
University of Houston

COLLABORATORS

Medical Collaborators:

Dr. D. Paniagua, M.D. (THI)

Dr. S. Little, M.D. (Methodist)

Dr. W. Zoghbi, MD. (Methodist)

Dr. C. Hartley, PhD. (Baylor CM)

Mathematicians:

J. Tambaca, (Univ Zagreb, CRO)

B. Piccoli (Rutgers, Camden)

A. Mikelic (U Lyon 1, FR)

R. Glowinski (UH)

Postdocs: A. Quaini (EPFL/UH), O. Boiarkine (UH)

Students: M. Bukac, S. Mabuza, Y. Yao, T. B. Kim (UH)

MOTIVATION

TO STUDY FLOW IN THE NETWORK OF HIGWAYS,
DATA NETWORK, OR ARTERIAL BLOOD FLOW NETWORK

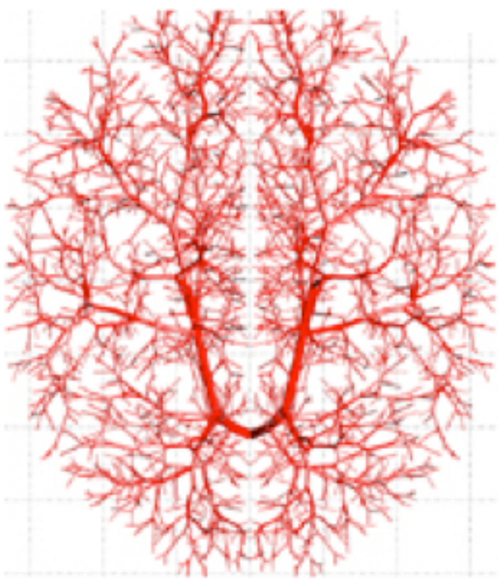

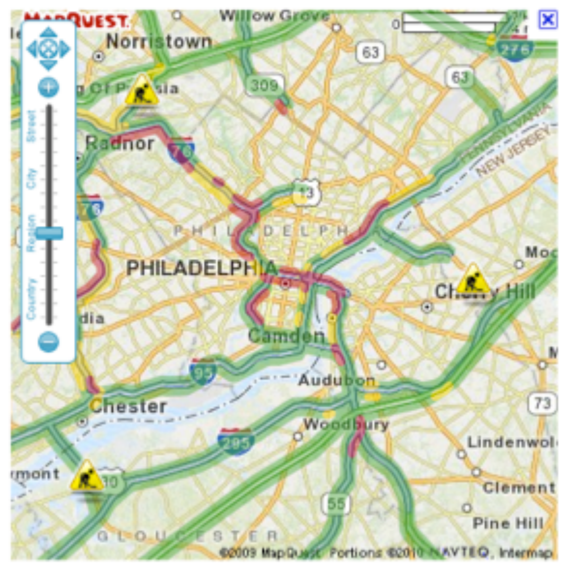

CEREBRAL VASCULAR NETWORK (LEFT) & NETWORK OF HIGHWAYS IN PHILADELPHIA (RIGHT)

MOTIVATION

TO STUDY THE STRUCTURAL PROPERTIES OF
MULTI-COMPONENT NET-LIKE STRUCTURES SUCH AS

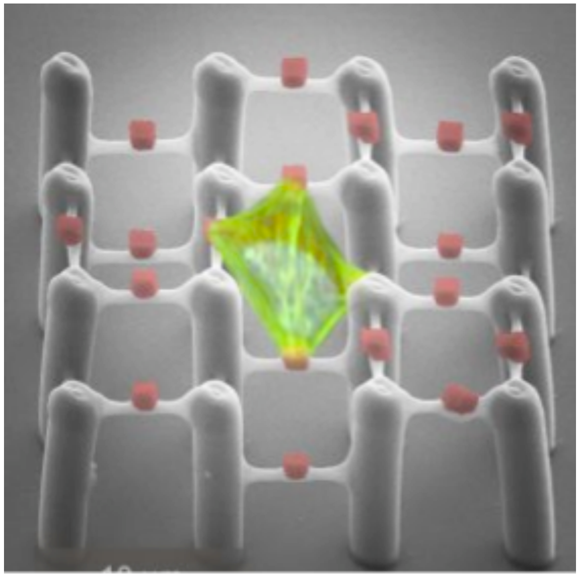

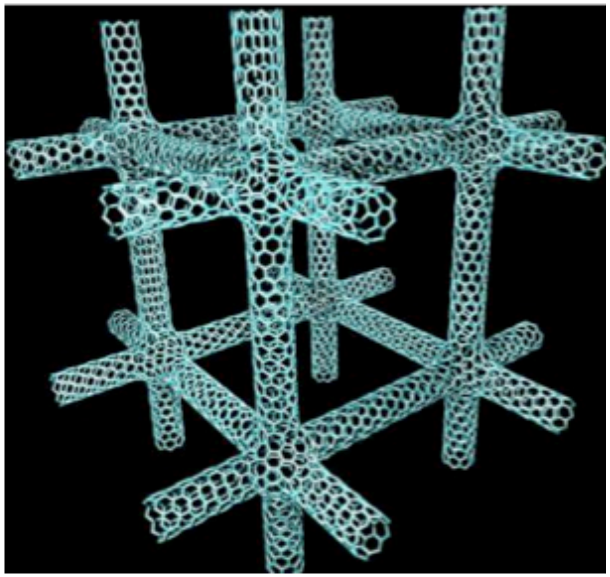

TISSUE SCAFFOLDS IN BIOMATERIALS (LEFT) & CARBON NANOTUBES IN MATERIALS SCIENCE(RIGHT)

MOTIVATION

TO STUDY THE STRUCTURAL PROPERTIES OF
MULTI-COMPONENT NET-LIKE STRUCTURES SUCH AS

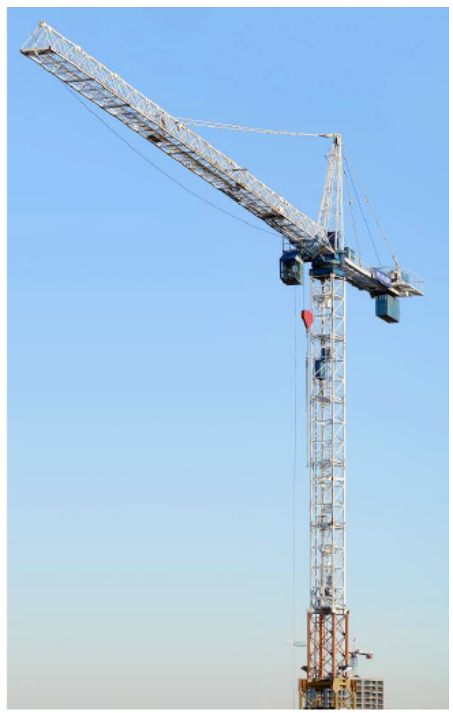

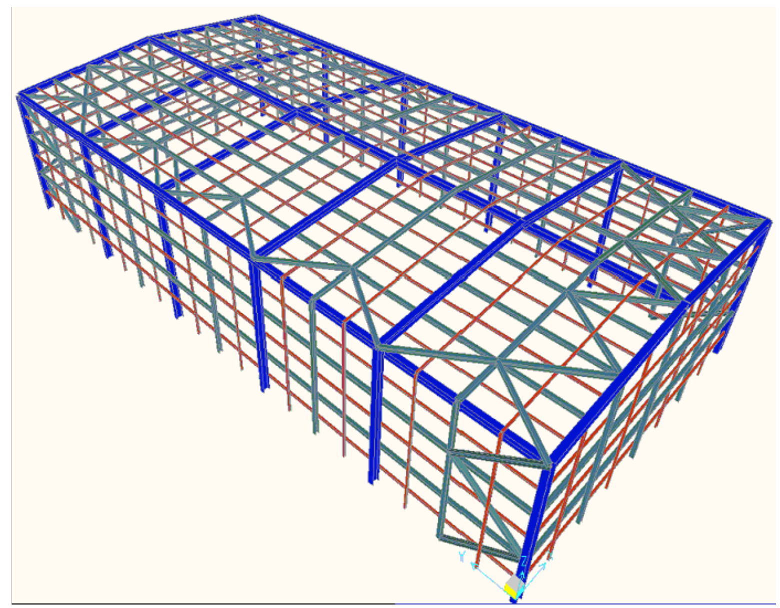

BRIDGES, CRANES, BUILDINGS MADE OF METALLIC FRAME STRUCTURES

MOTIVATION

TO STUDY THE STRUCTURAL PROPERTIES OF MULTI-COMPONENT NET-LIKE STRUCTURES SUCH AS

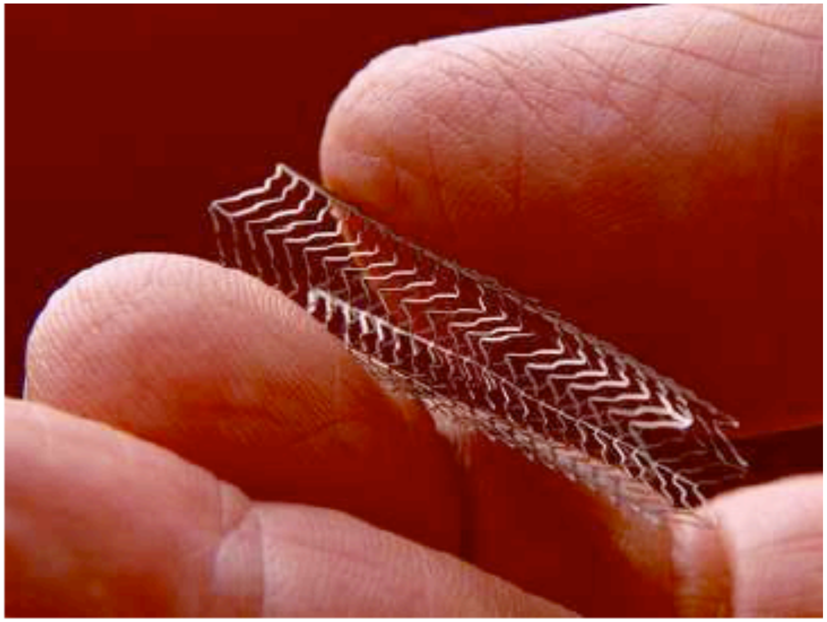

ENDOVASCULAR STENTS

HYPERBOLIC NETS and NETWORKS

Hyperbolic net/network is a term that will be used to describe a physical problem modeled by hyperbolic conservation laws defined on a collection of 1D domains forming a graph.

$$U_t + F(U)_x = 0$$

CONSERVATION LAW

$$U_t + F(U)_x = G(U)$$

BALANCE LAW

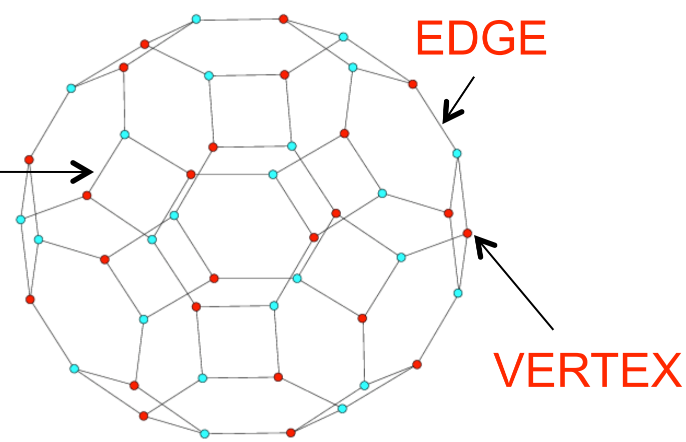

GRAPH

Hyperbolic nets and networks differ only in that hyperbolic nets do not have an a priori association with flow (e.g., stent (net) vs. arterial blood flow network).

HYPERBOLICITY

$$U_t + F(U)_x = 0, \;\; t > 0, x \in R$$

$$U = (x,t) - \text{ state variable}$$

$$U \in R^n, \;\; F : R^n \to R^n$$

$$F - \text{ smooth function}$$

A conservation law $U_t + F(U)_x = 0$ is said to be HYPERBOLIC if the eigenvalues of the Jacobian matrix F'(U) are all real.

(Same definition holds for a balance law $U_t + F(U)_x = G(U)$)

EXAMPLE: THE NONLINEAR WAVE SYSTEM

$$u_{tt} = (f(u)u_x)_x, \quad f(u) > 0 \quad \Longrightarrow \quad \begin{cases} u_t = w \\ v_t = w_x \\ w_t = (f(u)v)_x \end{cases}$$

$(w := u_t, \quad v := u_x)$

System: $U_t + F(U)_x = G(U)$ where $U = \begin{pmatrix} u \\ v \\ w \end{pmatrix}$, $F(U) = \begin{pmatrix} 0 \\ -w \\ -f(u)v \end{pmatrix}$ $G(U) = \begin{pmatrix} w \\ 0 \\ 0 \end{pmatrix}$

Jacobian matrix: $F'(U) = \begin{pmatrix} 0 & 0 & 0 \\ 0 & 0 & -1 \\ f'(u)v & -f(u) & 0 \end{pmatrix}$

Eigenvalues of the Jacobian: $F'(U) - \lambda I = \begin{pmatrix} -\lambda & 0 & 0 \\ 0 & -\lambda & -1 \\ f'(u)v & -f(u) & -\lambda \end{pmatrix} \Longrightarrow$ $\lambda_0 = 0,$ $\lambda_{1,2} = \pm\sqrt{f(u)},$

$\Longrightarrow$ **SYSTEM IS HYPERBOLIC**

with J. Tambaca

EXAMPLE: WAVE PROPAGATION IN A 3D NET MODELED BY THE NONLINEAR WAVE EQUATION

$u_{tt}=(f(u)u_x)_x$

$f(u)=0.5+u^2$

$$\begin{cases} u_t = w \\ v_t = w_x \\ w_t = (f(u)v)_x \end{cases}$$

Numerical simulation:
FEM (with P1)

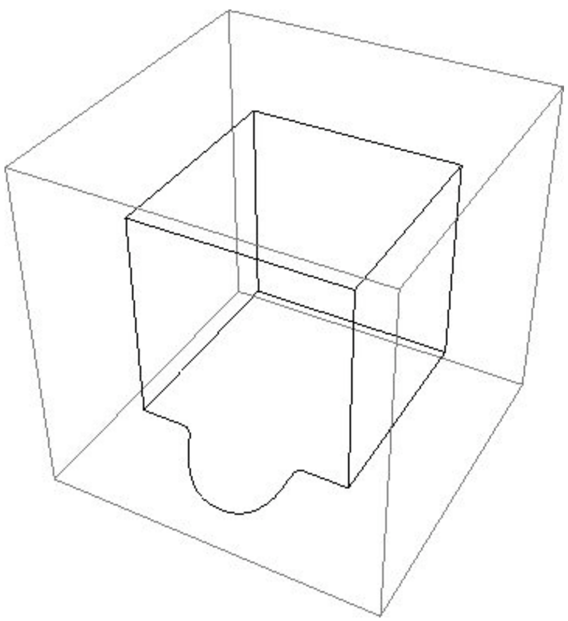

initial condition

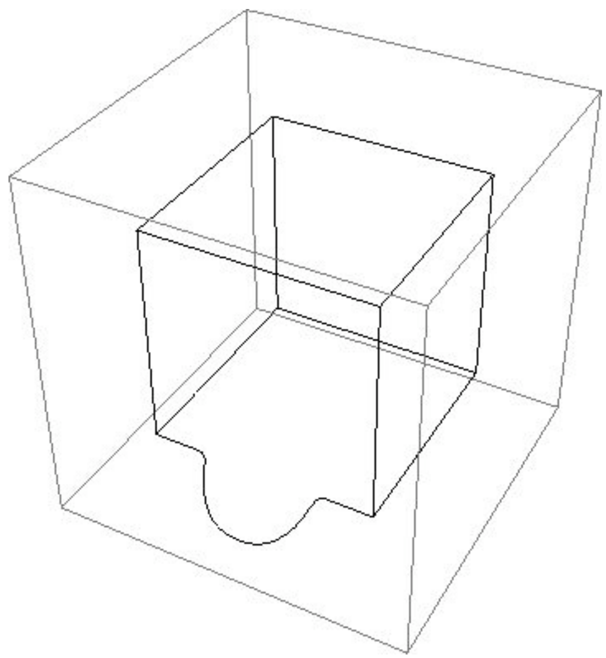

slow motion

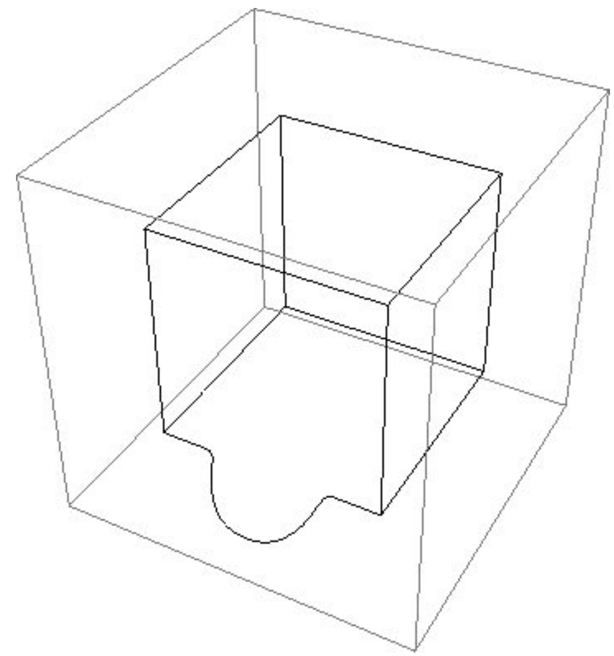

fast motion

COMMON PROPERTIES OF MOTIVATING PROBLEMS:

- GEOMETRY: the physical domain is multi-component, and net-like, which can be modeled as a graph

- PHYSICS: the physical/biological problem that holds on each domain component (edge of the graph) can be modeled by 1D hyperbolic conservation (or balance) laws.

$$U_t + F(U)_x = 0$$

CONSERVATION LAW

$$U_t + F(U)_x = G(U)$$

BALANCE LAW

$$U_t + F(U)_x = \varepsilon(D(U)U_x)_x$$

VISCOUS CONSERVATION LAW

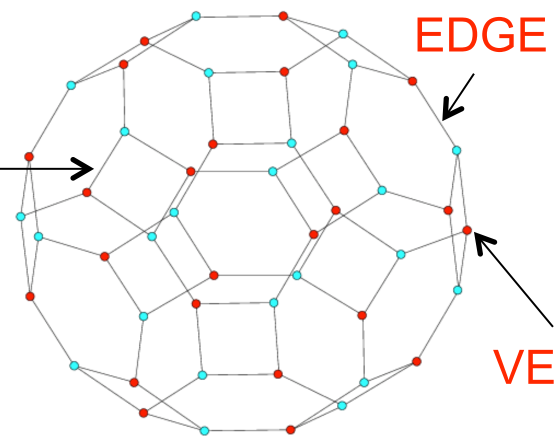

GRAPH

EXAMPLE: STRUCTURAL PROPERTIES OF VISCOUS GELLS, TISSUE SCAFFOLDS, OR CARBON NANOTUBES

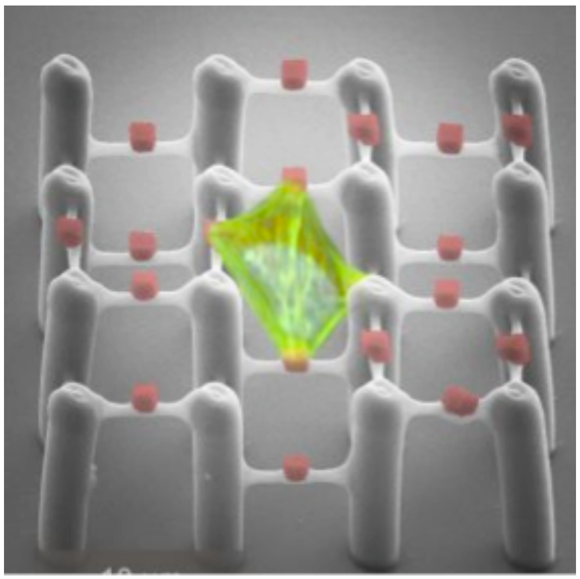

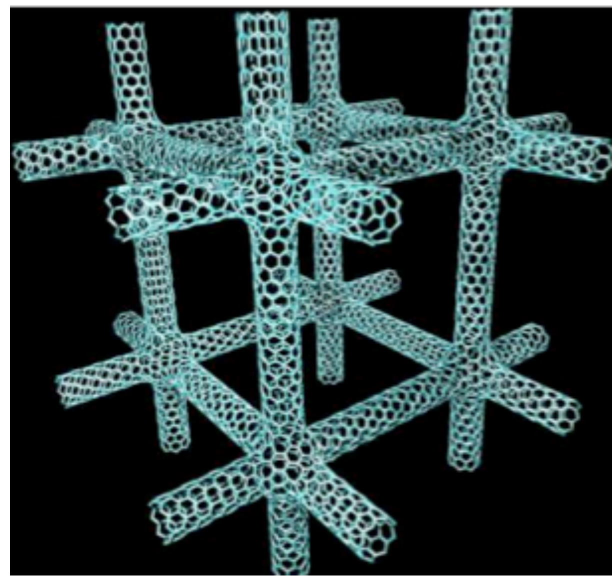

TISSUE SCAFFOLDS IN BIOMATERIALS (LEFT) & CARBON NANOTUBES IN MATERIALS SCIENCE(RIGHT)

$$U_t + F(U)_x = \varepsilon(D(U)U_x)_x$$

VISCOUS-HYPERBOLIC CONSERVATION LAWS

WE WILL FOCUS ON TWO EXAMPLES:

- MODELING OF ENDOVASCULAR STENTS AS AN EXAMPLE OF A HYPERBOLIC NET PROBLEM

- MODELING OF THE ARTERIAL NETWORK AS AN EXAMPLE OF A HYPERBOLIC NETWORK PROBLEM

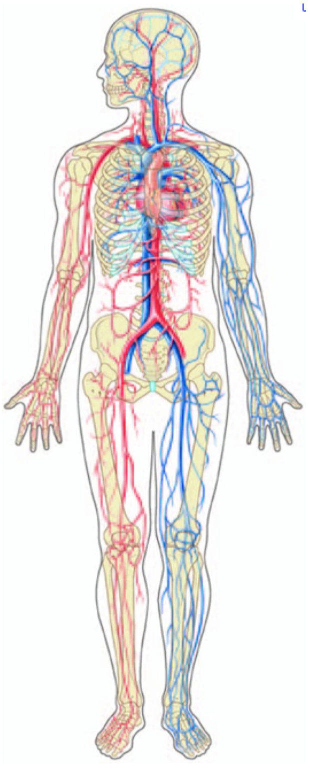

Before we continue, we need to recall some
basic theory of nonlinear hyperbolic conservation laws.

BASIC THEORY OF NONLINEAR CONSERVATION LAWS

$$U_t + F(U)_x = 0, \quad t > 0, x \in R$$

$$U = (x,t) - \text{ state variable}$$

$$U \in R^n, \quad F : R^n \to R^n$$

$$F - \text{ smooth function}$$

U – conserved quantity, F – flux function (the flux of U)

Integrate the PDE over an arbitrary interval [a,b]:

$$\frac{d}{dt}\int_a^b u(t,x)dx = -\int_a^b \mathrm{F}\,(u(t,x))_x dx = \mathrm{F}\,(u(t,a)) - \mathrm{F}(u(t,b))$$

Rate of change of u inside [a.b]

Flux of u that comes in – flux of u that goes out

CHARACTERISTICS

Consider the Cauchy problem: $\begin{cases} u_t + a(t,x,u)u_x = h(t,x,u) \\ u(0,x) = \bar{u}(x), \end{cases}$

Consider curves $x = x(t)$ such that: $\begin{cases} \frac{dx}{dt} = a(t,x,u) \\ x(0,y) = y \end{cases}$

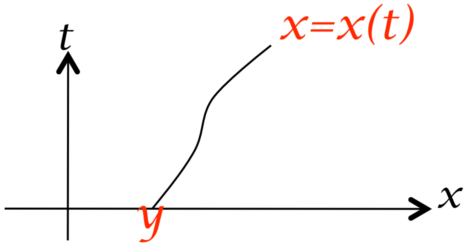

Then, along such curves, the derivative of $u(t,x(t))$ (as a function of t) is:

$$du/dt = u_t + a(t,x,u)\, u_x$$

The PDE implies: $du/dt = h(t,x,u)$.

Thus, along these curves, solution u of the conservation laws, satsfies an ODE!

The curves $x(t,y)$, y in $\mathbb{R}$, satisfying:
are called CHARACTERISTICS.

$$\begin{cases} \frac{dx}{dt} = a(t,x,u), \\ \frac{du}{dt} = h(t,x,u), \\ x(0,y) = y, \\ u(0,y) = \bar{u}(y). \end{cases}$$

CHARACTERISTICS

Systems: $\mathcal{U}_t + F(\mathcal{U})_x = 0$

$\mathcal{U}(0,x) = \mathcal{U}_o(x)$

Written in quasilinear form: $\mathcal{U}_t + F'(\mathcal{U})\, \mathcal{U}_x = 0$

$\mathcal{U}(0,x) = \mathcal{U}_o(x)$

The slopes of the characteristics are determined by the eigenvalues of the Jacobian F': $\lambda_1, \dots, \lambda_n$:

$$\begin{cases} \dfrac{dx_i}{dt} = \lambda_i, \quad i = 1,\dots,n \\ x_i(0) = y_i \end{cases}$$

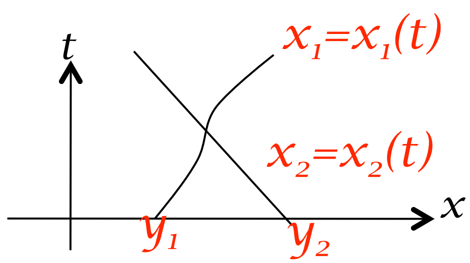

EXAMPLE: Burgers Equation (scalar)

$$u_t + u\, u_x = 0$$
$$u(0,x) = u_o(x)$$

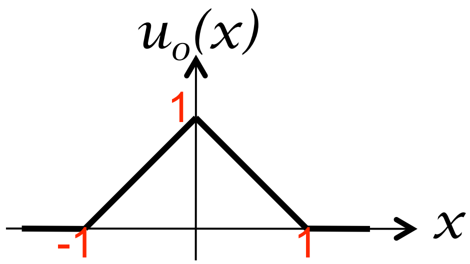

Characteristics: $dx/dt = u(t, x(t))$, along which $du/dt = 0$ (u is constant).

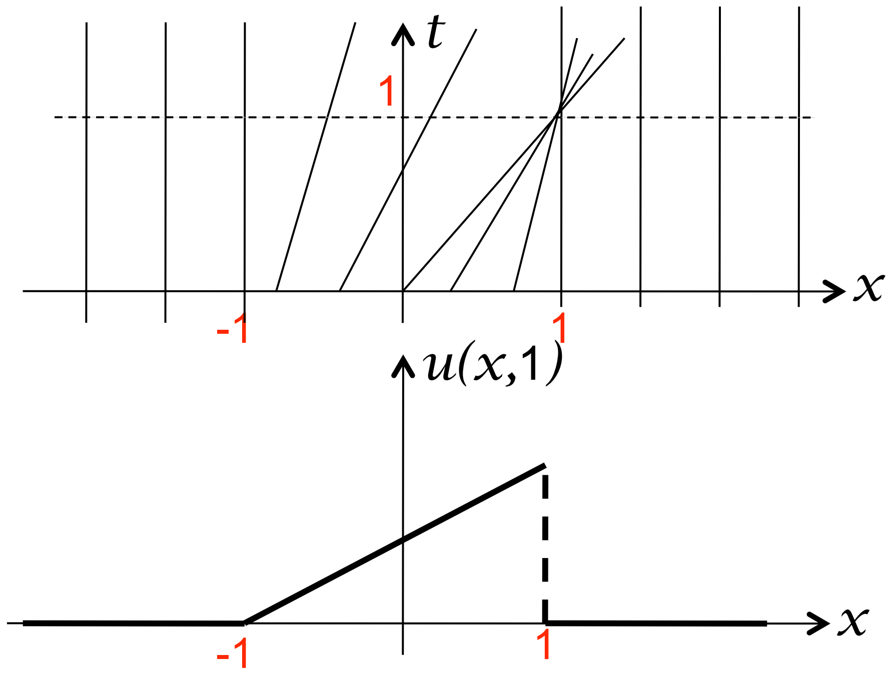

EXAMPLE: Burgers Equation (scalar)

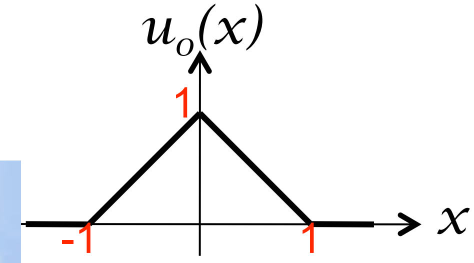

$$u_t + u\, u_x = 0$$

u

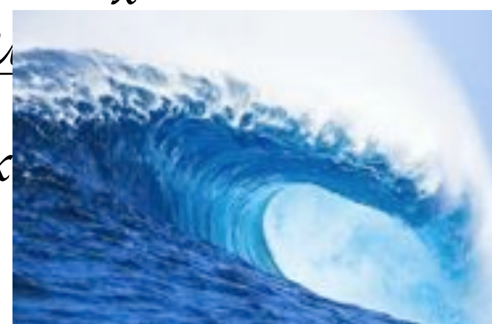

Characteristics: $dx/dt = u(t,x$ … $t = 0$ (u is constant).

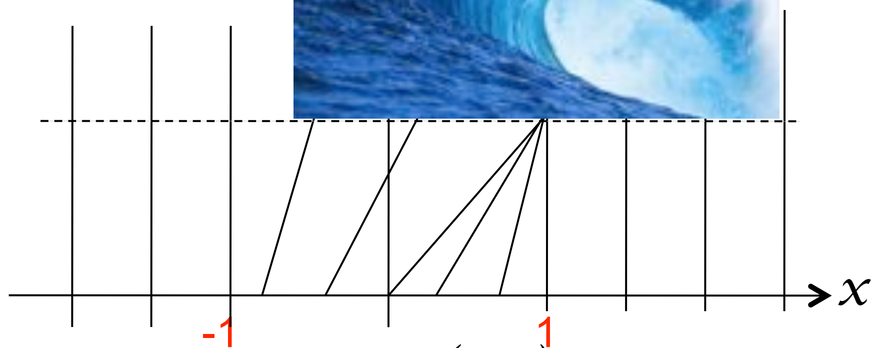

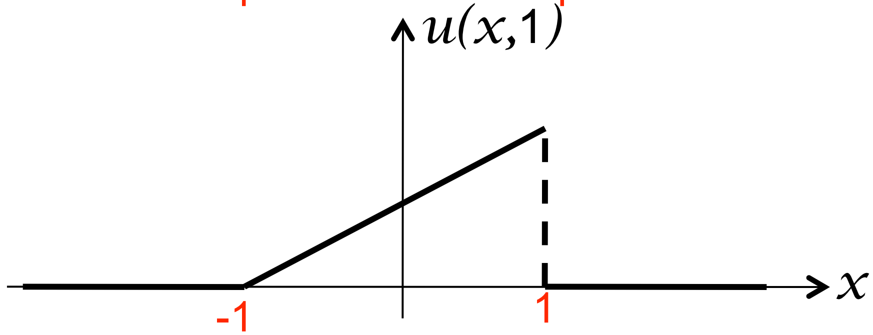

WEAK SOLUTIONS

Definition: A bounded and measurable function u is called a WEAK SOLUTION of the Cauchy problem

$$u_t + F(u)_x = 0$$
$$u(0,x) = u_o(x)$$

With bounded and measurable initial data u_o if for every C^1-function ψ with compact support in $[0,T) \times \mathbb{R}$ the following holds:

$$\int_0^T \int_{\mathbb{R}} \{u \cdot \psi_t + F'(u) \cdot \psi_x\}\, dx dt + \int_{\mathbb{R}} u_0(x) \cdot \psi(0,x) dx = 0.$$

Examples:

RIEMANN PROBLEM:

$$u_0(x) = \begin{cases} u_L, & x < 0 \\ u_R, & x < 0 \end{cases}$$

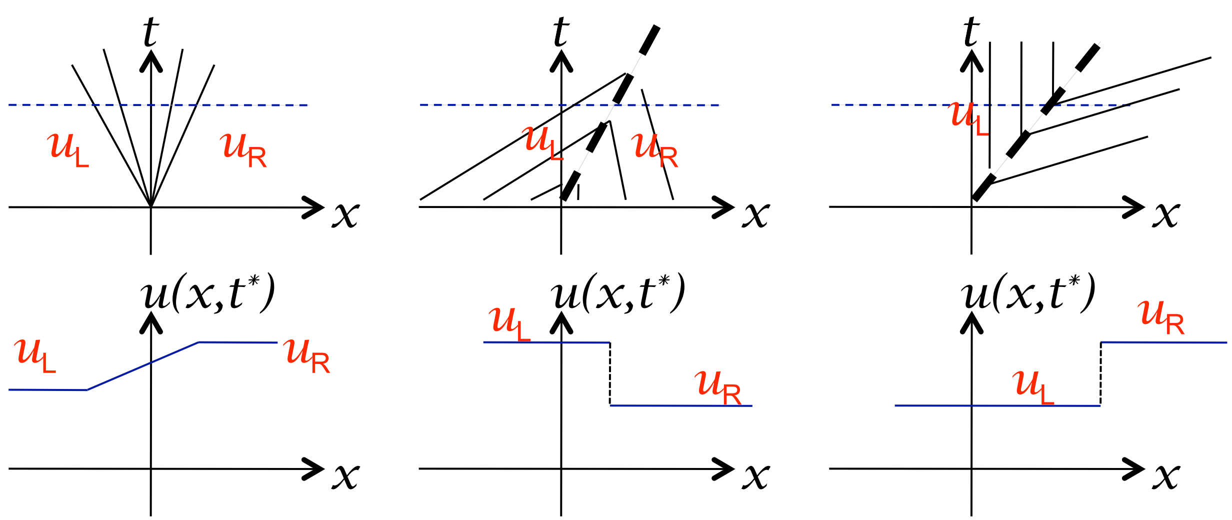

RAREFACTION

JUMP DISCONTINUITY (COMPRESSION SHOCK)

JUMP DISCONTINUITY (EXPANSION SHOCK)

WEAK SOLUTIONS

For convex F, rarefaction wave solution:

$$u(x,t) = \begin{cases} u_L, & x < F'(u_L)t \\ \mathrm{v}(x/t), & F'(u_L)t \le x \le F'(u_R)t \\ u_R, & x > F'(u_R)t \end{cases}$$

where $\mathrm{v}(\xi)$ is the solution of $F'(\mathrm{v}(\xi)) = \xi$.

Shock wave (jump discontinuity):

$$u(x,t) = \begin{cases} u_L, & x < st \\ u_R, & x > st \end{cases}$$

where s is the shock speed.

Examples:

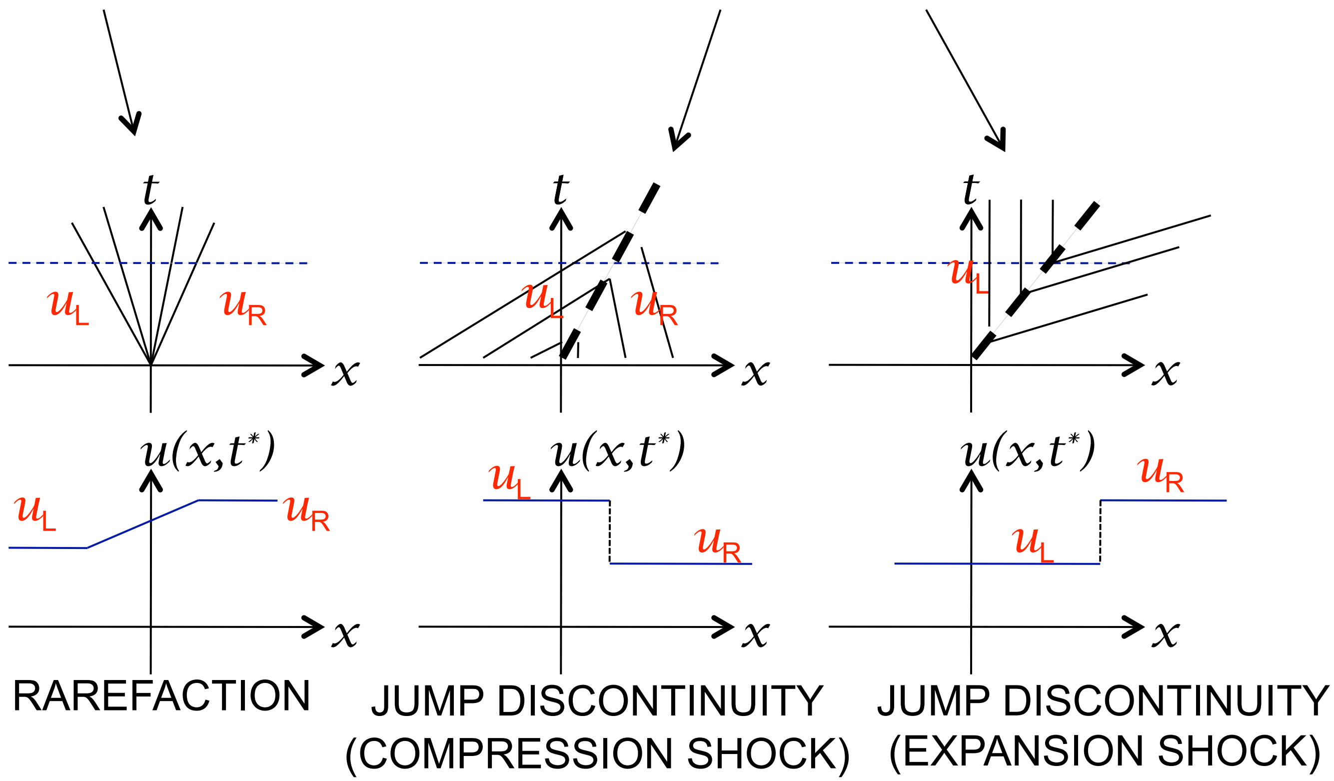

WEAK SOLUTIONS

Definition: A bounded and measurable function u is called a WEAK SOLUTION of the Cauchy problem

$$u_t + F(u)_x = 0$$
$$u(0,x) = u_o(x)$$

With bounded and measurable initial data u_o if for every C^1-function ψ with compact support in $[0,T) \times \mathbb{R}$ the following holds:

$$\int_0^T \int_{\mathbb{R}} \{u \cdot \psi_t + F(u) \cdot \psi_x\}\, dx dt + \int_{\mathbb{R}} u_0(x) \cdot \psi(0,x) dx = 0.$$

JUMP DISCONTINUITY:

$$-s(u_R - u_L) + (F(u_R) - F(u_L)) = 0$$

Rankine-Hugoniot Condition
(Jump Condition)

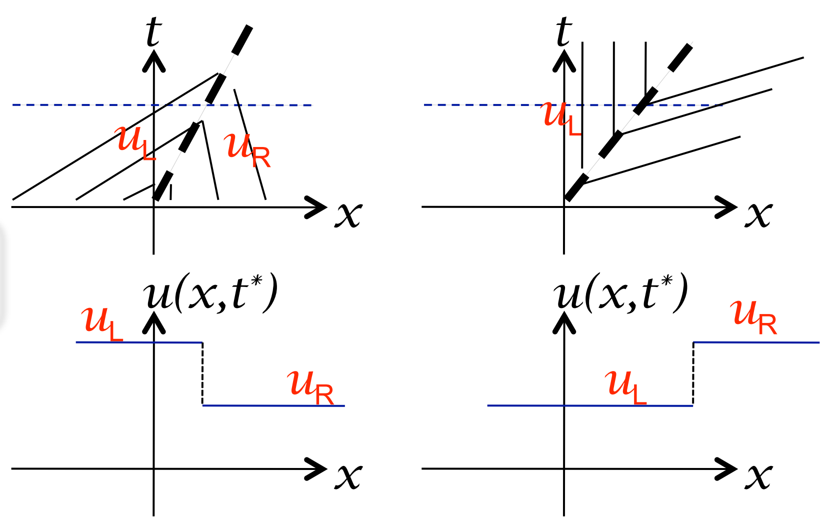

JUMP DISCONTINUITY (COMPRESSION SHOCK) JUMP DISCONTINUITY (EXPANSION SHOCK)

WEAK SOLUTIONS

Definition: A bounded and measurable function u is called a WEAK SOLUTION of the Cauchy problem

$$u_t + F(u)_x = 0$$
$$u(0,x) = u_o(x)$$

With bounded and measurable initial data u_o if for every C[1]-function ψ with compact support in $[0,T) \times \mathbb{R}$ the following holds:

$$\int_0^T \int_{\mathbb{R}} \{u \cdot \psi_t + F(u) \cdot \psi_x\}\, dx dt + \int_{\mathbb{R}} u_0(x) \cdot \psi(0,x) dx = 0.$$

Example:

RIEMANN PROBLEM:

$$u_0(x) = \begin{cases} u_L, & x < 0 \\ u_R, & x < 0 \end{cases}$$

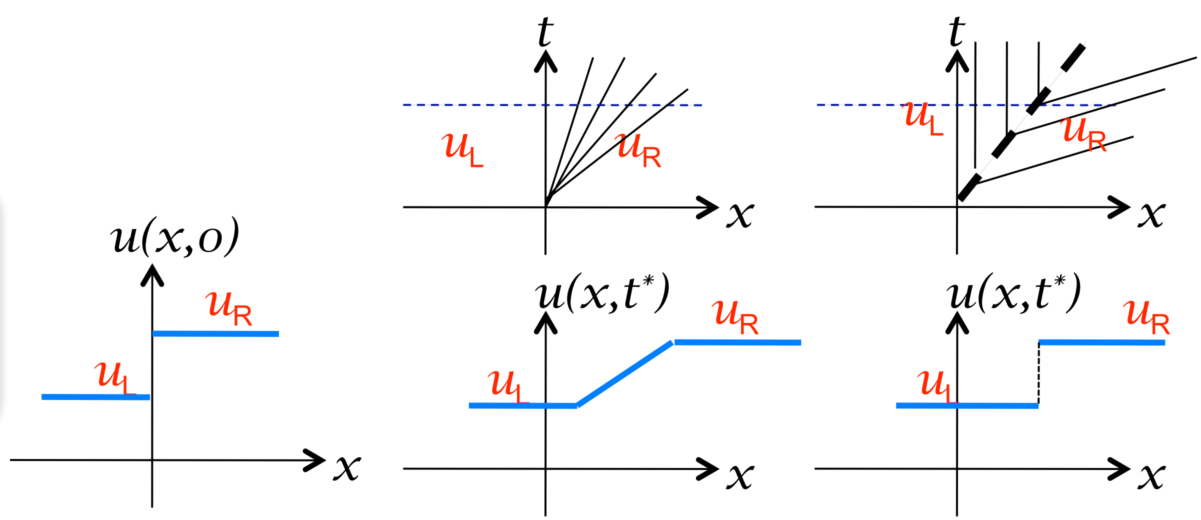

RAREFACTION

JUMP DISCONTINUITY (EXPANSION SHOCK)

WEAK SOLUTIONS

Definition: A bounded and measurable function u is called a WEAK SOLUTION of the Cauchy problem

$$u_t + F(u)_x = 0$$
$$u(0,x) = u_o(x)$$

With bounded and measurable initial data u_o if for every C^1-function ψ with compact support in $[0,T) \times \mathbb{R}$ the following holds:

$$\int_0^T \int_{\mathbb{R}} \{u \cdot \psi_t + F(u) \cdot \psi_x\}\, dx dt + \int_{\mathbb{R}} u_0(x) \cdot \psi(0,x) dx = 0.$$

Example:

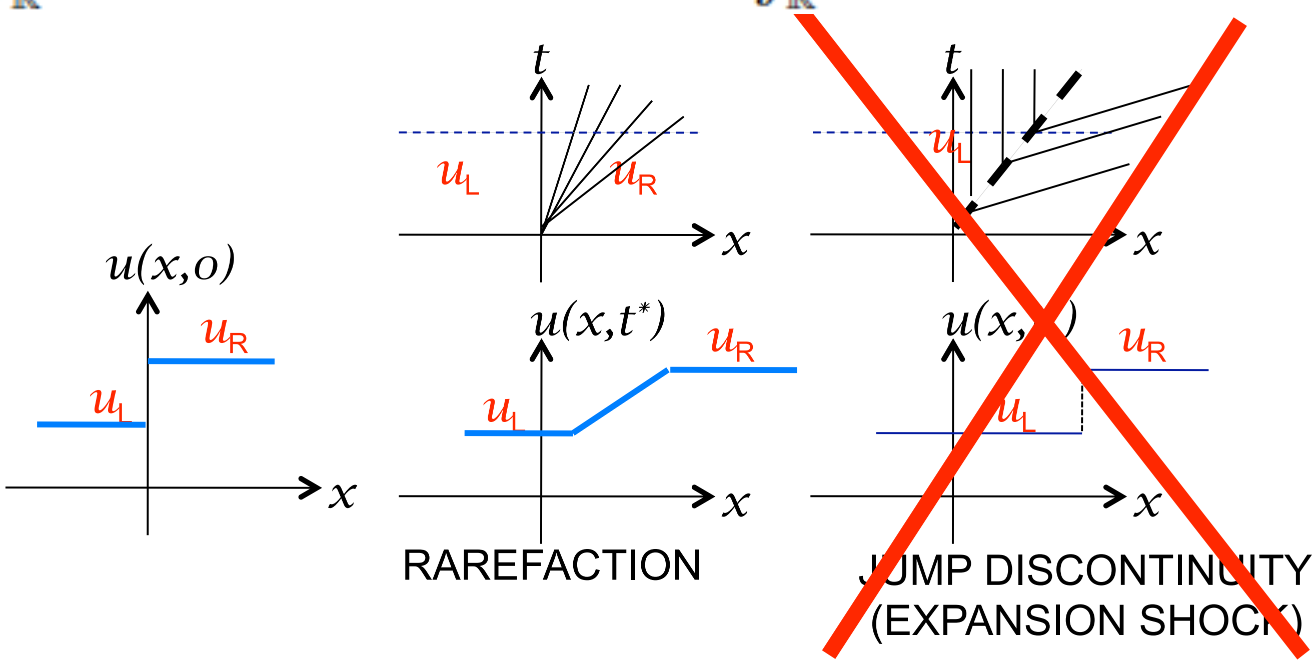

WEAK SOLUTIONS

Definition: A bounded and measurable function u is called a WEAK SOLUTION of the Cauchy problem

$$u_t + F(u)_x = 0$$
$$u(0,x) = u_o(x)$$

With bounded and measurable initial data u_o if for every C^1-function ψ with compact support in $[0,T) \times \mathbb{R}$ the following holds:

$$\int_0^T \int_{\mathbb{R}} \{u \cdot \psi_t + F(u) \cdot \psi_x\} \, dx dt + \int_{\mathbb{R}} u_0(x) \cdot \psi(0,x) dx = 0.$$

Examples:

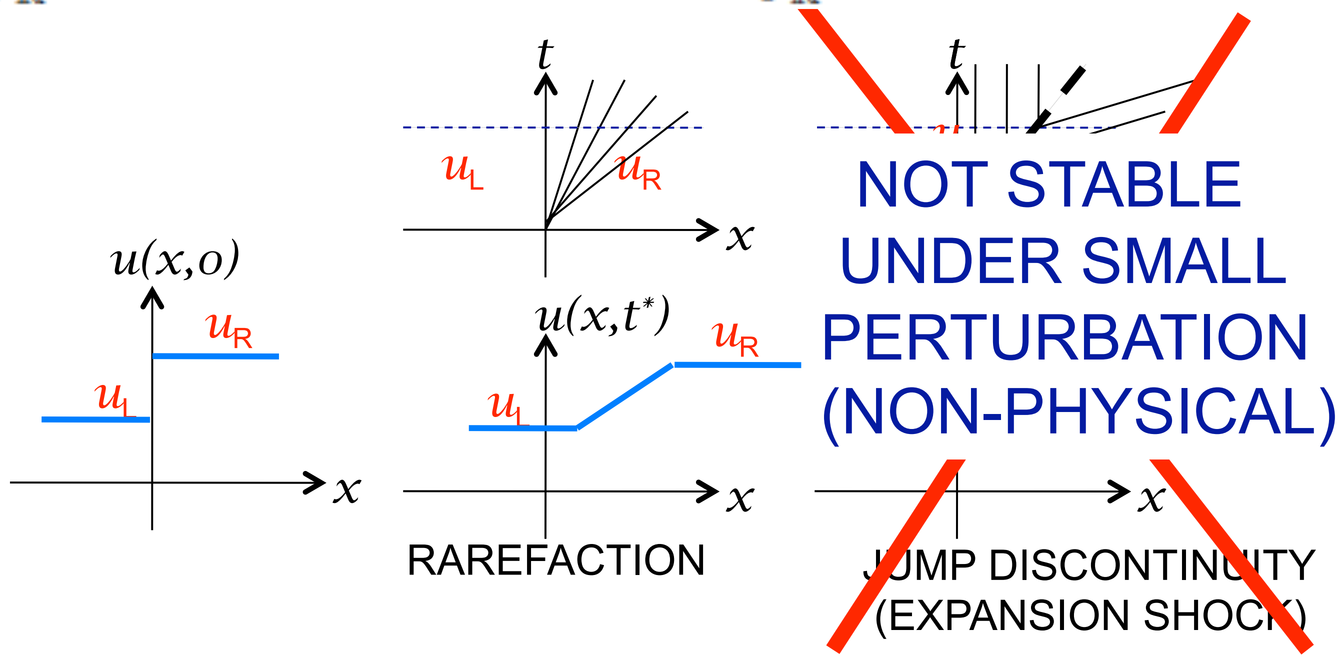

SHOCK ADMISSIBILITY (ENTROPY CRITERIA)

LAX ENTROPY CONDITION: A discontinuity propagating at speed s, given by the Rankine-Hugoniot condition

$$-s(u_R-u_L)+(F(u_R)-F(u_L))=0$$

Satisfies the entropy condition if

$$F'(u_L) > s > F'(u_R).$$

(Note that F' is the characteristic speed.)

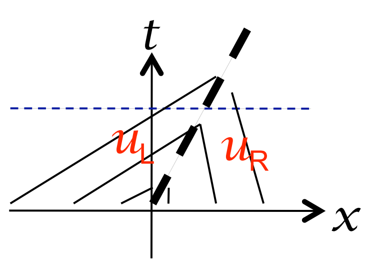

EXISTENCE OF A WEAK SOLUTION

(Glimm (1965), Lax (1953), Dafermos (1972), Bressan, Holden&Risebro, Serre, Smoller, DiPerna)

Functions of bounded Total Variation: $w : J \to \mathbb{R}$, J subset of $\mathbb{R}$

$$\mathrm{Tot.Var.}\, w = \sup \left\{ \sum_{j=1}^{N} |w(x_j) - w(x_{j-1})| \right\}$$

where $N \geqslant 1$, the points x_j belong to J for every $j \in \{0, \ldots, N\}$ and satisfy $x_0 < x_1 < \cdots < x_N$

Definition *We say that the function $w : J \to \mathbb{R}$ has bounded total variation if $Tot.Var.\, w < +\infty$. We denote with $BV(J)$ the set of all real functions $w : J \to \mathbb{R}$ with bounded total variation.*

Lemma *Let $w : J \to \mathbb{R}$ be a function with bounded total variation and $\bar{x}$ be a point in the interior of J. Then the limits*

$$\lim_{x \to \bar{x}^-} w(x), \qquad \lim_{x \to \bar{x}^+} w(x)$$

exist. Moreover the function w has at most countably many points of discontinuity.

EXISTENCE OF A WEAK SOLUTION

Theorem (GLOBAL EXISTENCE OR WEAK SOLUTIONS): Assume that the system

$$u_t + F(u)_x = 0$$
$$u(0,x) = u_o(x)$$

is strictly hyperbolic, and that each characteristic field is either linearly degenerate or genuinely nonlinear. Then there exists a constant $\delta_0 > 0$ such that, for every initial data in $L^1(R)$ with

$$\text{Tot. Var. } \{u_0\} \leq \delta_0$$

the Cauchy problem has a weak solution defined for all $t > 0$.

EXISTENCE OF A WEAK SOLUTION

Theorem (GLOBAL EXISTENCE OR WEAK SOLUTIONS): Assume that the system

$$u_t + F(u)_x = 0$$
$$u(0,x) = u_o(x)$$

is strictly hyperbolic, and that each characteristic field is either linearly degenerate or genuinely nonlinear. Then there exists a constant $\delta_0 > 0$ such that, for every initial data in $L^1(R)$ with

$$\text{Tot. Var. } \{u_0\} \leq \delta_0$$

the Cauchy problem has a weak solution defined for all $t > 0$.

Main ideas of the proof: based on the wave-tracking algorithm.

Main steps of the wave-tracking algorithm:

(1) approximate initial data with piece-wise constant functions

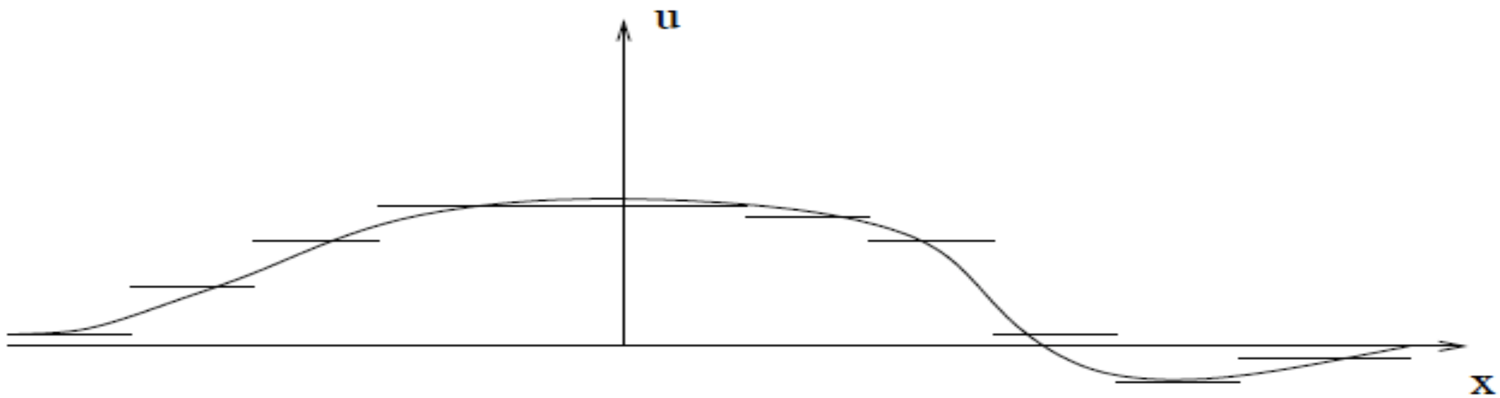

EXISTENCE OF A WEAK SOLUTION

Theorem (GLOBAL EXISTENCE OR WEAK SOLUTIONS): Assume that the system

$$u_t + F(u)_x = 0$$
$$u(0,x) = u_o(x)$$

is strictly hyperbolic, and that each characteristic field is either linearly degenerate or genuinely nonlinear. Then there exists a constant $\delta_0 > 0$ such that, for every initial data in $L^1(R)$ with

$$\text{Tot. Var. } \{u_0\} \leq \delta_0$$

the Cauchy problem has a weak solution defined for all $t > 0$.

Main ideas of the proof: based on the wave-tracking algorithm.

Main steps of the wave-tracking algorithm:

(1) approximate initial data with piece-wise constant functions

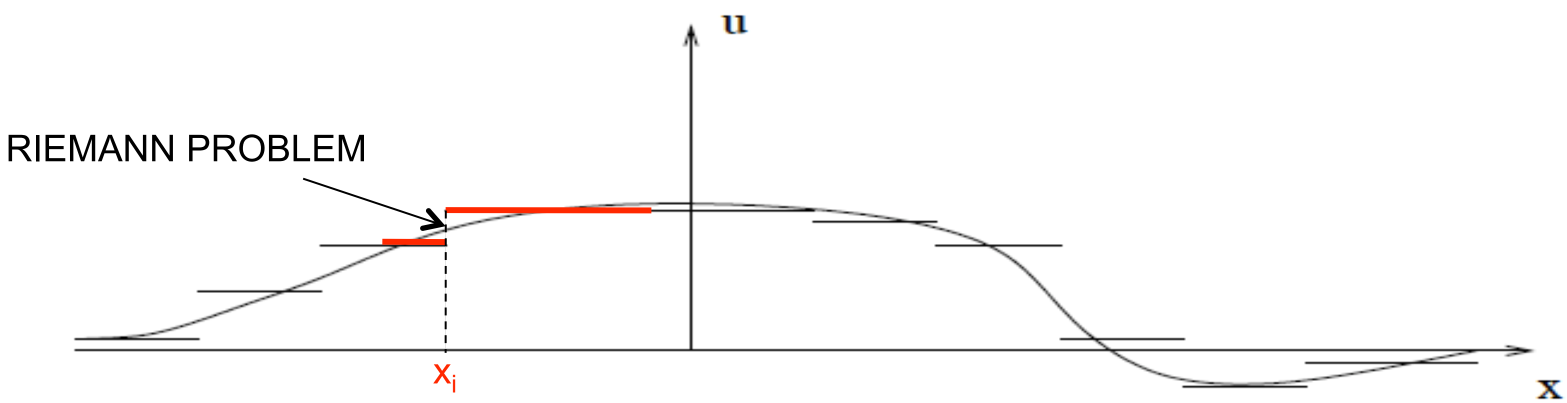

EXISTENCE OF A WEAK SOLUTION

Theorem (GLOBAL EXISTENCE OR WEAK SOLUTIONS): Assume that the system

$$u_t + F(u)_x = 0$$
$$u(0,x) = u_o(x)$$

is strictly hyperbolic, and that each characteristic field is either linearly degenerate or genuinely nonlinear. Then there exists a constant $\delta_0 > 0$ such that, for every initial data in $L^1(R)$ with

$$\text{Tot. Var. } \{u_0\} \leq \delta_0$$

the Cauchy problem has a weak solution defined for all t > 0.

Main ideas of the proof: based on the wave-tracking algorithm.

Main steps of the wave-tracking algorithm:

(1) approximate initial data with piece-wise constant functions

(2) solve at every point of discontinuity the corresponding Riemann problem

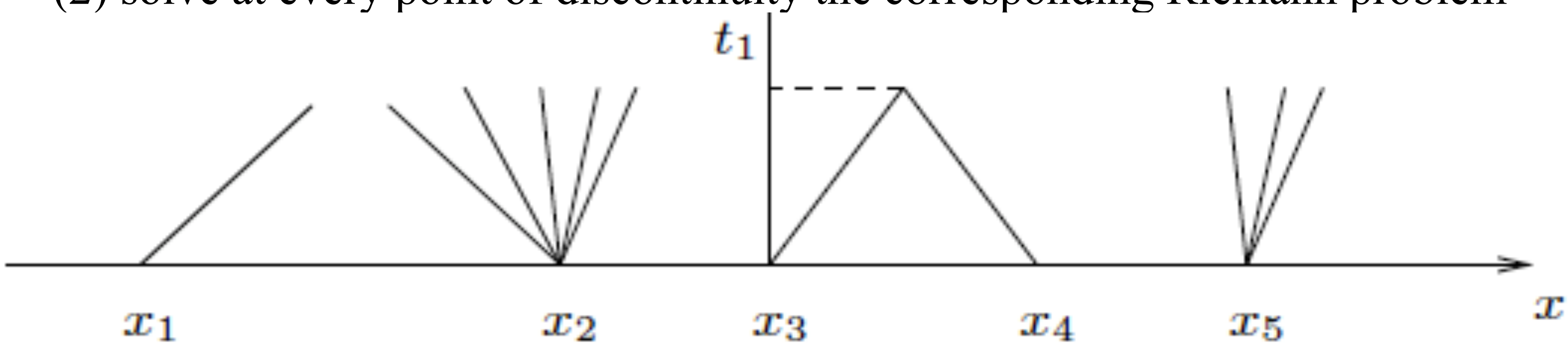

EXISTENCE OF A WEAK SOLUTION

Theorem (GLOBAL EXISTENCE OR WEAK SOLUTIONS): Assume that the system

$$u_t + F(u)_x = 0$$
$$u(0,x) = u_o(x)$$

is strictly hyperbolic, and that each characteristic field is either linearly degenerate or genuinely nonlinear. Then there exists a constant $\delta_0 > 0$ such that, for every initial data in $L^1(R)$ with

$$\text{Tot. Var. } \{u_0\} \leq \delta_0$$

the Cauchy problem has a weak solution defined for all $t > 0$.

Main ideas of the proof: based on the wave-tracking algorithm.

Main steps of the wave-tracking algorithm:

(1) approximate initial data with piece-wise constant functions

(2) solve at every point of discontinuity the corresponding Riemann problem

(3) approximate rarefaction waves with a fan of small shocks to get a piece-wise constant function until two waves interact

(4) repeat the process inductively starting with interaction times

(5) prove that the functions so constructed converge to a limit function, and that the limit function is an entropy solution

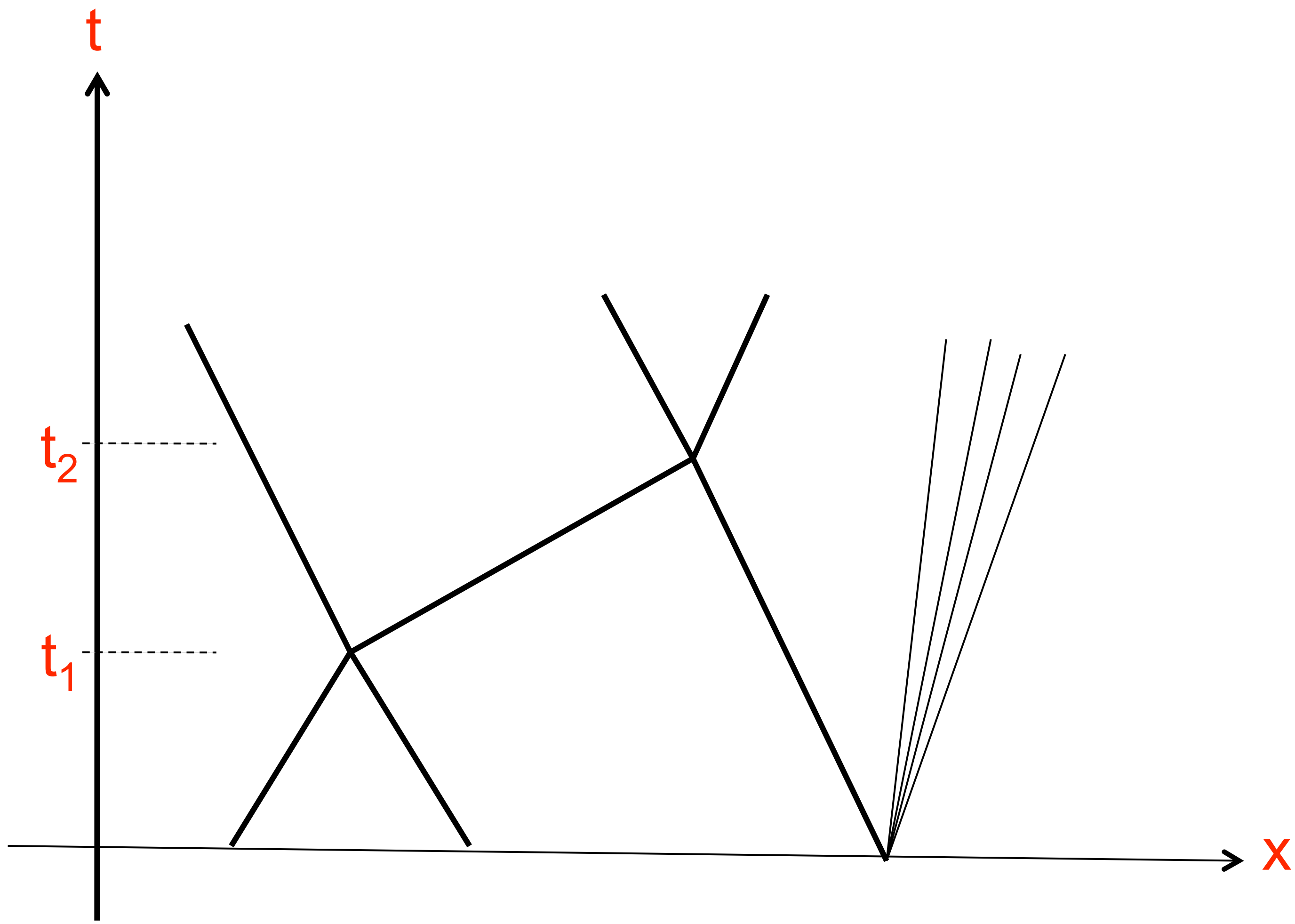

A wave-front tracking approximation

The algorithm produces a sequence of approximate solutions.
Convergence of the sequence is proved by a compactness argument,
Based on uniform bounds of the Total Variation.
More precisely, one needs to be able to control, via estimates:

(1) the number of waves
(2) the number of interactions between waves
(3) the total variation of the approximate solution

These estimates are trivial in the scalar case (single equation) since the number of waves decreases, as does the Total Variation of the solution.

In the systems case, due to the presence of more than one characteristic family, one needs to introduce simplified solutions to Riemann problems to be able to bound wave interactions between different families. The Total Variation increases in time, but only in the lower (quadratic) order contributions, and the control of over the Total Variation is obtained via the decrease in the Glimm's functional.

References:

Cauchy Problems: Dafermos (J Math Anal Appl, 1972), DiPerna (1976), Bressan (1992), Baiti and Jenssen (1998), Holden and Risebro (2002)

Cauchy Problems for Balance Laws: Amadori, Gosse and Guerra (2002)

Initial-Boundary Value Problems: Amadori and Colombo (1997), Donadello and Marson (2007)

Most recent summary with important references:
Alberto Bressan "Open questions in the theory of one-dimensional hyperbolic conservation laws," IMA Volumes in Mathematics and its Applications, Volume 153, 1-23, 2011 (Springer)

WEAK SOLUTION TO NETS AND NETWORK PROBLEMS

THERE IS NO GENERAL THEORY FOR EXISTENCE OF SOLUTIONS TO NONLINEAR HYPERBOLIC NET/NETWORK PROBLEMS!

NEED YOUNG, TALENTED MATHEMATICIANS TO WORK IN THIS AREA ☺

The main difficulties stem from the analysis of the wave interactions at net's vertices.

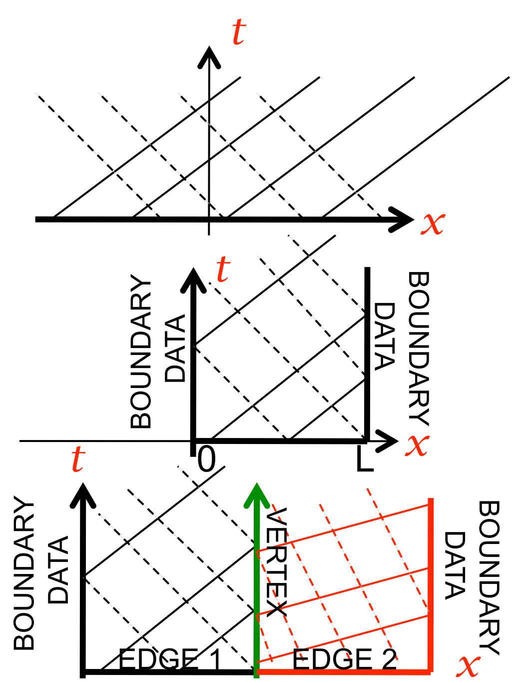

Cauchy problem: characteristics carrying information about solution extend to infinity.

Initial-boundary value problems: characteristics hit the boundary. If the boundary data is not "consistent" with the solution, a reflected wave forms.

Net/network problems: characteristics hit vertices, but the value of the solution at a vertex is NOT KNOWN a priori, but rather it depends on the solution ITSELF!

Example: 3D NET (CUBE)

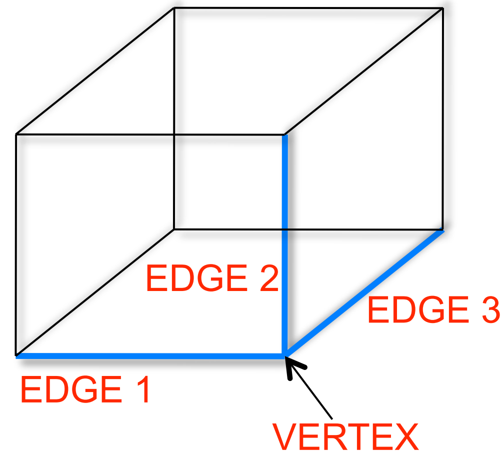

Suppose that on each edge, the nonlinear wave equation holds (modeling vibrations of each edge as a nonlinear string).

Characteristic structure:

Solution at the vertex depends on the solution on the entire net and on the coupling conditions at the vertex.

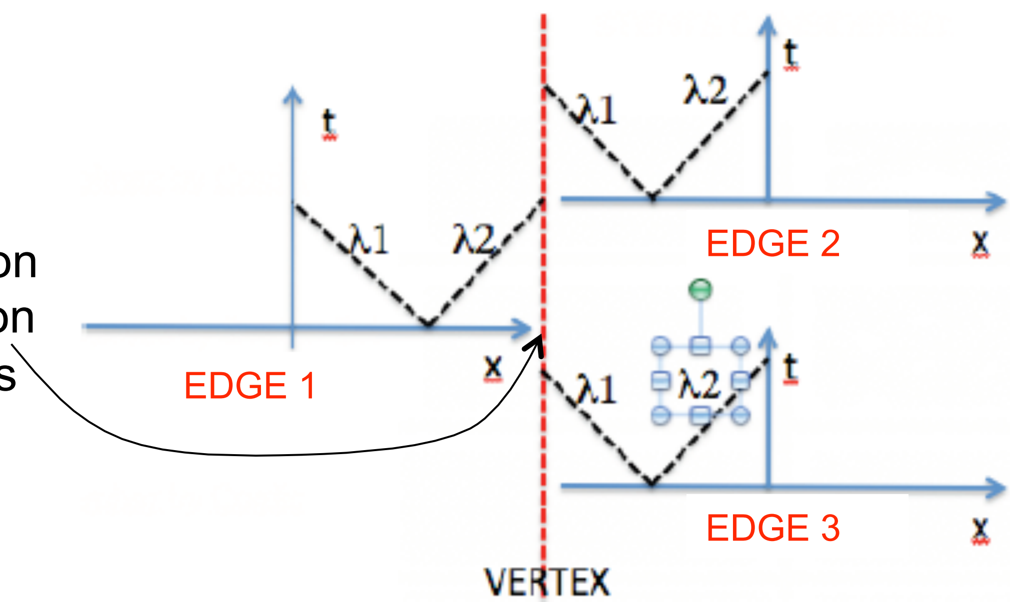

with J. Tambaca

WAVE PROPAGATION IN A 3D NET MODELED BY THE NONLINEAR WAVE EQUATION

$u_{tt}=(f(u)u_x)_x$

$f(u)=0.5+u^2$

$u_t = w$
$v_t = w_x$
$w_t = (f(u)v)_x$

Numerical simulation:
FEM (with P1)

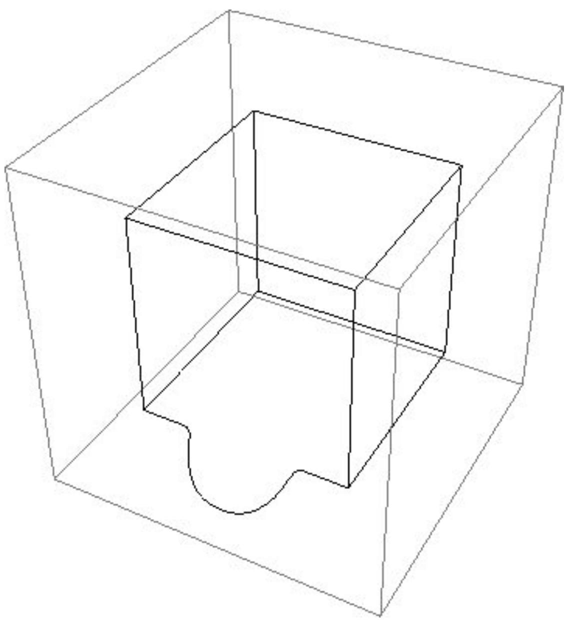

initial condition

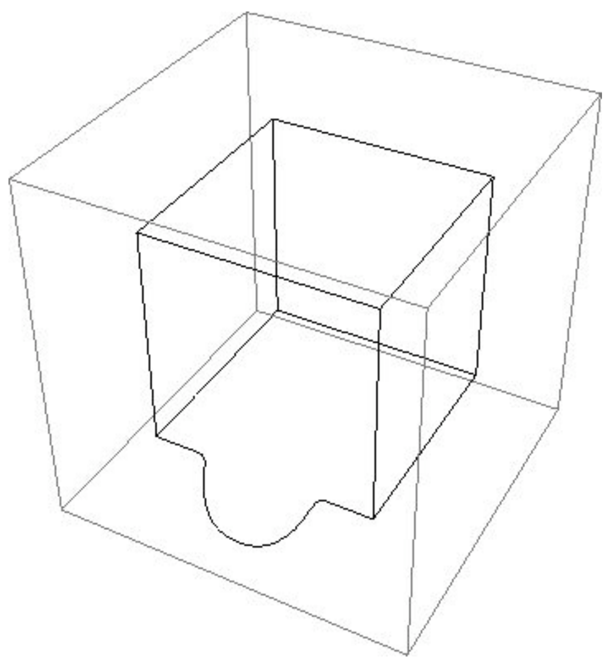

slow motion

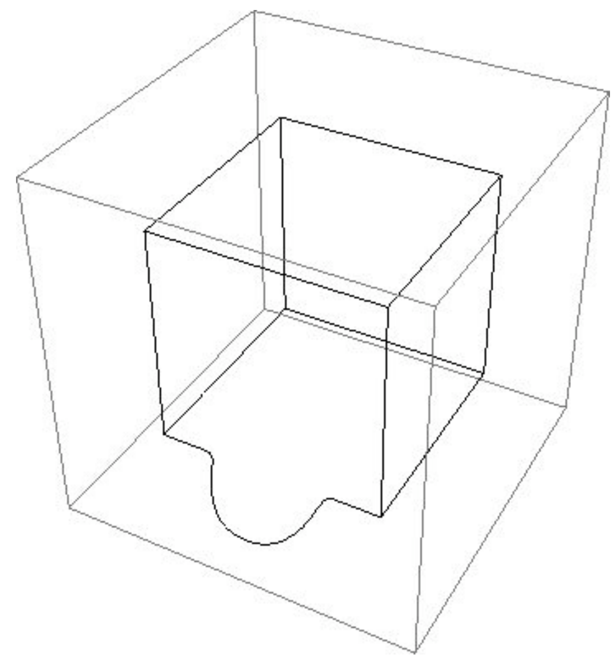

fast motion

with J. Tambaca

Propagation of waves for a linearized problem, and the interaction of waves at net’s vertices will be explicitly calculated later.

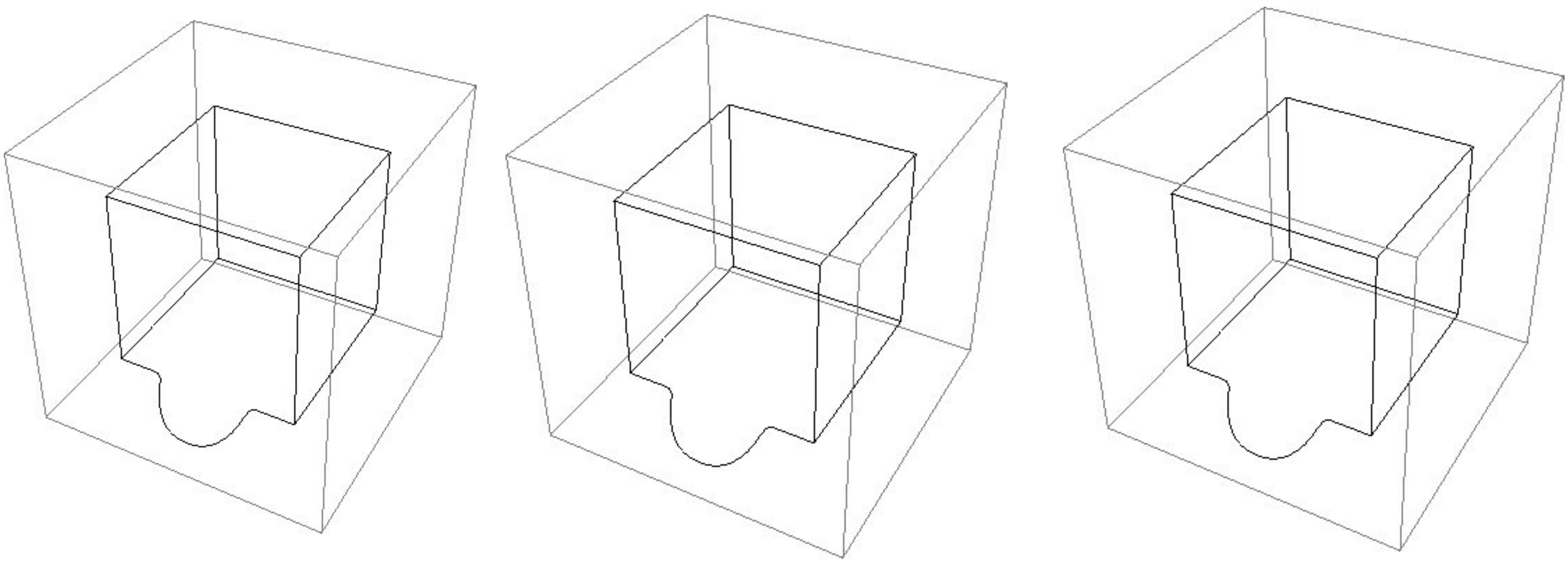

initial condition slow motion fast motion

THEORETICAL STUDY OF SOLUTIONS (NETs and NETWORKS)

1. The TV increases to the leading order, not to the lower, quadratic order. It was shown* that no total-variation-type functional is decreasing along the solutions in nets with loops, or when the characteristic condition is violated.

2. Estimating the number of waves interacting at each vertex is nontrivial. In nets and networks, the number of wave interactions at vertices may increase without a bound (e.g., in graphs with loops, or if the non-characteristic condition is not satisfied).

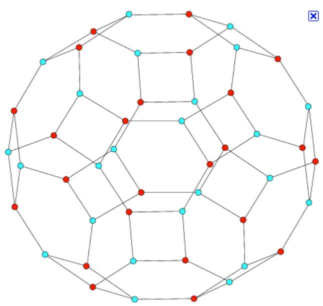

3. One needs an a priori bound on the value of the solution at each vertex to be able to use a compactness argument to establish convergence.

4. Solution estimates at vertices need to be done for a set of multi-Riemann problem data, the solutions of which are all coupled at the vertex via the physical (mathematical) coupling conditions.

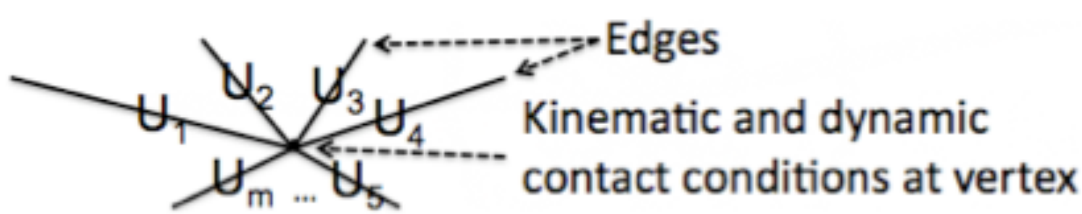

References:

*M. Garavello and B. Piccoli. *Traffic Flow on Networks*. Volume 1 of *AIMS Series on Applied Mathematics*. AIMS, 2006.

M. Garavello and B. Piccoli. Conservation laws on complex networks. *Ann. Inst. H. Poincaré Anal. Non Linéaire* 26 (5), 1925-1951, 2009.

M. Garavello and B. Piccoli. Traffic flow on a road network using the Aw-Rascle model. *Comm. Partial Differential Equations* 31 (1-3), 243–275, 2006.

S. Göttlich, M. Herty and A. Klar. Network models for supply chains. *Commun. Math. Sci.* 3 (4), 545–559, 2005.

K. Ammari and M. Jellouli. Stabilization of star-shaped networks of strings. *Differential Integral Equations*, 17, 1395–1410, 2004.

D. Armbruster, P. Degond, C. Ringhofer. A model for the dynamics of large queuing networks and supply chains. *SIAM J. Appl. Math.* 66 (3), 896–920, 2006.

G. Bretti, R. Natalini, B. Piccoli. Numerical approximation of a traffic flow model on networks. *Networks and Heterogeneous Media*, 1 (2006), pp. 57-84.

G.M. Coclite, M. Garavello and B. Piccoli. Traffic flow on a road network. (English summary) SIAM J. Math. Anal. 36 (6), 1862–1886, 2005.

R. M. Colombo, M. Herty and V. Sachers. On 2×2 conservation laws at a junction. *SIAM J. Math. Anal.* 40 (2), 605–622, 2008.

More details exemplifying the main difficulties in
the analysis and numerical simulation of net/network
problems will be presented later in the
lectures by considering some simplified problems
associated with our two main examples.

BACK TO TWO EXAMPLES:

- MODELING OF ENDOVASCULAR STENTS AS AN EXAMPLE OF A HYPERBOLIC NET PROBLEM

- MODELING OF THE ARTERIAL NETWORK AS AN EXAMPLE OF A HYPERBOLIC NETWORK PROBLEM

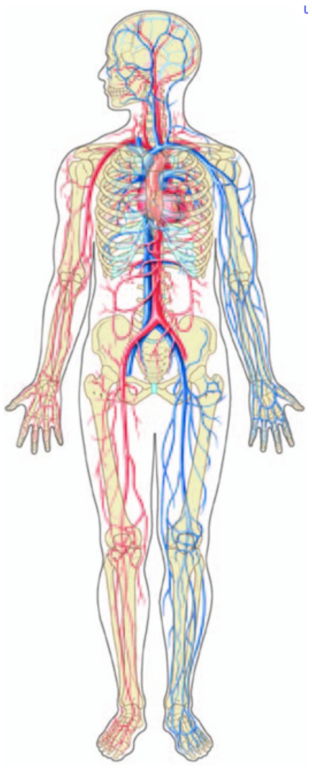

ENDOVASCULAR STENTS

- STENT: MESH TUBE THAT IS INSERTED INTO A NATURAL CONDUIT OF THE BODY TO PREVENT OR COUNTERACT A DISEASE-INDUCED LOCALIZED FLOW CONSTRICTION
- USED IN THE CARDIOVASCULAR SYSTEM, TRACHEOBRONCHIAL, BILIARY AND UROGENITAL SYSTEM
- STENTS PLAY CRUCIAL ROLE IN TREATMENT OF CORONARY ARTERY DISEASE

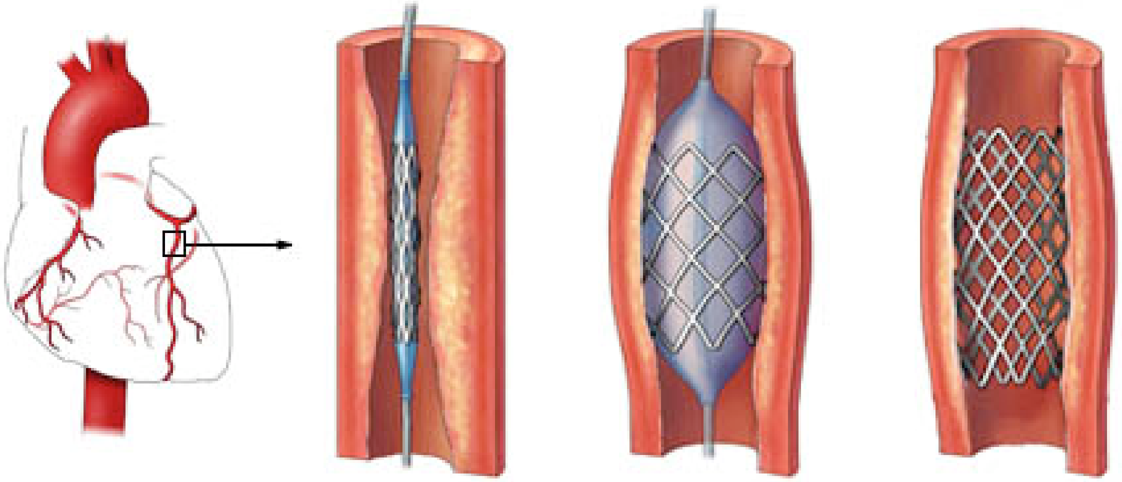

with J. Tambaca, M. Kosor
Dr. Paniagua, Dr. Fish

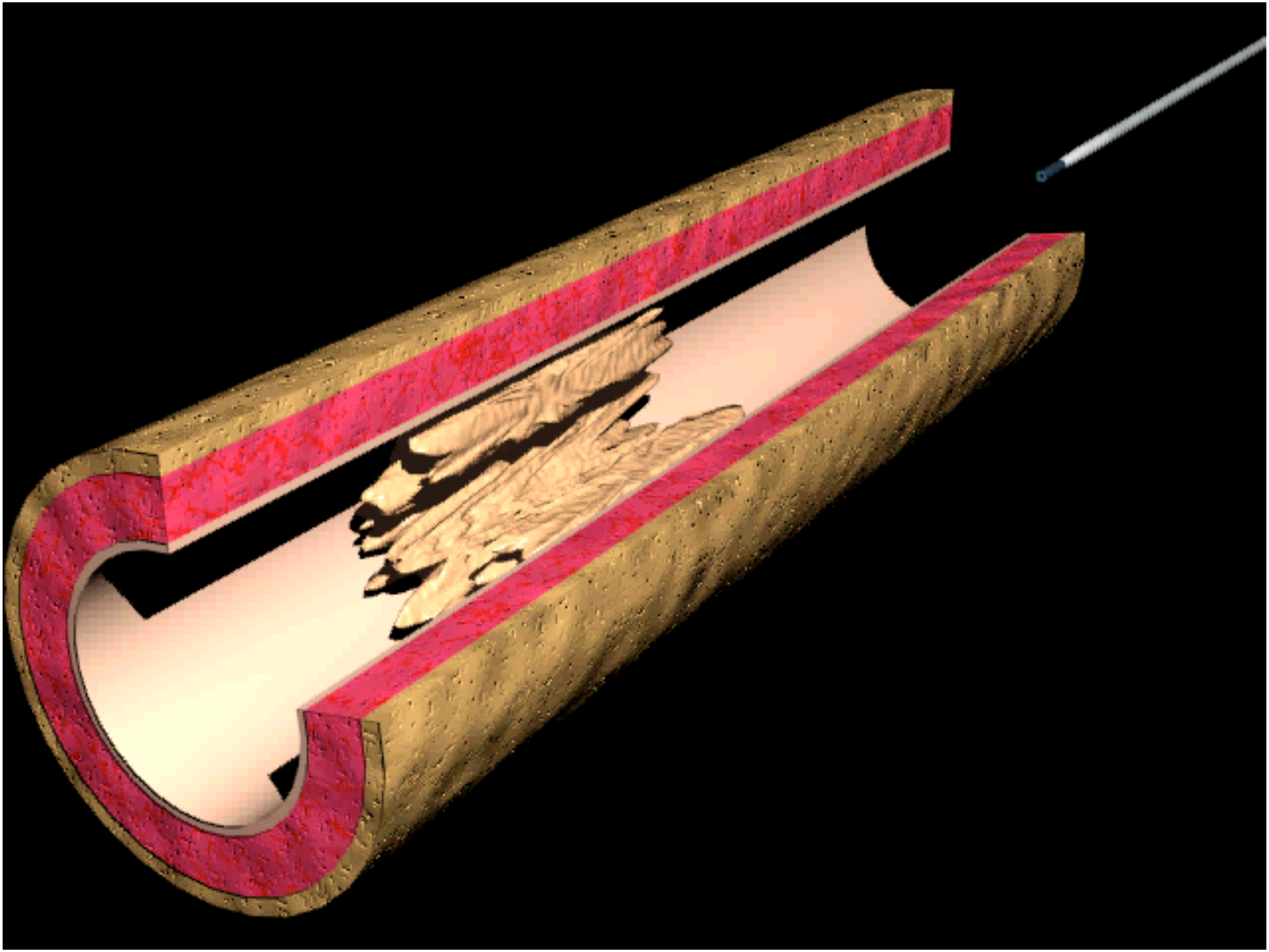

OPEN QUESTIONS

STUDY MECHANICAL PROPERTIES OF STENTS

- WHICH STENT IS APPROPRIATE FOR A GIVEN LESION?

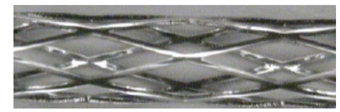

- WHICH STENTS ARE APPROPRIATE FOR TORTUOUS GEOMETRIES?

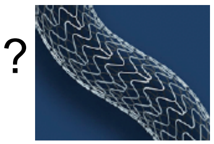

- WHAT IS THE OPTIMAL STENT DESIGN FOR THE CATHETER-BASED AORTIC VALVE REPLACEMENT?

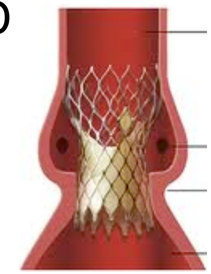

- WHAT IS THE STENT'S LONGITUDINAL STRAIGHTENING (BENDING RIGIDITY) AND HOW DOES IT DEPEND ON ITS GEOMETRY?
- LONGITUDINAL EXTENSION/SHORTENING DURING PULSATION?
- BIOCOMPATIBILITY and RESTENOSIS

J. Hao, T.W. Pan, S. Canic, R. Glowinski, D. Rosenstrauch. *A Fluid-Cell Interaction and Adhesion Algorithm for Tissue-Coating of Cardiovascular Implants*. SIAM J Multiscale Modeling and Simulation 7(4) 1669-1694 (2009)

MECHANICAL PROPERTIES OF STENTS

LARGE CARDIOVASCULAR LITERATURE

- CASE REPORTS
- Zarins, Mehta, Gyongyosi, Rieu, Sainsous,Ormiston, Webster, Dixon, Post, Kuntz, Mirkovitch, Sigwart, Garasic, Edelman, Rogers, Kastrati, Sigwart, Dyet, Watts, Ettles, Schomig, Rogers, Tseng, Edelman, Squire, Gruntzig, Mayler, Hanna,…

MODERATLY LARGE ENGINEERING LITERATURE

- SIMULATIONS USE 3D COMMERCIAL SOFTWARE
- Moore, Timmins, Berry, Dumoulin, Taylor, Bedoya, Schmidt, Behrens, Cochelin, Holzapfel, Gasser, Stadler, Magliavacca, Petrini, Colombo, Auricchio, Hoang, …

HELPED UNDERSTAND MANY STENT PERFORMANCE FEATURES!!!

DRAWBACKS:

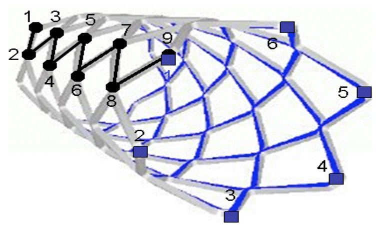

- 3D simulation of each stent strut is computationally very expensive
- thin and long structure: need extremely fine mesh to achieve reasonable accuracy (view 3Dstent)
- commercial software uses "black box" approach: do not know which models are used
- computationally prohibitive to include dynamic 3D stent modeling in a fluid-structure interaction solver

MECHANICAL PROPERTIES OF STENTS

LARGE CARDIOVASCULAR LITERATURE

- CASE REPORTS
- Zarins, Mehta, Gyongyosi, Rieu, Sainsous,Ormiston, Webster, Dixon, Post, Kuntz, Mirkovitch, Sigwart, Garasic, Edelman, Rogers, Kastrati, Sigwart, Dyet, Watts, Ettles, Schomig, Rogers, Tseng, Edelman, Squire, Gruntzig, Mayler, Hanna,…

MODERATLY LARGE ENGINEERING LITERATURE

- SIMULATIONS USE 3D COMMERCIAL SOFTWARE
- Moore, Timmins, Berry, Dumoulin, Taylor, Bedoya, Schmidt, Behrens, Cochelin, Holzapfel, Gasser, Stadler, Magliavacca, Petrini, Colombo, Auricchio, Hoang, …

HELPED UNDERSTAND MANY STENT PERFORMANCE FEATURES!!!

→ NEED FOR SIMPLIFIED, REDUCED MODELS (MULTI-COMPONENT, NET-BASED MODELS)

MODELING A STENT AS A HYPERBOLIC NET
MAIN IDEAS:

- DIMENSION REDUCTION: approximate the mechanical properties of each 3D slender stent strut by the 1D curved rod model

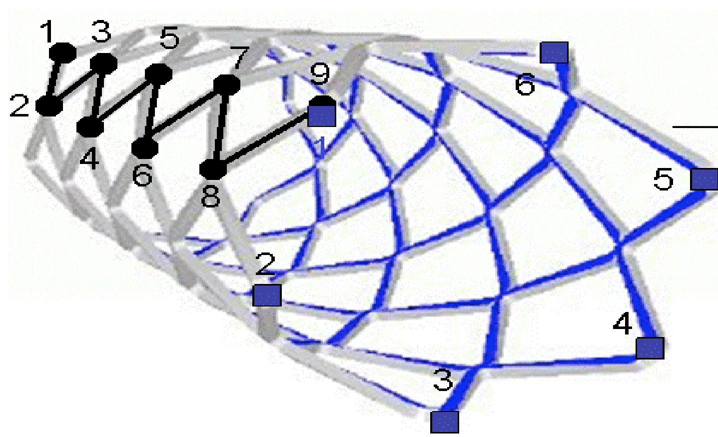

$$U_t + F(U)_x = G(U)$$

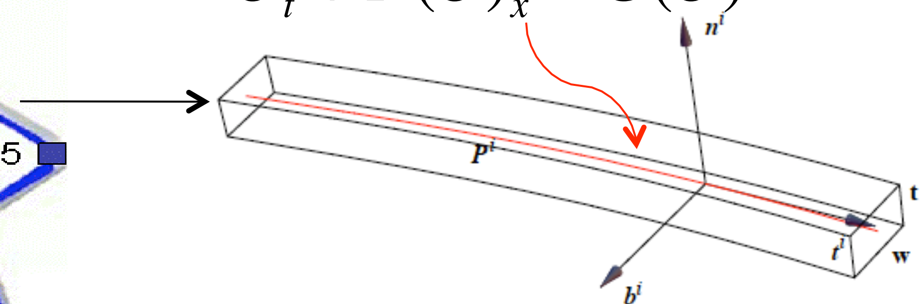

State variable U: captures the location of the middle line, and the rotation of the cross-sections

MAIN IDEAS (CONTINUED):

• GEOMETRY : define how 1D curved rods form a graph in 3D

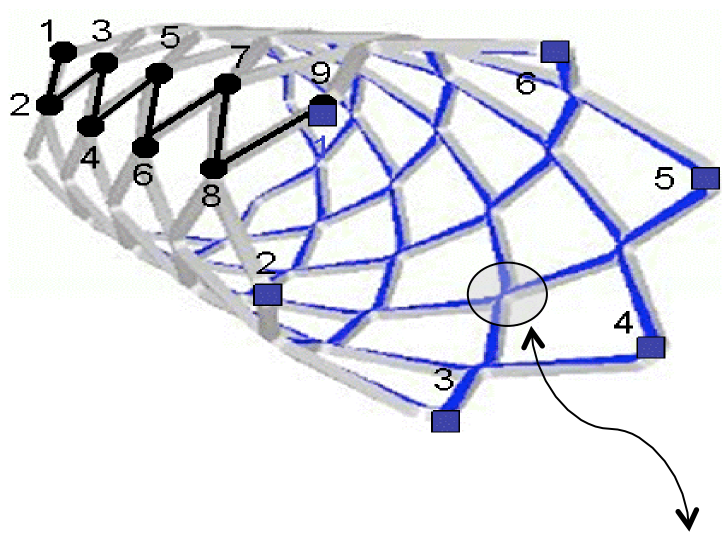

• MECHANICS OF CONTACT: define the contact conditions at graph's vertices defining the physics of contact, i.e., how curved rods (stent struts) meet (interact) at each vertex forming a graph (net) in 3D.

MODELING A STENT AS A HYPERBOLIC NET: SUMMARY

1. GEOMETRY: describing how individual components, such as stent struts, comprise a global net structure, such as stent.

2. PHYSICS: describing the mechanical properties of each individual net component (stent strut)

3. COUPLING CONDITIONS: describing the geometry and mechanics of contact between the net components, thereby forming a hyperbolic net in 3D consisting of 1D components.

STENT AS A HYPERBOLIC NET: DEFINITION OF A NET GEOMETRY

TOPOLOGY:

Net $\mathscr{N} = (\mathscr{V}, \mathscr{E})$: non-directed graph

$\mathscr{V}$ = set of graph vertices

$\mathscr{E}$ = family of non-ordered pairs of vertices (v,w)

(n_E – number of edges)

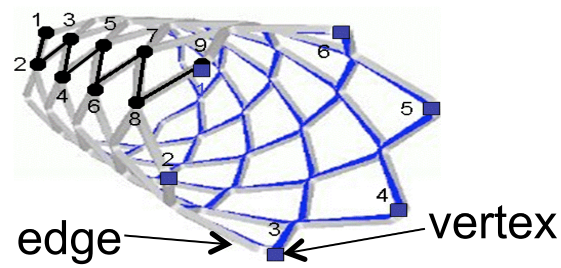

GEOMETRY: defined via:

(1) 1D parameterization P^i of each edge;

e.g., for a straight edge between v and w:

$$\mathbf{P}^i(s) = \mathbf{v} + s(\mathbf{v} - \mathbf{w})/\ell_i$$

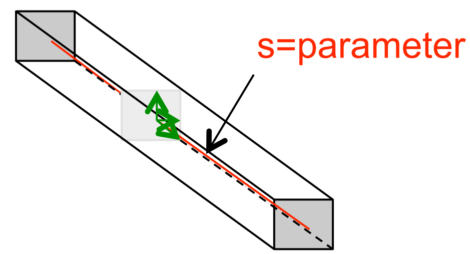

(2) definition of the normal and bi-normal vector functions defined at each point of the 1D net edge

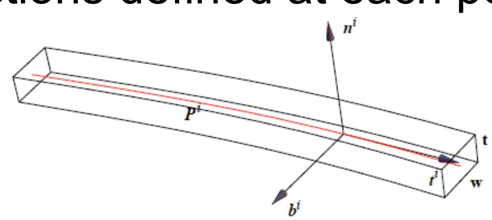

(1) 1D parameterization of each edge of a stent:

Denote by $e^i \in \mathscr{E}$ the i-th edge. The parameterization P^i of e^i is defined via a smooth, injective mapping

$$P^i : [0, \ell^i] \longrightarrow e^i$$

(Here: ℓ^i is the edge length, and P^i is the natural parameterization, i.e., the unit length parameterization)

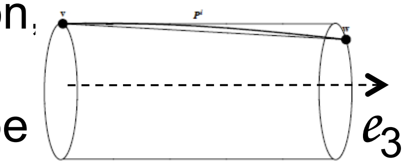

Stent struts lie on a (virtual) cylindrical surface, and so P^is can be defined via a projection onto the cylindrical surface of the straight rods

(2) Definition of the normal and bi-normal vector functions:

n^i, b^i – are smooth functions

$$n^i, b^i : [0, l^i] \to R^3$$

such that $\forall s \in [0, l^i]$ we have $(P^i, n^i, b^i) \in SO(3)$

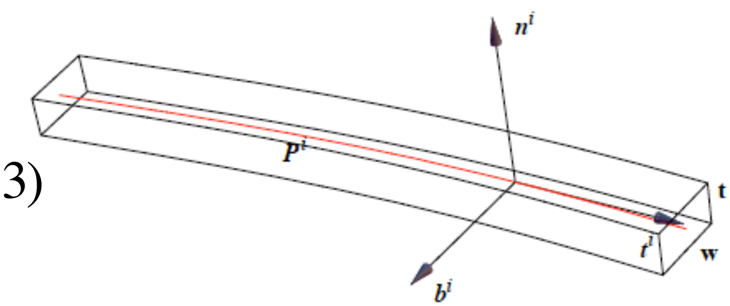

We define:

$$t^i(s_1) = \frac{(\mathbf{P}^i)'(s_1)}{\|(\mathbf{P}^i)'(s_1)\|}, \quad \mathbf{n}^i(s_1) = \frac{(\mathbf{I} - \mathbf{P})\mathbf{P}^i(s_1)}{\|(\mathbf{I} - \mathbf{P})\mathbf{P}^i(s_1)\|}, \quad \mathbf{b}^i(s_1) = t^i(s_1) \times \mathbf{n}^i(s_1),$$

where P is the orthogonal projection with the standard scalar product onto axis of symmetry of the stent cylinder (aligned with e_3)

(1) 1D parameterization of each edge of a stent:

Denote by $e^i \in \mathcal{E}$ the i-th edge. The parameterization P^i of e^i is defined via a smooth, injective mapping

$$P^i : [0, \ell^i] \longrightarrow e^i$$

(Here: ℓ^i is the edge length, and P^i is the natural parameterization, i.e., the unit length parameterization)

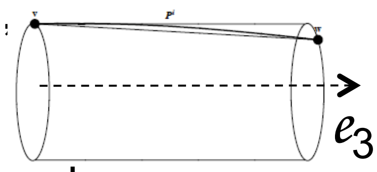

Stent struts lie on a (virtual) cylindrical surface, and so P^is can be defined via a projection onto the cylindrical surface of the straight rods

(2) Definition of the normal and bi-normal vector functions:

THE STENT NET DOMAIN: $\Omega = \bigcup_{i=1}^{n_E} P^i(0, l_i)$

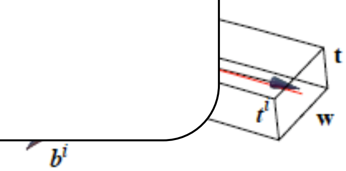

We define:

$$t^i(s_1) = \frac{(\mathbf{P}^i)'(s_1)}{\|(\mathbf{P}^i)'(s_1)\|}, \quad \mathbf{n}^i(s_1) = \frac{(\mathbf{I} - \mathbf{P})\mathbf{P}^i(s_1)}{\|(\mathbf{I} - \mathbf{P})\mathbf{P}^i(s_1)\|}, \quad \mathbf{b}^i(s_1) = t^i(s_1) \times \mathbf{n}^i(s_1),$$

where P is the orthogonal projection with the standard scalar product onto axis of symmetry of the stent cylinder (aligned with e_3)

STENT AS A HYPERBOLIC NET: PHYSICS

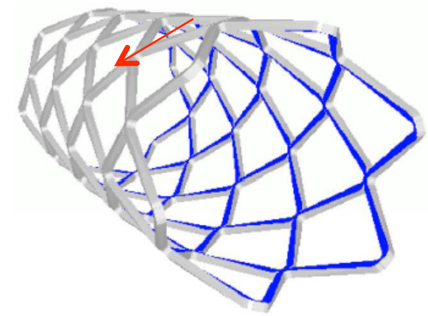

MECHANICAL PROPERTIES OF STENT STRUTS

STENT STRUTS: slender bodies → lower dimensional theories

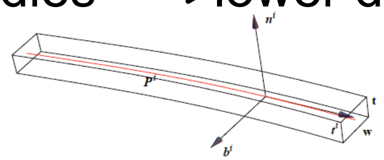

STRUT DEFORMATION: dominant in bi-normal direction

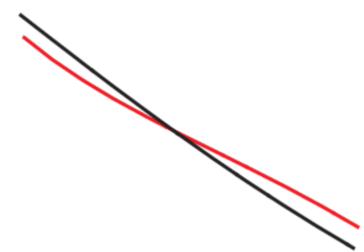

↓

ANTMAN – COSSERAT CURVED ROD MODEL

captures: deformation of the middle line in all 3 spatial directions + rotation of the cross-sections of the curved rod

THE ANTMAN-COSSERAT CURVED ROD MODEL

FOR ONE STENT STRUT (ONE NET EDGE)!

$$\partial_t(\mathbf{g}(\mathbf{U})) = \partial_s(\mathbf{h}(\mathbf{U})) + \mathbf{k}(\mathbf{U}), \quad t > 0, s \in [0, l]$$

HYPERBOLIC BALANCE LAW

STATE VARIABLE: $\mathbf{U} = (\boldsymbol{d}_1, \boldsymbol{d}_2, \boldsymbol{d}_3, \boldsymbol{u}, \boldsymbol{y}, \boldsymbol{\omega}, \boldsymbol{p})$ 21 UNKNOWNS

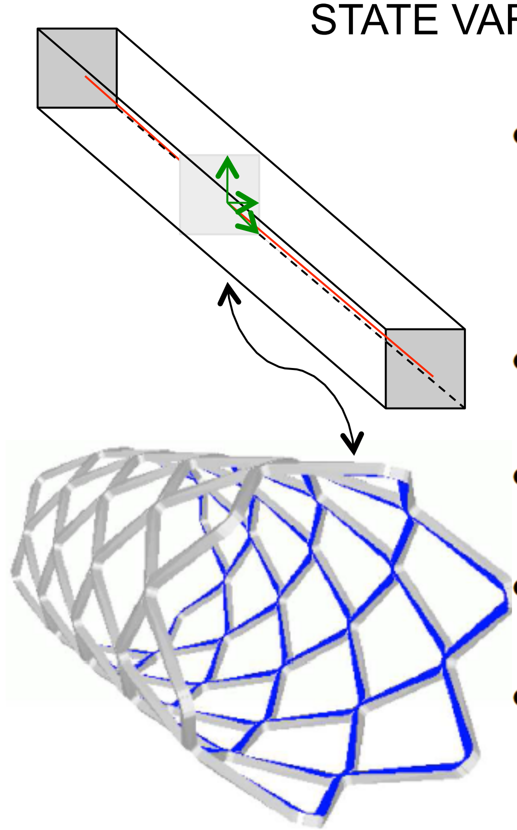

- $(\boldsymbol{d}_1, \boldsymbol{d}_2, \boldsymbol{d}_3)$ is the local coordinate system defined by the **cross-sections** of the curved rod. The cross-sections are spanned by the vector functions $\boldsymbol{d}_1$ and $\boldsymbol{d}_2$, where $\boldsymbol{d}_3 := \boldsymbol{d}_1 \times \boldsymbol{d}_2$. Vectors $\{\boldsymbol{d}_1, \boldsymbol{d}_2, \boldsymbol{d}_3\}$ are orthonormal;
- components u_i of $\boldsymbol{u}$ in the local basis $\{\boldsymbol{d}_i\}$ $(\boldsymbol{u} = \sum_{i=1}^3 u_i \boldsymbol{d}_i)$ measure **flexure** (u_1 and u_2), and **torsion** (u_3);
- components v_i of $\boldsymbol{y} := \partial_s \boldsymbol{r}$ in the local basis $\{\boldsymbol{d}_i\}$ $(\boldsymbol{y} = \sum_{i=1}^3 v_i \boldsymbol{d}_i)$ measure **shear** (v_1 and v_2), and **dilatation** (v_3);
- $\boldsymbol{\omega}$, which is defined via $\partial_t \boldsymbol{d}_i := \boldsymbol{\omega} \times \boldsymbol{d}_i, i = 1, 2, 3$, is associated with **angular velocity** of the cross-sections of the curved rod;
- $\boldsymbol{p} := \partial_t \boldsymbol{r}$ describes the **velocity of the middle line** of the curved rod.

THE ANTMAN-COSSERAT CURVED ROD MODEL

$$\partial_t(\mathbf{g}(\mathbf{U})) = \partial_s(\mathbf{h}(\mathbf{U})) + \mathbf{k}(\mathbf{U}), \quad t > 0, s \in [0, l]$$

HYPERBOLIC BALANCE LAW

STATE VARIABLE: $\mathbf{U} = (\boldsymbol{d}_1, \boldsymbol{d}_2, \boldsymbol{d}_3, \boldsymbol{u}, \boldsymbol{y}, \boldsymbol{\omega}, \boldsymbol{p})$ 21 UNKNOWNS

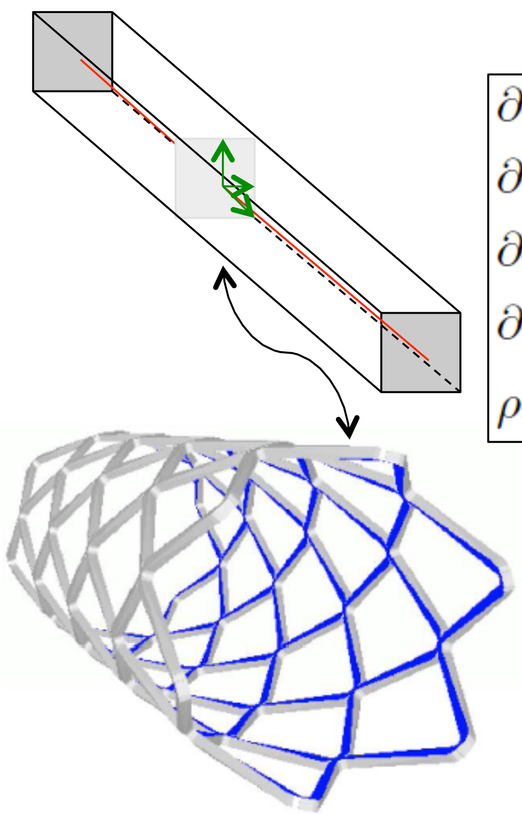

$$\partial_t \boldsymbol{d}_i = \boldsymbol{\omega} \times \boldsymbol{d}_i, \quad i = 1, 2, 3$$

$$\partial_t \boldsymbol{u} = \partial_s \boldsymbol{\omega} - \boldsymbol{u} \times \boldsymbol{\omega},$$

$$\partial_t \boldsymbol{y} = \partial_s \boldsymbol{p},$$

$$\partial_t(\rho \mathbf{D}\mathbf{J}\mathbf{D}^T \boldsymbol{\omega}) = \partial_s \left(\mathbf{D}\mathsf{m}(\mathbf{D}^T \boldsymbol{u}, \mathbf{D}^T \boldsymbol{y}))\right) + \boldsymbol{y} \times \left(\mathbf{D}\mathsf{n}(\mathbf{D}^T \boldsymbol{u}, \mathbf{D}^t \boldsymbol{y})\right) + \boldsymbol{l}$$

$$\rho A \partial_t \boldsymbol{p} = \partial_s \left(\mathbf{D}\mathsf{n}(\mathbf{D}^T \boldsymbol{u}, \mathbf{D}^T \boldsymbol{y})\right) + \boldsymbol{f}.$$

CONSTITUTIVE EQ.
(HYPERELASTIC MATERIAL)

EVOLUTION OF THE CROSS-SECTIONS

COMPATIBILITY AMONG 2ND ORDER DERIVATIVES

$$\boldsymbol{y}_t = \boldsymbol{r}_{st} = \boldsymbol{r}_{ts} = \boldsymbol{p}_s$$

BALANCE OF ANGULAR AND LINEAR MOMENTUM

THE ANTMAN-COSSERAT MODEL

The model is in the form

$$\partial_t(\mathbf{g}(\mathbf{U})) = \partial_s(\mathbf{h}(\mathbf{U})) + \mathbf{k}(\mathbf{U}), \quad t > 0, s \in [0, l]$$

BALANCE LAW

Need to verify if the model is hyperbolic.

Hyperbolic conservation laws have certain common solution properties that can be used to study solutions of hyperbolic net problems.

MATHEMATICAL PROPERTIES OF THE SYSTEM

- 21 X 21 SYSTEM

$$\partial_t \boldsymbol{d}_i = \boldsymbol{\omega} \times \boldsymbol{d}_i, \quad i = 1, 2, 3$$
$$\partial_t \boldsymbol{u} = \partial_s \boldsymbol{\omega} - \boldsymbol{u} \times \boldsymbol{\omega},$$
$$\partial_t \boldsymbol{y} = \partial_s \boldsymbol{p},$$
$$\partial_t(\rho \mathbf{D} \mathbf{J} \mathbf{D}^T \boldsymbol{\omega}) = \partial_s \left(\mathbf{D} \mathsf{m}(\mathbf{D}^T \boldsymbol{u}, \mathbf{D}^T \boldsymbol{y}) \right) + \boldsymbol{y} \times \left(\mathbf{D} \mathsf{n}(\mathbf{D}^T \boldsymbol{u}, \mathbf{D}^t \boldsymbol{y}) \right) + \boldsymbol{l}$$
$$\rho A \partial_t \boldsymbol{p} = \partial_s \left(\mathbf{D} \mathsf{n}(\mathbf{D}^T \boldsymbol{u}, \mathbf{D}^T \boldsymbol{y}) \right) + \boldsymbol{f}.$$

$$u_t = w$$
$$v_t = w_x$$
$$w_t = (f(u)v)_x$$

- HYPERBOLICITY IS ASSOCIATED WITH THE FORM OF CONSTITUTIVE EQS.

$$\nabla(\mathsf{m}, \mathsf{n}) := \begin{bmatrix} \partial \mathsf{m}/\partial \mathsf{u} & \partial \mathsf{m}/\partial \mathsf{v} \\ \partial \mathsf{n}/\partial \mathsf{u} & \partial \mathsf{n}/\partial \mathsf{v} \end{bmatrix}$$

POSITIVE DEFINITE ⇒ HYPERBOLICITY

- EIGENVALUES OF THE JACOBIAN: 9 ARE ZERO, 12 ARE $\pm\sqrt{\mu_i}$, $\mu_i > 0$

Antman*: physically reasonable hyperelastic materials have positive definite $\nabla(\mathsf{m}, \mathsf{n})$

* S.S. Antman "Nonlinear problems of elasticity," Springer 2005.

MATHEMATICAL STRUCTURE IS SIMILAR TO THE NONLINEAR WAVE EQUATION SYSTEM

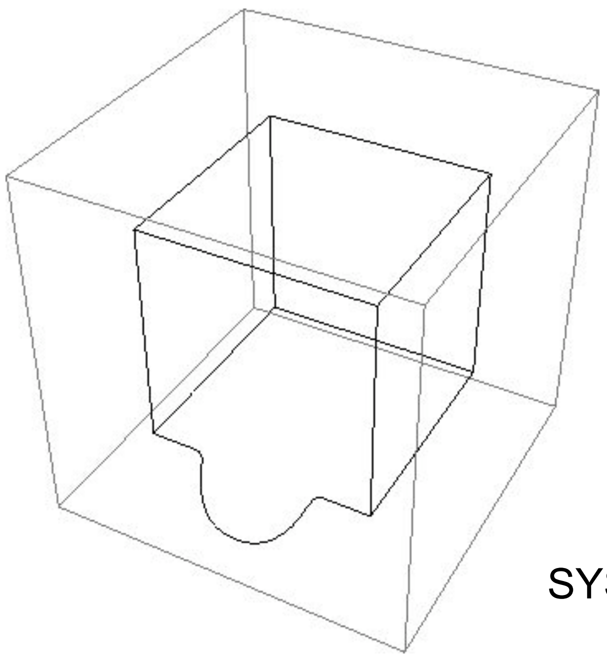

$$u_{tt} = (f(u)u_x)_x, \quad f(u) > 0$$

$$\begin{cases} u_t = w & \text{(no spatial derivative)} \\ v_t = w_x & \text{(compatibility of 2}^{\text{nd}}\text{ order partial deriv.)} \\ w_t = (f(u)v)_x & \text{(balance of forces)} \end{cases}$$

SYSTEM IS OF THE FORM: $\boxed{U_t + F(U)_x = G(U)}$

EIGENVALUE OF THE JACOBIAN F'(U): $\lambda_0 = 0,\ \lambda_{1,2} = \pm\sqrt{f(u)},\ f(u) > 0$

REAL EIGENVALUES: SYSTEM IS HYPERBOLIC

THE COUPLING CONDITIONS AT NET's VERTICES

Two types of coupling conditions are physically reasonable and are consistent with the global weak formulation of the problem:

1. KINEMATIC COUPLING CONDITION: continuity of velocities of middle lines and of cross-sections at each vertex.

2. DYNAMIC COUPLING CONDITION: the sum of all contact forces at each vertex is zero, and the sum of all contact moments at each vertex is zero.

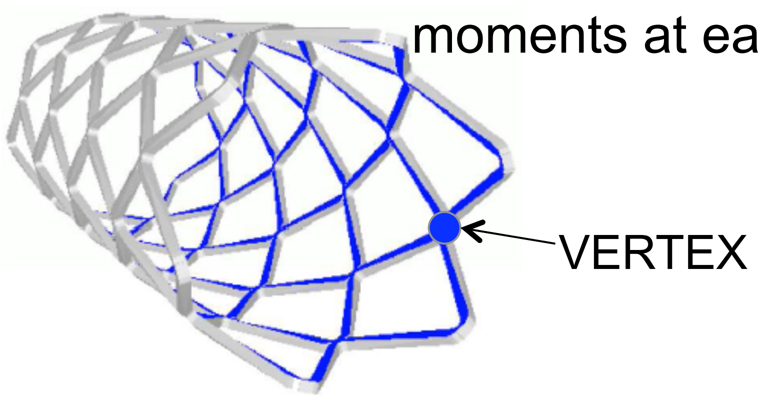

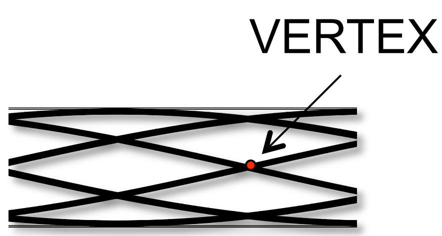

J. Tambaca, I. Velcic, Derivation of the nonlinear bending–torsion model for a junction of elastic rods. Proceedings of the Royal Society of Edinburgh. A: Mathematics. Accepted. (justif. curved rods)
Dominique Blanchard, Georges Griso, Asymptotic behavior of structures made of straight rods. Submitted. (justification; straight rods)

EXAMPLE: THE NONLINEAR WAVE EQUATION

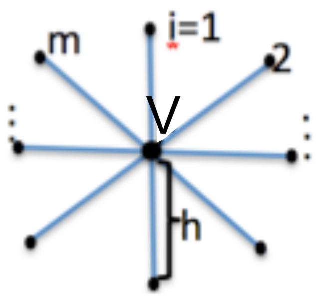

Consider an initial-boundary value problem for the nonlinear wave equation on a simple net consisting of m edges connected at one vertex V:

$$u_{tt} = (f(u)u_x)_x, \quad f(u) > 0$$

$$\left.\begin{aligned} u(x,0) &= u_0(x) \\ u_t(x,0) &= u_1(x) \end{aligned}\right\} \text{ Initial conditions}$$

Boundary conditions at vertices $V_1, \ldots, V_m$

(Recall: u – displacement of a vibrating string, u_t- velocity)

The set of all vertices $\mathscr{V}$ ={V,V_1,…,V_m}. The set of all edges $\mathscr{E}$ ={{V,V_1},…,{V,V_m}}.

Parameterize all the edges so that they “begin” at V, and “end” at V_i:

$$P^i(s) = V + s(V_i - V)/h, \ \ s \in (0,h)$$

CONTACT CONDITIONS AT VERTEX V:

(1) THE KINEMATIC CONTACT CONDITION: $u_1 = \ldots = u_m$

(here u_i is the limiting value of u at vertex V, on e_i)

This also implies: $(u_t)_1 = \ldots = (u_t)_m$ (continuity of velocity at V)

(2) THE DYNAMIC CONTACT CONDITION:

Contact force: $f(u)u_x$

Sum of contact forces = 0 at V: $$\sum_{\substack{edges \\ i=1}}^{n_E} (f(u)u_x)_i = 0$$

WEAK FORMULATION

The problem: $u_{tt} = (f(u)u_x)_x, \;\; \text{on} \;\; e_1$

....

$$u_{tt} = (f(u)u_x)_x, \;\; \text{on} \;\; e_m$$

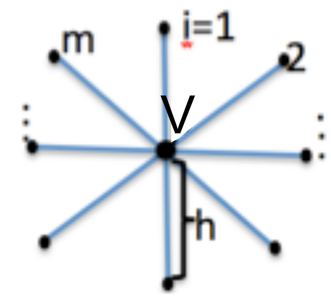

with initial and boundary conditions defined for each e_i.
Recall, the boundary conditions at V are the coupling (contact) conditions.

We multiply each equation by a test function ϕ_i defined on e_i, and then sum over all the edges defining the net domain $\Omega = \bigcup_{i=1}^{n_E} P^i(0,l_i)$, where P^i is a parameterization of the edge e_i :

$$\sum_{i=1}^{n_E} \{u_{tt} - (f(u)u_x)_x\}_i \phi_i = 0$$

Define the test space for the displacement:

$$V = \{\phi = (\phi_1, ..., \phi_m) \ : \ \phi_k \in H^1([0,h]), \underbrace{\phi_1(0) = ... = \phi_m(0)}_{\text{KINEMATIC COUPLING COND.}}\}$$

After the integration by parts:

$$\frac{d^2}{dt^2}\sum_{i=1}^{m}\int_0^h u_i\phi_i dx \ + \ \sum_{i=1}^{m}\int_0^h f(u_i)\partial_x u_i \partial_x \phi_i dx = \sum_{i=1}^{m} f(u_i(h,t))\partial_x u_i(h,t)\phi_i(h)$$
$$- \ \sum_{i=1}^{m} f(u_i(0,t))\partial_x u_i(0,t)\phi_i(0), \qquad \forall \phi = (\phi_1, ..., \phi_m) \in V.$$

Define the test space for the displacement:

$$V = \{\phi = (\phi_1, ..., \phi_m) \ : \ \phi_k \in H^1([0,h]), \underbrace{\phi_1(0) = ... = \phi_m(0)}_{\text{KINEMATIC COUPLING COND.}}\}$$

After the integration by parts:

$$\frac{d^2}{dt^2}\sum_{i=1}^{m}\int_0^h u_i\phi_i dx \ + \ \sum_{i=1}^{m}\int_0^h f(u_i)\partial_x u_i \partial_x \phi_i dx = \sum_{i=1}^{m} f(u_i(h,t))\partial_x u_i(h,t)\phi_i(h)$$
$$- \sum_{i=1}^{m} f(u_i(0,t))\partial_x u_i(0,t)\phi_i(0), \qquad \forall \phi = (\phi_1, ..., \phi_m) \in V.$$

Kinematic coupling condition embedded in the test space implies that all $\phi_i(0)$ have the same value (at V)

Define the test space for the displacement:

$$V = \{\phi = (\phi_1, ..., \phi_m) \; : \; \phi_k \in H^1([0,h]), \underbrace{\phi_1(0) = ... = \phi_m(0)}_{\text{KINEMATIC COUPLING COND.}}\}$$

After the integration by parts:

$$\frac{d^2}{dt^2}\sum_{i=1}^{m}\int_0^h u_i\phi_i dx \; + \; \sum_{i=1}^{m}\int_0^h f(u_i)\partial_x u_i \partial_x \phi_i dx = \sum_{i=1}^{m} f(u_i(h,t))\partial_x u_i(h,t)\phi_i(h)$$

$$- \underbrace{\sum_{i=1}^{m} f(u_i(0,t))\partial_x u_i(0,t)}_{=0}\phi_i(0), \qquad \forall \phi = (\phi_1, ..., \phi_m) \in V.$$

DYNAMIC COUPLING CONDITION

Kinematic coupling condition embedded in the test space implies that all $\phi_i(0)$ have the same value (at V)

Define the test space for the displacement:

$$V = \{\phi = (\phi_1, ..., \phi_m) \ : \ \phi_k \in H^1([0,h]), \underbrace{\phi_1(0) = ... = \phi_m(0)}_{\text{KINEMATIC COUPLING COND.}}\}$$

After the integration by parts:

Boundry conditions at outer vertices.

$$\frac{d^2}{dt^2}\sum_{i=1}^{m}\int_0^h u_i\phi_i dx + \sum_{i=1}^{m}\int_0^h f(u_i)\partial_x u_i \partial_x \phi_i dx = \sum_{i=1}^{m} f(u_i(h,t))\partial_x u_i(h,t)\phi_i(h)$$
$$- \underbrace{\sum_{i=1}^{m} f(u_i(0,t))\partial_x u_i(0,t)}_{=0}\phi_i(0), \qquad \forall \phi = (\phi_1, ..., \phi_m) \in V.$$

DYNAMIC COUPLING CONDITION

Kinematic coupling condition embedded in the test space implies that all $\phi_i(0)$ have the same value (at V)

WEAK FORMULATION

$$\frac{d^2}{dt^2}\sum_{i=1}^{m}\int_0^h u_i\phi_i dx \;+\; \sum_{i=1}^{m}\int_0^h f(u_i)\partial_x u_i \partial_x \phi_i dx = \sum_{i=1}^{m} f(u_i(h,t))\partial_x u_i(h,t)\phi_i(h)$$

$$\forall \phi = (\phi_1, ..., \phi_m) \in V.$$

supplemented with the initial conditions

WEAK FORMULATION

$$\frac{d^2}{dt^2}\sum_{i=1}^{m}\int_0^h u_i\phi_i dx \;+\; \sum_{i=1}^{m}\int_0^h f(u_i)\partial_x u_i \partial_x \phi_i dx = \sum_{i=1}^{m} f(u_i(h,t))\partial_x u_i(h,t)\phi_i(h)$$

$$\forall \phi = (\phi_1, ..., \phi_m) \in V.$$

supplemented with the initial conditions

This formulation is particularly suitable for a FEM approximation of the net problem.

with J. Tambaca

WAVE PROPAGATION IN A 3D NET
MODELED BY THE NONLINEAR WAVE EQUATION

$u_{tt}=(f(u)u_x)_x$

$f(u)=0.5+u^2$

$u_t= w$
$v_t = w_x$
$w_t= (f(u)v)_x$

<u>Numerical simulation</u>:
FEM (with P1)

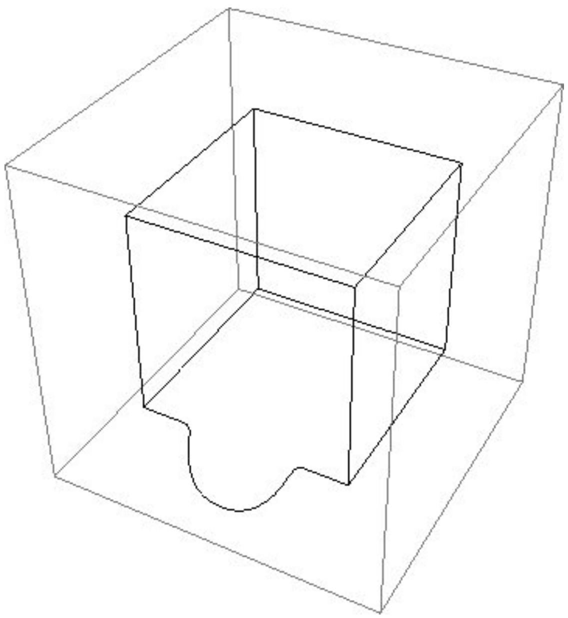

initial condition

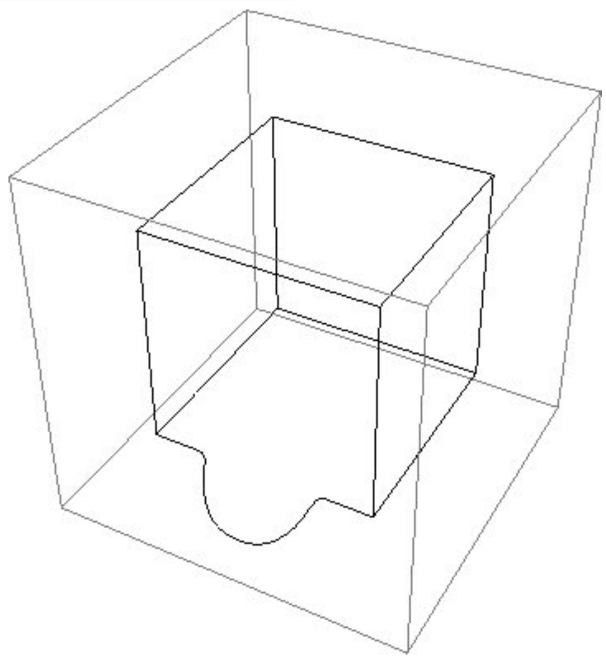

slow motion

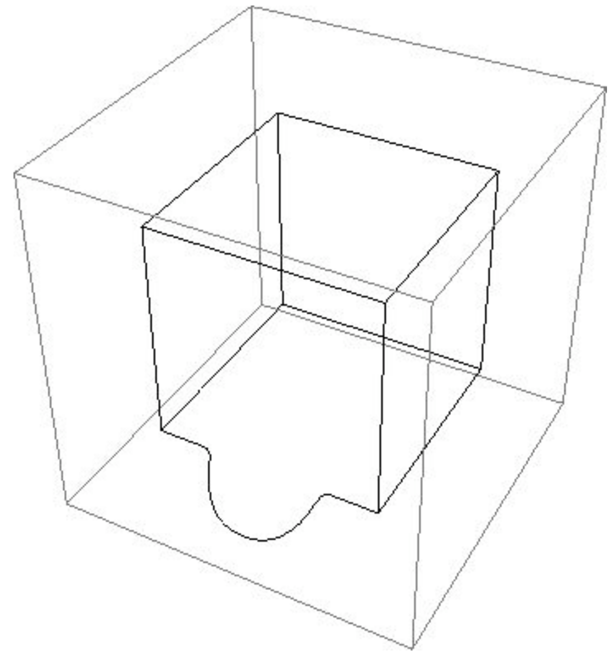

fast motion

WAVE INTERACTIONS AT VERTICES FORM A MOVING BOUNDARY PROBLEM

FINDING SMOOTH SOLUTION USING THE METHOD OF CHARACTERISTICS

The linear wave equation: $u_{tt} = (f(x)u_x)_x, \quad f(x) > 0, \quad x \in \mathbb{R}, t > 0$

Change of variables: $u_t = w, \quad u_x = v,$ obtain first-order system:

$$\begin{aligned} v_t &= w_x, \\ w_t &= (f(x)v)_x \end{aligned}$$

System in quasilinear form:

$$\begin{pmatrix} v \\ w \end{pmatrix}_t = \underbrace{\begin{pmatrix} 0 & 1 \\ f(x) & 0 \end{pmatrix}}_{\text{Jacobian of the flux function}} \begin{pmatrix} v \\ w \end{pmatrix}_x + \begin{pmatrix} 0 \\ f'(x)v \end{pmatrix}$$

Eigenvalues of the Jacobian: $\lambda_{1,2} = \pm\sqrt{f(x)}$

We have 2 families of characteristics:

$$\frac{dx_1}{dt} = \lambda_1 = -\sqrt{f(x)}, \quad \frac{dx_2}{dt} = \lambda_2 = \sqrt{f(x)}$$

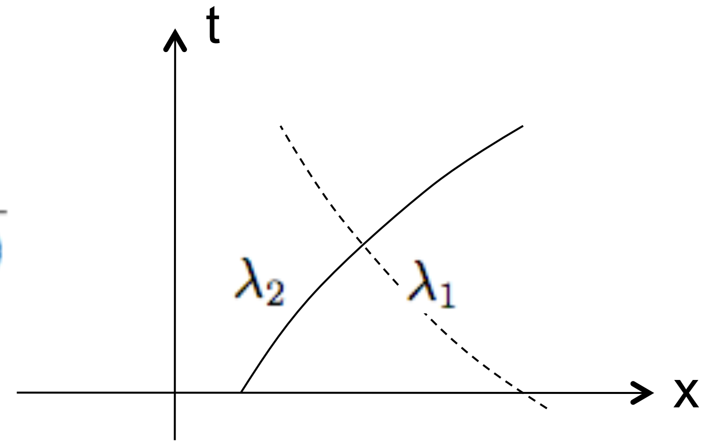

Eigenvectors of the Jacobian matrix:

$$r_1 = \begin{pmatrix} 1 \\ \lambda_1 \end{pmatrix} = \begin{pmatrix} 1 \\ -\sqrt{f(x)} \end{pmatrix}$$

$$r_2 = \begin{pmatrix} 1 \\ \lambda_2 \end{pmatrix} = \begin{pmatrix} 1 \\ \sqrt{f(x)} \end{pmatrix}$$

$$l_1 = \begin{pmatrix} -\lambda_2 \\ 1 \end{pmatrix} = \begin{pmatrix} \sqrt{f(x)} \\ 1 \end{pmatrix}, \quad l_1 \cdot r_2 = 0$$

$$l_2 = \begin{pmatrix} -\lambda_1 \\ 1 \end{pmatrix} = \begin{pmatrix} \sqrt{f(x)} \\ 1 \end{pmatrix}, \quad l_2 \cdot r_1 = 0$$

To study (smooth) solutions, we can use Riemann Invariants, or Characteristic Variables (generalizes to nonlinear 2x2 problems).

Main Idea: Diagonalize the system and find which combination of the unknown functions satisfies an ODE along the characteristics.

Start from
$$u_t + AU_x = F$$

Multiply by a left eigenvector:
$$l_i^T U_t + l_i^T A \, l_i \, l_i^T U_x = l_i F, \quad i = 1, 2.$$

Obtain the diagonal system:
$$l_i^T U_t + \lambda_i l_i^T U_x = l_i F, \quad i = 1, 2.$$

OR:
$$l_1^T U_t + \lambda_1 l_1^T U_x = l_1^T F,$$
$$l_2^T U_t + \lambda_2 l_2^T U_x = l_2^T F.$$

Define:
$$(w_i)_t = l_i^T U_t$$
$$(w_i)_x = l_i^T U_x$$

For a constant-coeff. system we have:
$$(w_i)_t = l_i^T U_t = (l_i^T U)_t,$$
$$(w_i)_x = l_i^T U_x = (l_i^T U)_x.$$

Functions w_i satisfy:

$$(w_1)_t + \lambda_1 (w_1)_x = l_1^T F,$$
$$(w_2)_t + \lambda_2 (w_2)_x = l_2^T F$$

Thus, w_i satisfies an ODE:

$$\frac{dw_i}{dt} = l_i^T F \text{ along } \frac{dx_i}{dt} = \lambda_i.$$

Functions w_i are called RIEMANN INVARIANTS (CHARACTERISTIC VARIABLES).

For the linear wave equation:

$$w_1 = \sqrt{f(x)}v + w,$$
$$w_2 = -\sqrt{f(x)}v + w,$$

When f(x) = 1:

$$w_1 = v + w,$$
$$w_2 = -v + w$$

and w_i is constant along $\frac{dx_i}{dt} = \lambda_i$

We can recover smooth solutions:

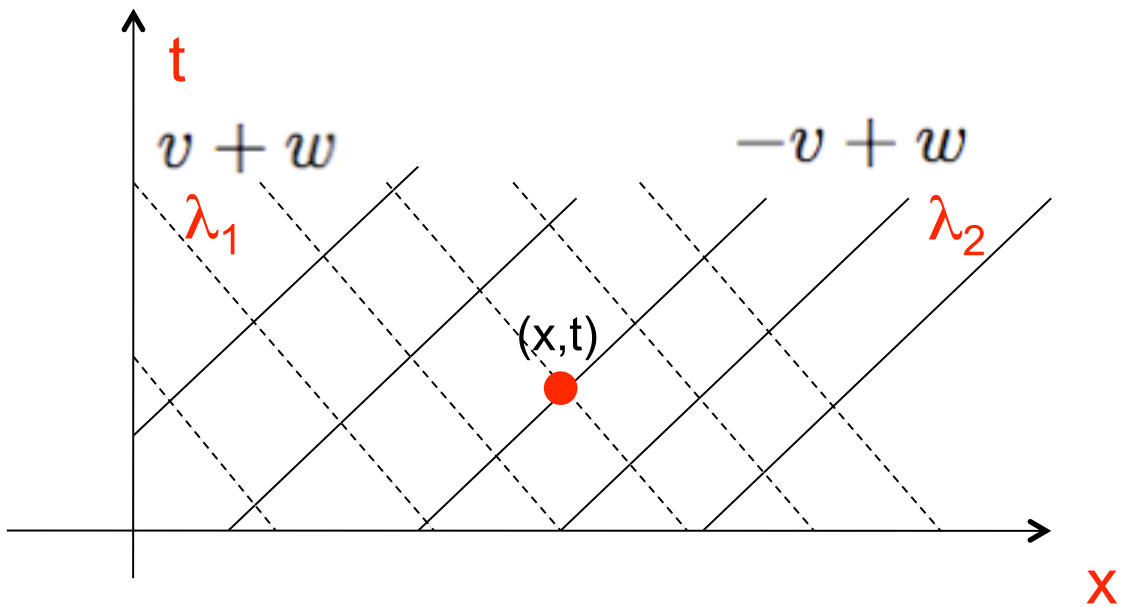

$$\begin{cases} (-v+w)(x,t) = (-v_0+w_0)(x-t) \\ (v+w)(x,t) = (v_0+w_0)(x+t) \end{cases}$$

Suppose:
w_0 is 0

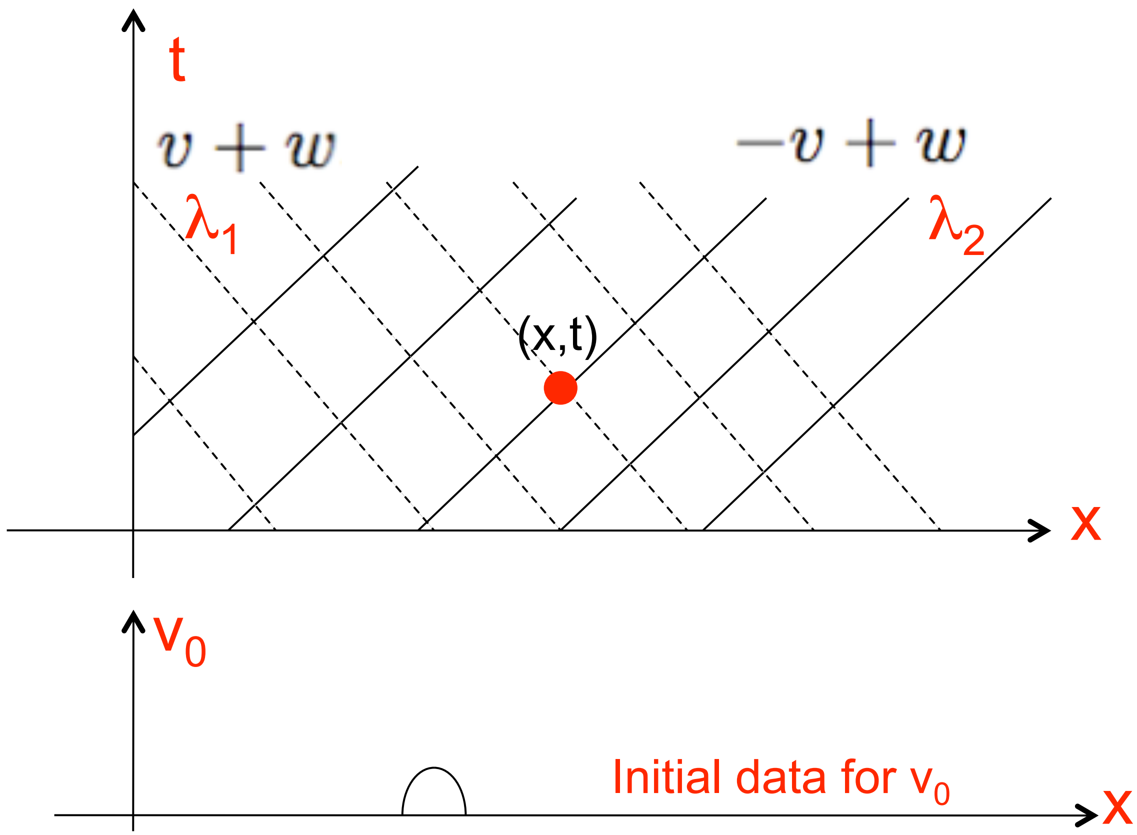

$$\begin{cases} (-v+w)(x,t) = (-v_0+w_0)(x-t) \\ (v+w)(x,t) = (v_0+w_0)(x+t) \end{cases}$$

Suppose:
w_0 is 0

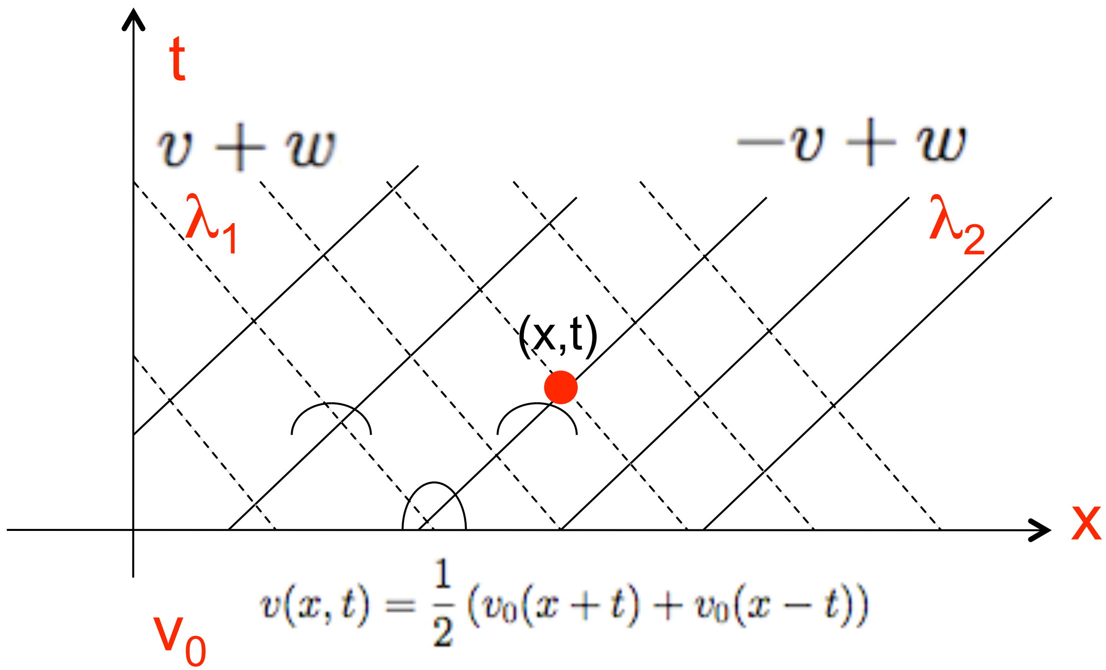

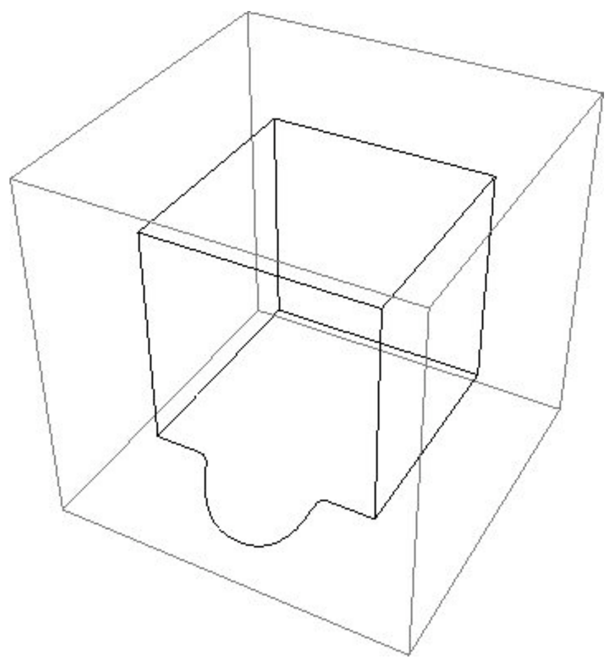

INTERACTION OF WAVES WITH VERTICES

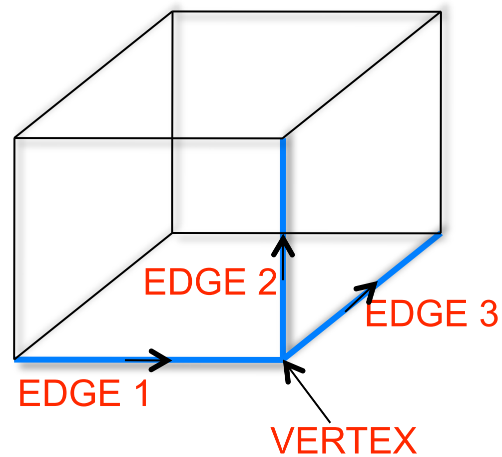

NEED TO BE ABLE TO RECOVER 6 UNKNOWNS: $v^1, v^2, v^3, w^1, w^2, w^3$

We have 3 equations from the coupling conditions:

1. Continuity of velocity: $w^1 = w^2$

   $w^1 = w^3$

2. Balance of forces: $v^1 = v^2 + v^3$

NEED 3 MORE CONDITIONS TO HAVE A WELL-DEFINED PROBLEM!

INTERACTION OF WAVES WITH VERTICES

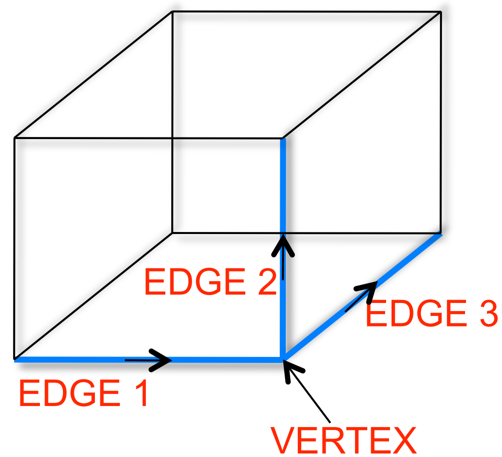

NEED TO BE ABLE TO RECOVER 6 UNKNOWNS: $v^1, v^2, v^3, w^1, w^2, w^3$

We have 3 equations from the coupling conditions:

1. Continuity of velocity: $w^1 = w^2$
   $w^1 = w^3$

2. Balance of forces: $v^1 = v^2 + v^3$

NEED INFORMATION FROM PDE ABOUT THE WAVES COMING TO THE VERTEX.

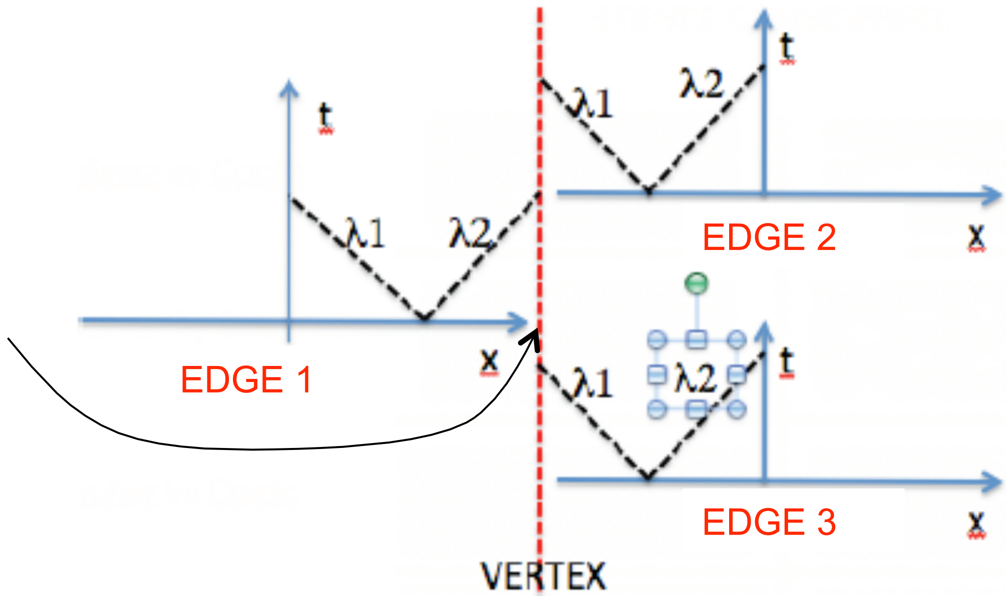

Use Riemann Invariants along the characteristic approaching the vertex.

$$-v^1 + w^1 = C^1$$
$$v^2 + w^2 = C^2$$
$$v^3 + w^3 = C^3.$$

Obtain a system of 6 equations in 6 unknowns:

$$
\begin{aligned}
w^1 &= w^2 \\
w^1 &= w^3 \\
v^1 &= v^2 + v^3 \\
-v^1 + w^1 &= C^1 \\
v^2 + w^2 &= C^2 \\
v^3 + w^3 &= C^3.
\end{aligned}
$$

→

$$
\begin{aligned}
w^1 = w^2 = w^3 &= 1/3(C_1 + C_2 + C_3) \\
v^2 &= -1/3C_1 - +2/3C_2 - 1/3C_3 \\
v^3 &= -1/3C_1 - 1/3C_2 + 2/3C_3 \\
v^1 &= -2/3C_1 + 1/3C_2 + 1/3C_3.
\end{aligned}
$$

(double check the signs ☺)

Nonlinear 2x2 problems with smooth solutions can be “solved” using Riemann Invariants.

Riemann Invariants do not exist for general nxn systems. Also, when shocks develop, even in 2x2 systems, Riemann Invariants cannot be used.

There is no general theory about how to construct the solutions at vertices.
One suggestion (Piccoli et al.) is to solve all possible Riemann problems at each vertex, and chose the values of the solution at the vertex so that the RP solutions only contain the waves traveling to the interior of the edge (avoids loss of information).

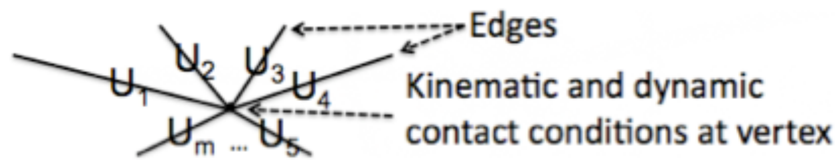

This approach leads to a nonlinear problem at each vertex that is not necessarily well-posed, especially for large systems, and is not easily solved numerically even when there exists a unique solution!

Our suggestion:

WEAK FORMULATION

$$\frac{d^2}{dt^2}\sum_{i=1}^{m}\int_0^h u_i\phi_i dx \;+\; \sum_{i=1}^{m}\int_0^h f(u_i)\partial_x u_i \partial_x \phi_i dx = \sum_{i=1}^{m} f(u_i(h,t))\partial_x u_i(h,t)\phi_i(h)$$

$$\forall \phi = (\phi_1, ..., \phi_m) \in V.$$

supplemented with the initial conditions

- incorporates one coupling condition in the solution space
- enforces the other coupling condition in the weak sense
- this approach incorporates, at the same time, both the coupling condition and the information from the PDE simultaneously

STENT AS A HYPERBOLIC NET

Used similar ideas for the stent problem, formulated in the weak form similar to the nonlinear wave system.

CONTACT CONDITIONS:

1. **CONT. OF VEL.**
2. **BALANCE OF FORCES AND MOMENTS**

(at vertices)

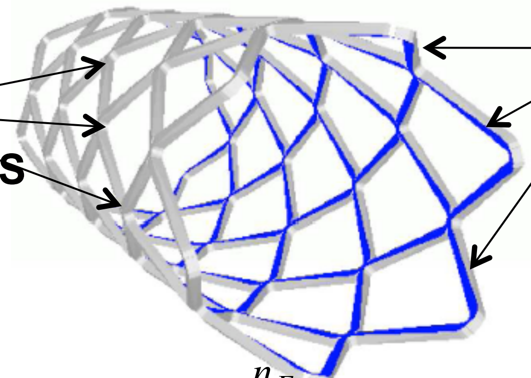

ANTMAN-COSSERAT MODEL

(on edges/stent struts)

$$\Omega = \bigcup_{i=1}^{n_E} P^i(0,l_i)$$

P^i – parameterization of edges of $\mathscr{N} = (\mathscr{V}, \mathscr{E})$

Problem (example): STENT RESPONSE TO UNIFORM PRESSURE LOAD

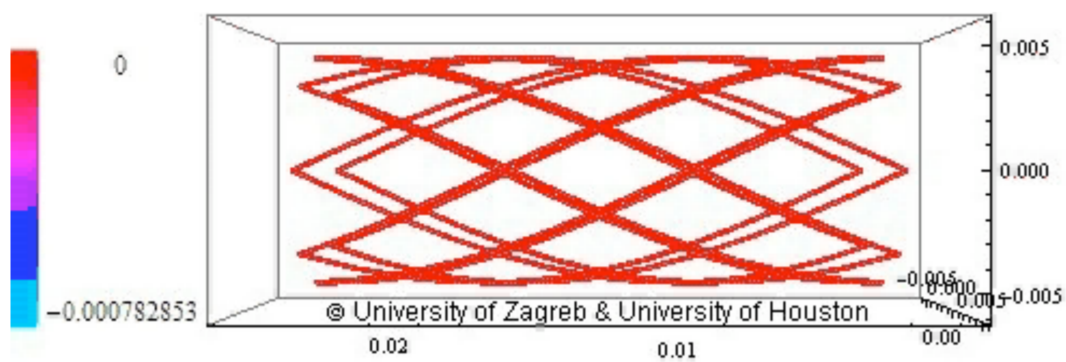

COMPARISON WITH FULL 3D SIMULATIONS

- STATIC PROBLEM
- LINEARIZED ANTMAN-COSSERAT MODEL: small deformation of an already expanded stent
- 3D SIMULATION: FreeFem++, P2 elements; computational mesh h=1/10,…1/60.
- 1D SIMULATION: in-house FEM code in C++

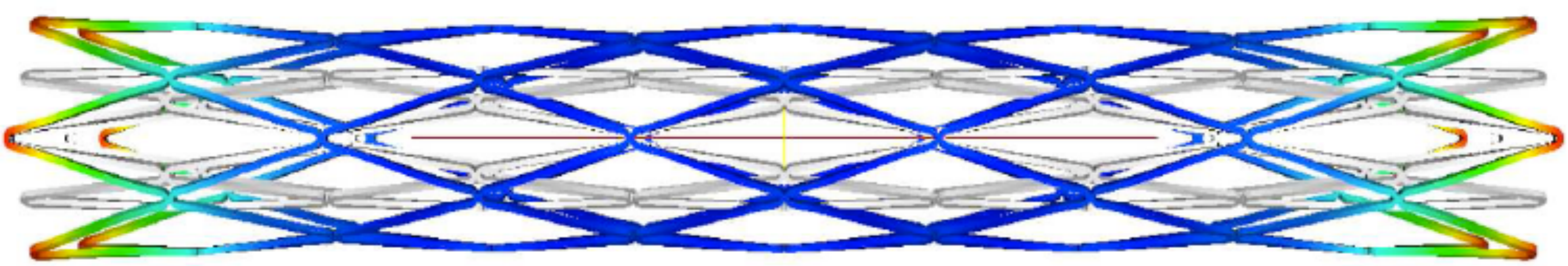

COMPARISON WITH FULL 3D SIMULATIONS

1D SIMULATION

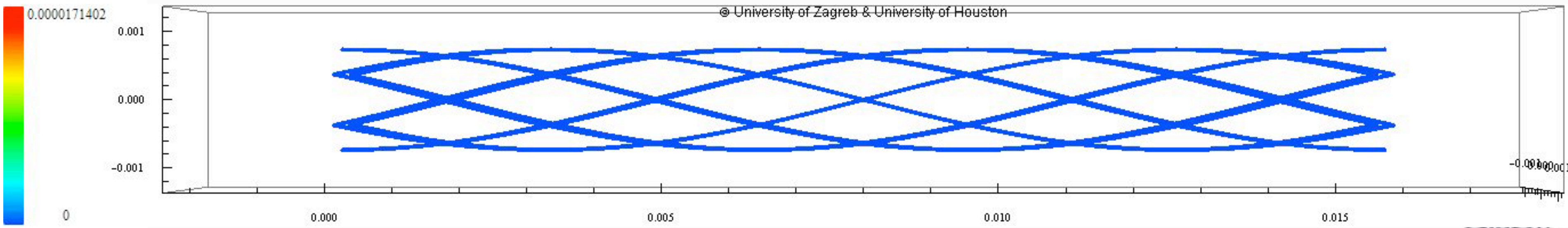

30x displacement magnification

3D SIMULATION

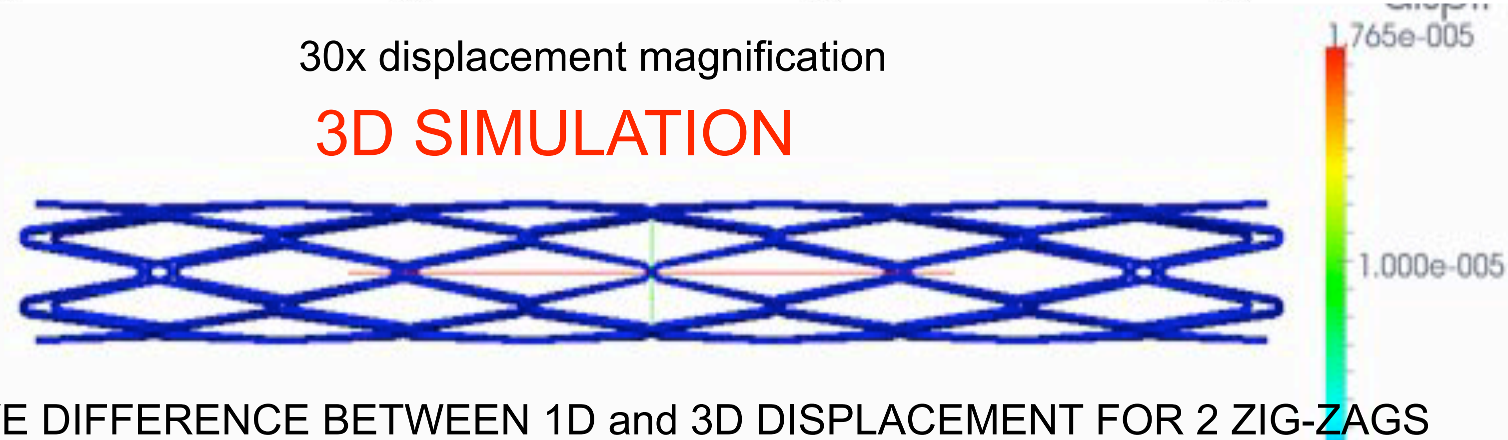

QUANTITATIVE DIFFERENCE BETWEEN 1D and 3D DISPLACEMENT FOR 2 ZIG-ZAGS

3D simulations converge with mesh refinement to 1D solution with #3D nodes: 211337 v.s. #1D nodes: 474 for 2.7% diff.

THE REDUCED MODEL PROVIDES:

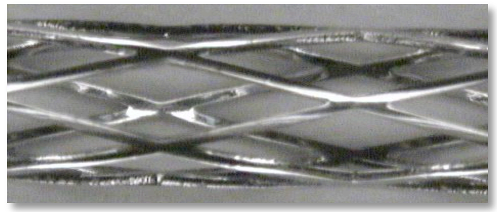

- SIGNIFICANT COMPUTATIONAL SAVINGS

- INCREASED ACURACY in DISPLACEMENT CALCULATIONS

- EFFECTIVE PRESSURE-DISPLACEMENT RELATIONSHIP FROM LEADING-ORDER ENERGY FORMULATION
  (IMPORTANT for NUMERICAL FLUID-STRUCTURE INTERACT. STUDIES)

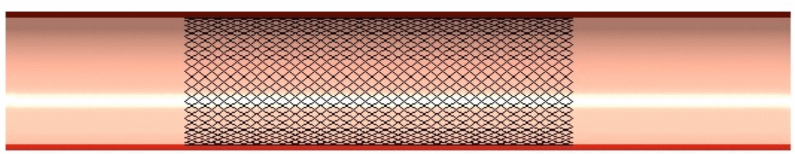

J. Tambaca, M. Kosor, S. Canic and D. Paniagua. Mathematical Modeling of Endovascular Stents. *SIAM J Applied Mathematics* 70 (6), 1922–1952, 2010.

•CORONARY STENT RESPONSE TO COMPRESSION AND TO BENDING (DEFORMATION OF STENTS IN THEIR EXPANDED STATE)

STENTS CONSIDERED:

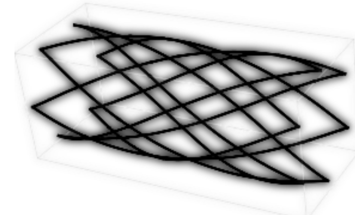

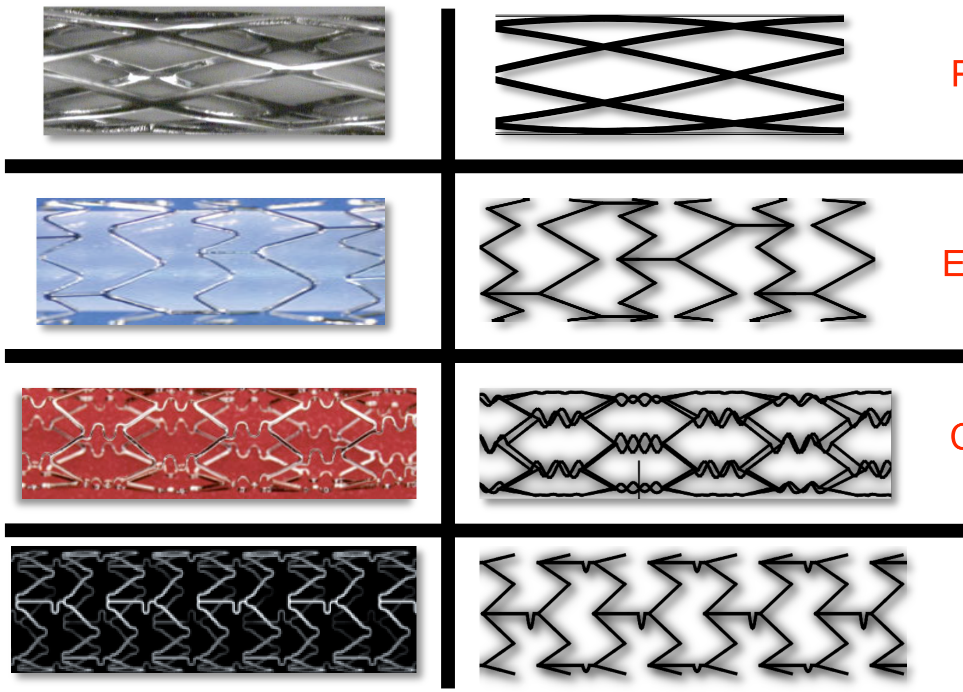

Palmaz by Cordis — Palmaz-like stent mesh

Express by Boston Sci. — Express-like stent mesh

Cypher by Cordis — Cypher-like stent mesh

Xience by Abbott — Xience-like stent mesh

•USING THIS APPROACH: HELPED IN OPTIMAL DESIGN OF STENT FOR TRANSCATHETER AORTIC VALVE REPLACEMENT (with Private Consortium in Houston)

Movie Gallery of Coronary Stents Exposed to Compression and Bending

Compression | **Bending**

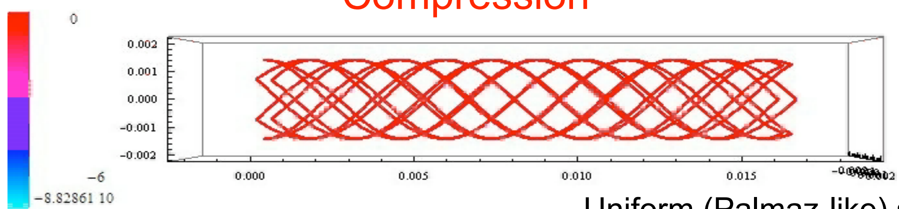
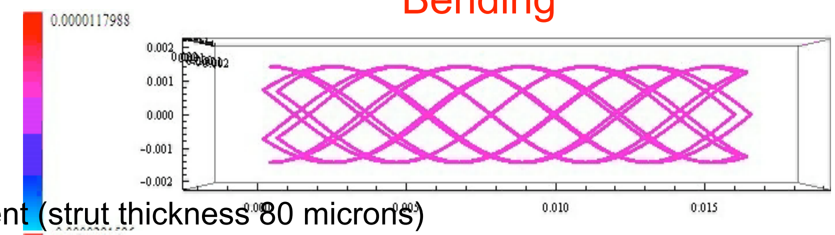

Uniform (Palmaz-like) stent (strut thickness 80 microns)

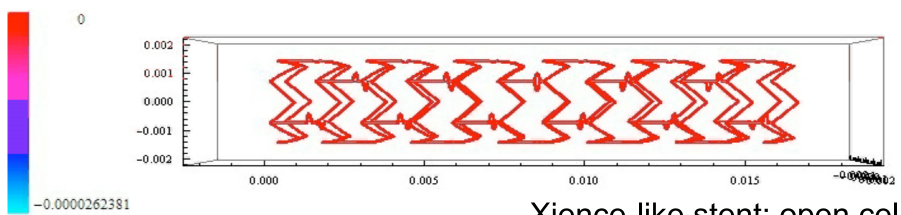
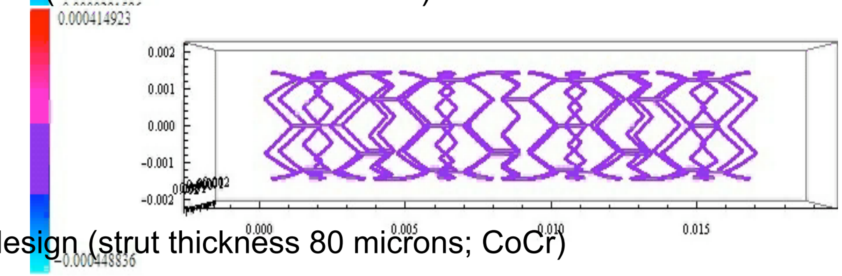

Xience-like stent; open cell design (strut thickness 80 microns; CoCr)

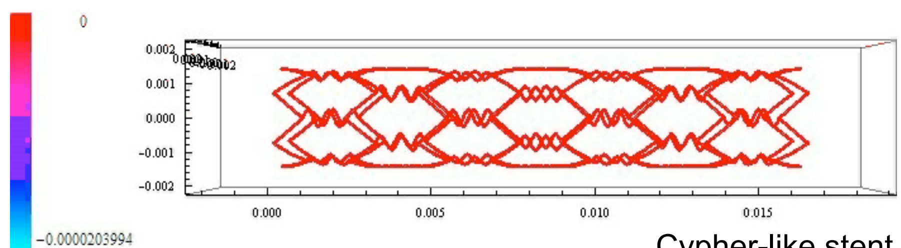
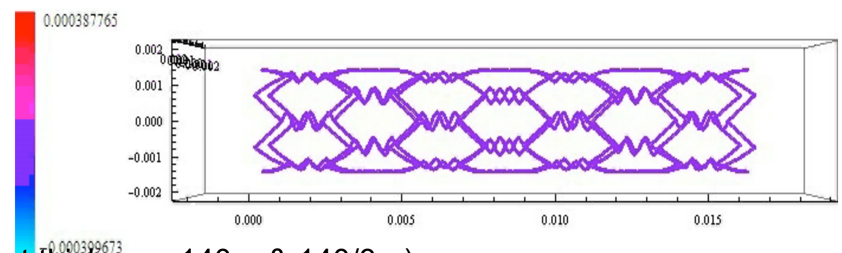

Cypher-like stent (strut thickness 140 μ & 140/3 μ)

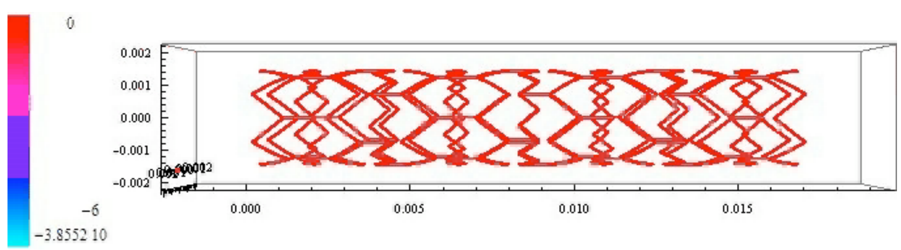
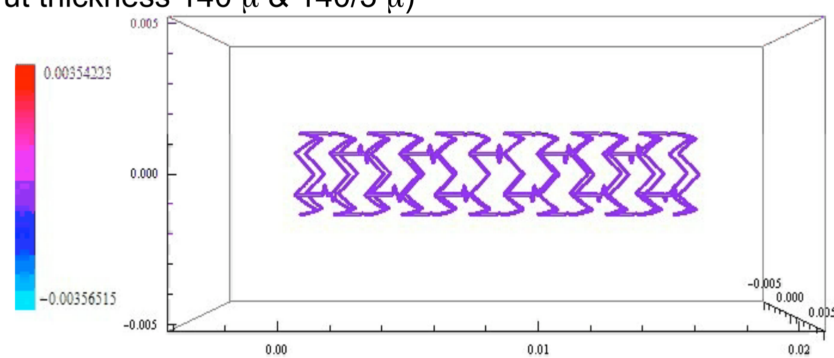

Express-like stent; open cell design (strut thickness 132 μ)

CONCLUSIONS

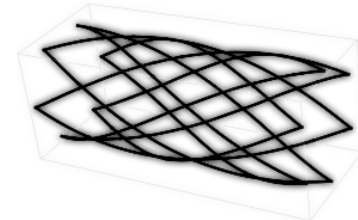

•Palmaz-like stent is by far the hardest stent with respect to both compression and bending (should not be clinically applied in tortuous geometries [*])

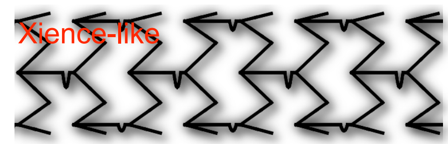

• open-cell design provides more flexibility to bending (important since longitudinal straightening effect of rigid stent has been clinically associated with increased incidence of major adverse cardiovascular events [*])

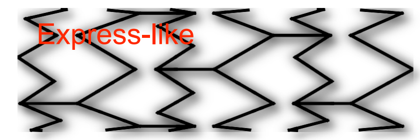

• Express-like stent has high flexibility (bending) while keeping high radial strength (radial displacement: 0.24%) (important to avoid buckling of bent stents)

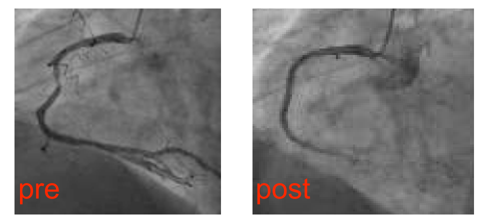

• Xience-like stent has the smallest longitudinal extension under cyclic loading ("in phase" circumferential rings; not "opposing") (clinically important when landing a stent in an "angle" area formed by a native artery)

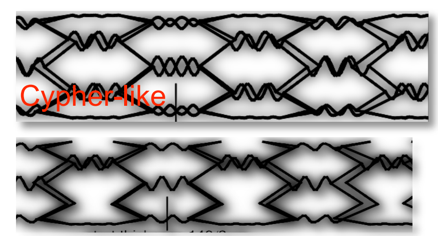

• New design: more flexibility than Express with higher radial strength: Cypher-like stent with open-cell design

Computer-generated Cypher-like stent with open cell design

*Gyongyosi et al. Longitudinal straightening effect of stents is an additional predictor for major adverse cardiac events. J American College of Cardiology 35 (2000)

References:

J. Tambaca, M. Kosor, S. Canic and D. Paniagua. Mathematical Modeling of Endovascular Stents. *SIAM J Applied Mathematics* 70 (6), 1922–1952, 2010.

S. Canic and J. Tambaca. Cardiovascular Stents as PDE Nets: 1D vs. 3D. *IMA J Appl. Math.* Conditionally accepted 2011.

J. Tambaca, S. Canic and D. Paniagua. A Novel Approach to Modeling Coronary Stents Using a Slender Curved Rod Model: A Comparison Between Fractured Xience-like and Palmaz-like Stents. *Applied and Numerical PDEs* (eds. W. Fitzgibbon, Yu. Kuznetsov, P. Neittaanmaki, J. Periaux and O. Pironneau), Springer, 41-58, 2010.

J. Tambaca, S. Canic, D. Paniagua, and D. Fish. Mechanical Behavior of Fully Expanded Commercially Available Endovascular Coronary Stents in the US. *Texas Heart Institute Journal.* Accepted 2011.

S. S. Antman. *Nonlinear Problems of Elasticity.* Springer, New York, 2005.

E. Cosserat and F. Cosserat. Theorie des corps deformable, Hermann, Paris 1909.

J. Tambaca, I Velcic. Derivation of the nonlinear bending–torsion model for a junction of elastic rods. *Proceedings of the Royal Society of Edinburgh, Section: A Mathematics* In print 2011.

ARTERIAL BLOOD FLOW NETWORKS

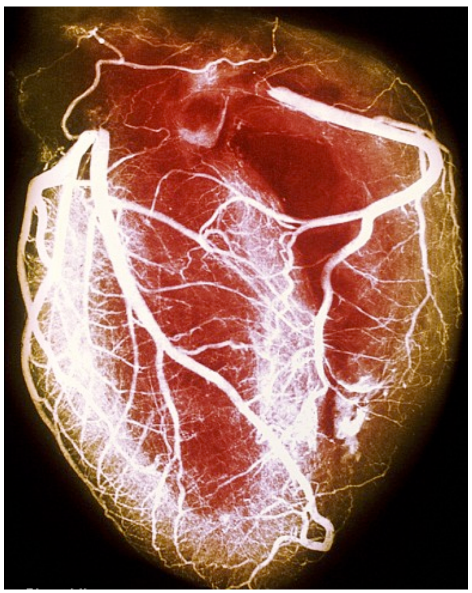

network of coronary arteries

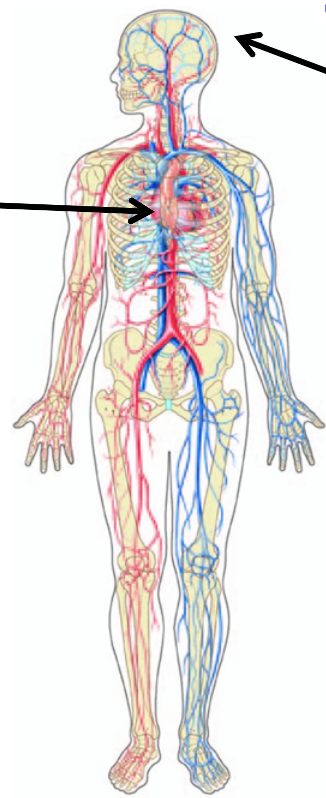

human cardiovascular
network (principal arteries)

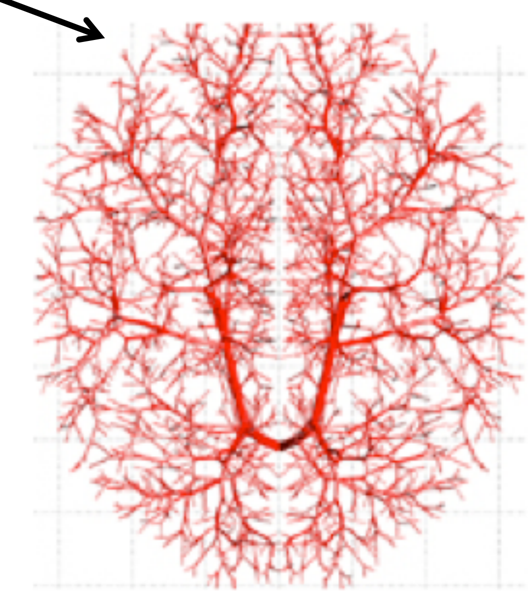

cerebral arterial network

• THE COMPLEXITY OF THE HUMAN CARDIOVASCULAR SYSTEM RENDERS THE NUMERICAL SIMULATION OF THE ENTIRE CARDIOVASCULAR SYSTEM USING FULL 3D FSI MODELS COMPUTATIONALLY PROHIBITIVE

• MULTI-SCALE APPROACHES HAVE BEEN DEVELOPED THAT COUPLE 3D SIMULATIONS OF SMALLER SEGMENTS WITH 1D SIMULATIONS OF LARGER (NETWORK) SEGMENTS (Quarteroni et al., Veneziani et al.)

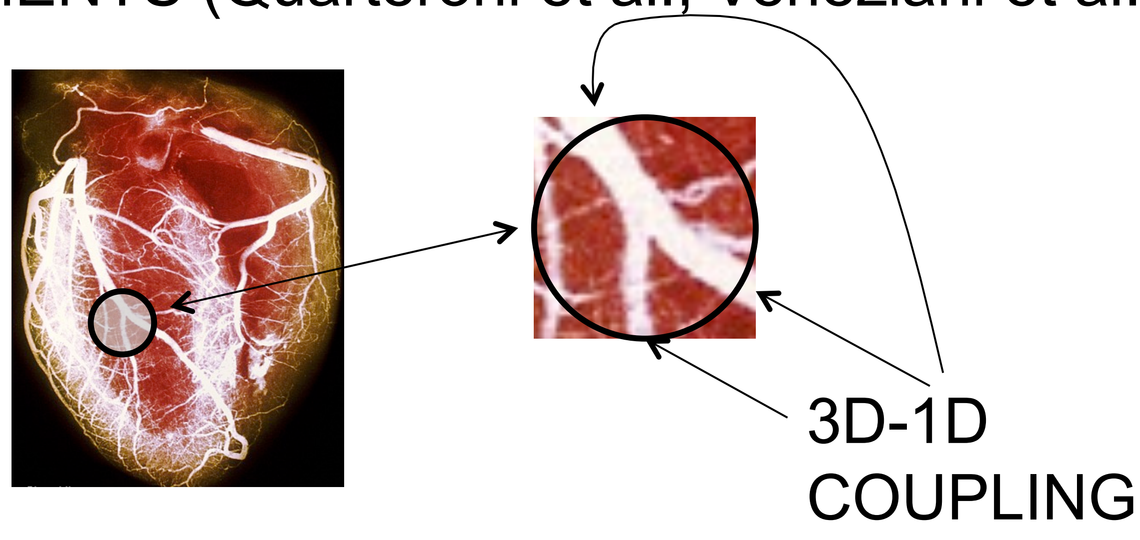

REDUCED 1D-BASED NETWORK MODELS

- CAN MODEL “BOUNDARY CONDITIONS” FOR 3D SIMULATIONS

- CAPTURES THE FLOW OF A VISCOUS, INCOMPRESSIBLE FLUID IN A **STRAIGHT** VESSEL WITH **SMALL ASPECT RATIO** (axial velocity dominant; details to follow)

- CAPTURES THE PRESSUE AND ARTERIAL WAVE PROPAGATION IN THE VASCULAR NETWORK
(e.g., study of blood pressure in elderly upon standing up
Olufsen et al.)

BASICS FOR THE 1D BLOOD FLOW MODEL IN ONE COMPLIANT, CYLINDRICAL ARTERY

Domain:

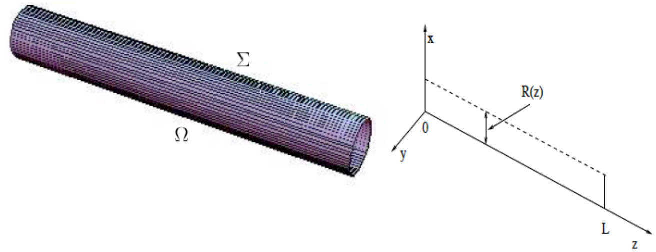

Reference cylinder:

$$\Omega = \left\{ x = (r\cos\theta, r\sin\theta, z) \in \mathbb{R}^3 : r \in (0, R(z)), \theta \in (0, 2\pi), z \in (0, L) \right\}$$

Lateral boundary:

$$\Sigma = \left\{ x = (R(z)\cos\theta, R(z)\sin\theta, z) \in \mathbb{R}^3 : \theta \in (0, 2\pi), z \in (0, L) \right\}$$

Deformed cylinder:

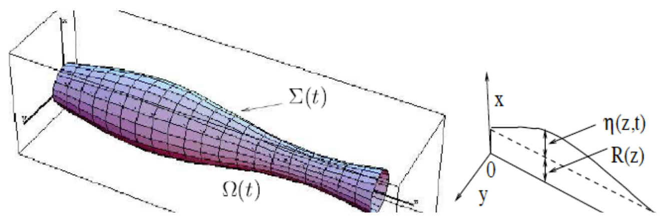

$$\Omega(t) = \{ (r\cos\theta, r\sin\theta, z) \in \mathbb{R}^3 : r \in (0, R(z) + \eta(t,z)), \theta \in (0, 2\pi), z \in (0, L) \}$$

Lateral boundary:

$$\Sigma(t) = \{ ((R(z) + \eta(t,z))\cos\theta, (R(z) + \eta(t,z))\sin\theta, z) \in \mathbb{R}^3 : \theta \in (0, 2\pi), z \in (0, L) \}$$

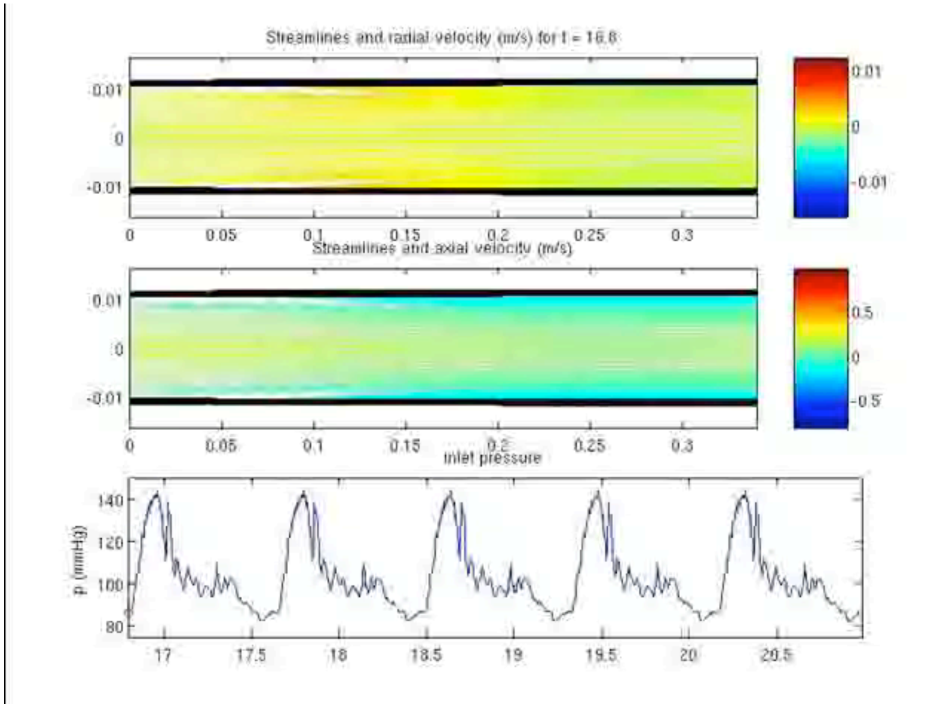

Streamlines and radial velocity (m/s) for t = 16.8
0.01
0
-0.01
0
0.05
0.1
0.15
0.2
0.25
0.3
Streamlines and axial velocity (m/s)
0.5
-0.5
inlet pressure
p (mmHg)
140
120
100
80
17
17.5
18
18.5
19
19.5
20
20.5

Basic assumptions (full model):

- medium-to-large arteries: blood can be modeled as a viscous, incompressible, Newtonian fluid
- models for vessel wall dynamics: elastic/viscoelastic
- only radial displacement will be taken into account
- small displacement, and small displ. gradient: linear elasticity/viscoelasticity

Basic assumptions (dimension reduction: reduced model):

- long and narrow (slender) domain (artery): i.e., small aspect ratio $\varepsilon = R/L$;
- axially symmetric flow
- constant or slowly varying vessel radius

FULL FLUID-STRUCTURE INTERACTION MODEL IN CYLINDRICAL COORDINATES

FLUID: Navier-Stokes equations for an incompressible, viscous, Newtonian fluid

$$\rho_F\left(\frac{\partial v_r}{\partial t}+v_r\frac{\partial v_r}{\partial r}+v_z\frac{\partial v_r}{\partial z}\right)+\frac{\partial p}{\partial r} = \mu\left(\frac{\partial^2 v_r}{\partial r^2}+\frac{\partial^2 v_r}{\partial z^2}+\frac{1}{r}\frac{\partial v_r}{\partial r}-\frac{v_r}{r^2}\right)$$

Balance of radial momentum

$$\rho_F\left(\frac{\partial v_z}{\partial t}+v_r\frac{\partial v_z}{\partial r}+v_z\frac{\partial v_z}{\partial z}\right)+\frac{\partial p}{\partial z} = \mu\left(\frac{\partial^2 v_z}{\partial r^2}+\frac{\partial^2 v_z}{\partial z^2}+\frac{1}{r}\frac{\partial v_z}{\partial r}\right)$$

Balance of axial momentum

$$\frac{\partial v_r}{\partial r}+\frac{\partial v_z}{\partial z}+\frac{v_r}{r} = 0.$$

Conservation of mass (incompressibility cond)

STRUCTURE: homogeneous, isotropic, linearly viscoelastic membrane (Kelvin-Voigt viscosity), displacing in radial direction only

$$f_r = h\rho_w\frac{\partial^2\eta}{\partial t^2}+\frac{Eh}{1-\sigma^2}\frac{1}{R^2}\eta+p_{\mathrm{ref}}\frac{\eta}{R}+\frac{hC_v}{R^2}\frac{\partial\eta}{\partial t}$$

2nd Newton's Law of Motion (balance of forces)

FULL FLUID-STRUCTURE INTERACTION MODEL IN CYLINDRICAL COORDINATES

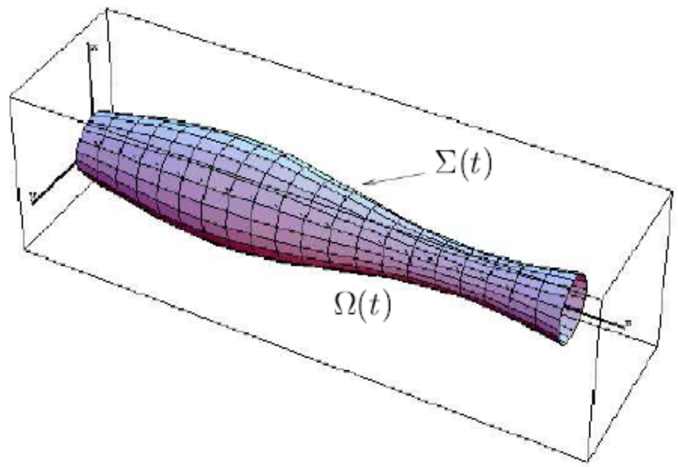

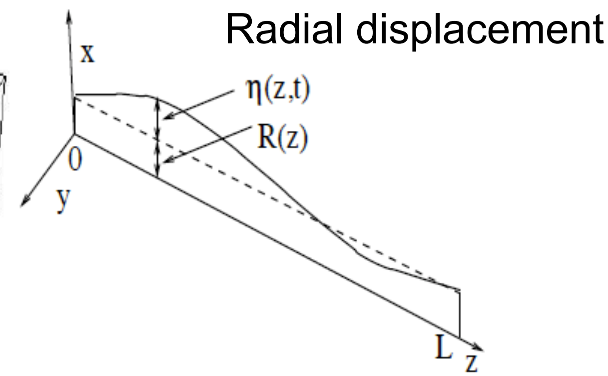

Outside force

Membrane acceleration

Linear elasticity

Pre-stress

Viscoelasticity

STRUCTURE: homogeneous, isotropic, linearly viscoelastic membrane (Kelvin-Voigt elasticity), displacing in radial direction only

$$f_r = h\rho_w \frac{\partial^2 \eta}{\partial t^2} + \frac{Eh}{1-\sigma^2}\frac{1}{R^2}\eta + p_{\mathrm{ref}}\frac{\eta}{R} + \frac{hC_v}{R^2}\frac{\partial \eta}{\partial t}$$

2nd Newton's Law of Motion (balance of forces)

COUPLING BETWEEN THE FLUID AND STRUCTURE

- THE KINEMATIC CONDITION: continuity of velocity at the fluid-structure interface Σ(t) (no slip)

$$v_r(R+\eta(z,t),z,t) = \frac{\partial \eta(z,t)}{\partial t}, \quad v_z(R+\eta(z,t),z,t) = 0$$

- THE DYNAMIC CONDITION: balance of contact forces at the fluid-structure interface Σ(t)

$$f_r = [(p - p_{\text{ref}})\mathbf{I} - 2\mu D(\boldsymbol{v})]\,\boldsymbol{n} \cdot \boldsymbol{e}_r \left(1 + \frac{\eta}{R}\right) \sqrt{1 + (\partial_z \eta)^2}$$

COUPLING BETWEEN THE FLUID AND STRUCTURE

- THE KINEMATIC CONDITION: continuity of velocity at the fluid-structure interface $\Sigma(t)$ (no slip)

$$v_r(R+\eta(z,t),z,t) = \frac{\partial \eta(z,t)}{\partial t}, \quad v_z(R+\eta(z,t),z,t) = 0$$

- THE DYNAMIC CONDITION: balance of contact forces at the fluid-structure interface $\Sigma(t)$

$$f_r = [(p - p_{\text{ref}})\mathbf{I} - 2\mu D(\boldsymbol{v})]\, \boldsymbol{n} \cdot \boldsymbol{e}_r \left(1 + \frac{\eta}{R}\right) \sqrt{1 + (\partial_z \eta)^2}$$

Normal component of fluid stress Jacobian of the Eulerian-Lagrangian tranf.

MEMBRANE CONTACT FORCE FLUID CONTACT FORCE

$$f_r = h\rho_w \frac{\partial^2 \eta}{\partial t^2} + \frac{Eh}{1-\sigma^2}\frac{1}{R^2}\eta + p_{\text{ref}}\frac{\eta}{R} + \frac{hC_v}{R^2}\frac{\partial \eta}{\partial t}$$

BENCHMARK PROBLEM IN FSI in BLOOD FLOW

LATERAL BOUNDARY CONDITION: COUPLING BETWEEN FLUID AND STRUCTURE:

1. CONTINUITY OF VELOCITY (NO-SLIP)
2. BALANCE OF CONTACT FORCE

INLET BOUNDARY CONDITION

$p + \rho_F v_z^2/2 = P_0(t) + p_{\mathrm{ref}}$

(dynamic pressure)

(normal stress)

η - given

$\mathrm{v}_r = 0$

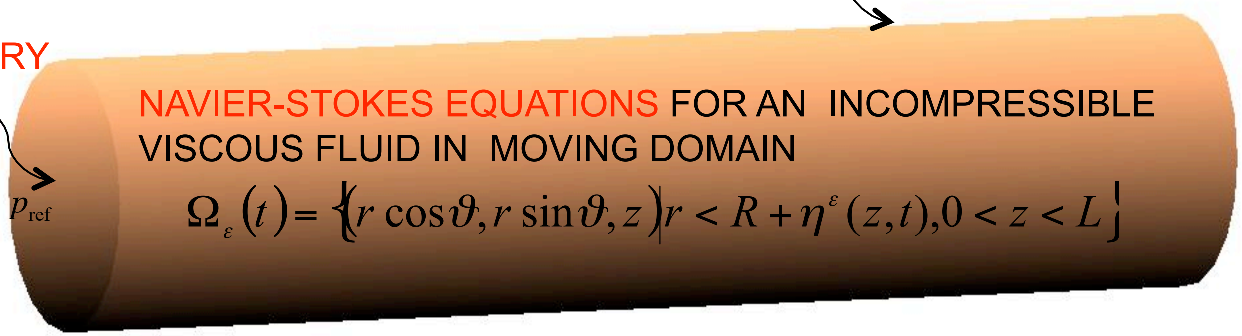

NAVIER-STOKES EQUATIONS FOR AN INCOMPRESSIBLE VISCOUS FLUID IN MOVING DOMAIN

$$\Omega_\varepsilon(t) = \{(r\cos\vartheta, r\sin\vartheta, z) \,|\, r < R + \eta^\varepsilon(z,t), 0 < z < L\}$$

OUTLET BOUNDARY CONDITION

$p + \rho_F v_z^2/2 = P_1(t) + p_{\mathrm{ref}}$

(dynamic pressure)

(normal stress)

η - given

$\mathrm{v}_r = 0$

INITIAL CONDITIONS $\eta^\varepsilon = \dfrac{\partial \eta^\varepsilon}{\partial t} = 0, \ \mathrm{v} = 0$

DIMENSION REDUCTION: REDUCED MODELS

1. Introduce non-dimensional variables
2. Derive model in non-dimensional form
3. Use the fact that R/L =: ε is small
4. "Average" the equations across the "slender" direction (dimension reduction; problems with closure)
5. Write a hierarchy of equations in terms of $\varepsilon^0, \varepsilon^1, \varepsilon^2, ..$
6. Ignore the terms of order ε^2 and smaller
7. Derive the reduced equations that approximate the full problem to ε^2 accuracy
8. Prove that as ε goes to 0, the full model "converges" to the reduced model (error estimates)

THE NON-DIMENSIONAL PROBLEM

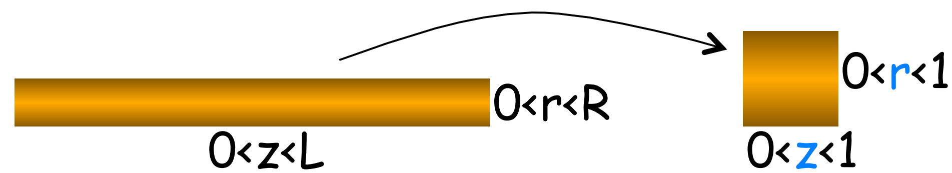

THE NON-DIMENSIONAL VARIABLES:

- the independent variables $r = R\tilde{r}, \quad z = L\tilde{z}, \quad t = \frac{1}{\omega}\tilde{t}$
- the dependent variables $\boldsymbol{v} = V\tilde{\boldsymbol{v}},\ \eta = \Xi\tilde{\eta}$ and $p = \rho_F V^2 \tilde{p}$

ASYMPTOTIC EXPANSIONS:

$$\begin{aligned} \boldsymbol{v} &= V\left\{\tilde{\boldsymbol{v}}^0 + \varepsilon\tilde{\boldsymbol{v}}^1 + \cdots\right\} \\ \eta &= \Xi\left\{\tilde{\eta}^0 + \varepsilon\tilde{\eta}^1 + \cdots\right\} \\ p &= \rho_F V^2\left\{\tilde{p}^0 + \varepsilon\tilde{p}^1 + \cdots\right\} \end{aligned}$$

Plug into the Navier-Stokes equations and ignore the terms of order ε^2 or smaller.

Energy estimates imply:

$$\omega = \frac{1}{L}\sqrt{\frac{1}{\rho_F}\left(\frac{hE}{R(1-\sigma^2)} + p_{\text{ref}}\right)} \qquad 2V = \frac{\mathcal{P}}{\sqrt{\rho_F}}\left(\frac{hE}{R(1-\sigma^2)} + p_{\text{ref}}\right)^{-\frac{1}{2}} \qquad 2\Xi = \mathcal{P}R\left(\frac{hE}{R(1-\sigma^2)} + p_{\text{ref}}\right)^{-1}$$

ENERGY

$$\frac{\rho}{2}\frac{d}{dt}\int_{\Omega(t)}|v|^2 dx + \frac{\pi R}{2}\rho_s h \frac{d}{dt}\int_0^L \left|\frac{\partial \eta}{\partial t}\right|^2 dz + \frac{d}{dt}E(t) + V_s(t) + V_f(t) = W_{in}(t) - W_{out}(t).$$

where

$$E(t) = \frac{\pi R}{2}\int_0^L C_0|\eta| + C_1\left|\frac{\partial \eta}{\partial z}\right|^2 + C_2\left|\frac{\partial^2 \eta}{\partial z^2}\right|^2 dz, \quad V_s(t) = \pi R\int_0^L D_0\left|\frac{\partial \eta}{\partial t}\right|^2 + D_1\left|\frac{\partial^2 \eta}{\partial t \partial z}\right|^2 + D_2\left|\frac{\partial^3 \eta}{\partial t \partial z^2}\right|^2 dz, \quad V_f(t) = 2\mu\|D(v)\|^2_{L^2(\Omega(t))},$$

$$W_{in}(t) = \int_0^R P_1(t) v_z|_{z=0}\, r dr, \quad W_{out}(t) = \int_0^R P_2(t) v_z|_{z=L}\, r dr.$$

A PRIORI ESTIMATES (when inertial forces dominate viscous forces)

$$\frac{1}{L}\|\eta^\varepsilon(t)\|^2_{L^2} \le 4R^2\frac{R^2(1-\sigma^2)^2}{h^2E^2}\frac{1}{B^2}P^2$$

$$\frac{1}{\pi R^2 L}\|u^\varepsilon(t)\|^2_{L^2} \le \frac{4}{\rho}\frac{R(1-\sigma^2)}{hE}\frac{1}{B}P^2$$

→

$$\frac{1}{L}\|\eta^\varepsilon(t)\|_{L^2(0,L)} \le 0.0012$$

10% of R

THE ε^2 APPROX. OF THE NAVIER-STOKES EQs IN NON-DIMENSIONAL FORM

$$\begin{aligned} \mathrm{Sh}\frac{\partial \tilde{v}_z}{\partial \tilde{t}} + \tilde{v}_z\frac{\partial \tilde{v}_z}{\partial \tilde{z}} + \tilde{v}_r\frac{\partial \tilde{v}_z}{\partial \tilde{r}} + \frac{\partial \tilde{p}}{\partial \tilde{z}} &= \frac{1}{\mathrm{Re}}\left\{\frac{1}{\tilde{r}}\frac{\partial}{\partial \tilde{r}}\left(\tilde{r}\frac{\partial \tilde{v}_z}{\partial \tilde{r}}\right)\right\}, \\ \frac{\partial}{\partial \tilde{r}}(\tilde{r}\tilde{v}_r) + \frac{\partial}{\partial \tilde{z}}(\tilde{r}\tilde{v}_z) &= 0, \\ \frac{\partial \tilde{p}}{\partial \tilde{r}} &= 0. \end{aligned}$$

Here $\boxed{\tilde{v}_r := \tilde{v}_r^1 + \varepsilon\tilde{v}_r^2}$ so that $v_r^\varepsilon = \varepsilon V\left(\tilde{v}_r + \mathcal{O}(\varepsilon^2)\right)$, $\boxed{\tilde{v}_z := \tilde{v}_z^0 + \varepsilon\tilde{v}_z^1}$ so that $v_z^\varepsilon = V\left(\tilde{v}_z + \mathcal{O}(\varepsilon^2)\right)$, $\boxed{\tilde{p} := \tilde{p}^0 + \varepsilon\tilde{p}^1}$ so that $p^\varepsilon = \rho_F V^2\left(\tilde{p} + \mathcal{O}(\varepsilon^2)\right)$ and $\boxed{\tilde{\eta} := \tilde{\eta}^0 + \varepsilon\tilde{\eta}^1}$ so that $\eta^\varepsilon = \Xi\left(\tilde{\eta} + \mathcal{O}(\varepsilon^2)\right)$. The Strouhal and the Reynolds numbers are given by

$$\boxed{Sh = \frac{L\omega}{V} \quad \text{and} \quad Re = \frac{\rho_F V R^2}{\mu L}.}$$

THE ε^2 APPROX. OF THE NAVIER-STOKES EQs IN NON-DIMENSIONAL FORM

$$
\begin{aligned}
\mathrm{Sh}\frac{\partial \tilde{v}_z}{\partial \tilde{t}} + \tilde{v}_z \frac{\partial \tilde{v}_z}{\partial \tilde{z}} + \tilde{v}_r \frac{\partial \tilde{v}_z}{\partial \tilde{r}} + \frac{\partial \tilde{p}}{\partial \tilde{z}} &= \frac{1}{\mathrm{Re}}\left\{\frac{1}{\tilde{r}}\frac{\partial}{\partial \tilde{r}}\left(\tilde{r}\frac{\partial \tilde{v}_z}{\partial \tilde{r}}\right)\right\}, \\
\frac{\partial}{\partial \tilde{r}}(\tilde{r}\tilde{v}_r) + \frac{\partial}{\partial \tilde{z}}(\tilde{r}\tilde{v}_z) &= 0, \\
\frac{\partial \tilde{p}}{\partial \tilde{r}} &= 0.
\end{aligned}
$$

HYDROSTATIC APPROXIMATION → $\frac{\partial \tilde{p}}{\partial \tilde{r}} = 0$

Here $\tilde{v}_r := \tilde{v}_r^1 + \varepsilon\tilde{v}_r^2$ so that $v_r^\varepsilon = \varepsilon V(\tilde{v}_r + \mathcal{O}(\varepsilon^2))$, $\tilde{v}_z := \tilde{v}_z^0 + \varepsilon\tilde{v}_z^1$ so that $v_z^\varepsilon = V(\tilde{v}_z + \mathcal{O}(\varepsilon^2))$, $\tilde{p} := \tilde{p}^0 + \varepsilon\tilde{p}^1$ so that $p^\varepsilon = \rho_F V^2(\tilde{p} + \mathcal{O}(\varepsilon^2))$ and $\tilde{\eta} := \tilde{\eta}^0 + \varepsilon\tilde{\eta}^1$ so that $\eta^\varepsilon = \Xi(\tilde{\eta} + \mathcal{O}(\varepsilon^2))$. The Strouhal and the Reynolds numbers are given by

DESCRIBES UNSTEADY, OSCILLATING FLOW →

$$
Sh = \frac{L\omega}{V} \quad \text{and} \quad Re = \frac{\rho_F V R^2}{\mu L}.
$$

← RATIO OF INERTIAL FORCES TO VISCOUS FORCES

THE ε^2 APPROX. OF THE NAVIER-STOKES EQs IN NON-DIMENSIONAL FORM

$$\begin{aligned} \mathrm{Sh}\frac{\partial \tilde{v}_z}{\partial \tilde{t}} + \tilde{v}_z\frac{\partial \tilde{v}_z}{\partial \tilde{z}} + \tilde{v}_r\frac{\partial \tilde{v}_z}{\partial \tilde{r}} + \frac{\partial \tilde{p}}{\partial \tilde{z}} &= \frac{1}{\mathrm{Re}}\left\{\frac{1}{\tilde{r}}\frac{\partial}{\partial \tilde{r}}\left(\tilde{r}\frac{\partial \tilde{v}_z}{\partial \tilde{r}}\right)\right\}, \\ \frac{\partial}{\partial \tilde{r}}(\tilde{r}\tilde{v}_r) + \frac{\partial}{\partial \tilde{z}}(\tilde{r}\tilde{v}_z) &= 0, \\ \frac{\partial \tilde{p}}{\partial \tilde{r}} &= 0. \end{aligned}$$

HYDROSTATIC APPROXIMATION → $\frac{\partial \tilde{p}}{\partial \tilde{r}} = 0$

Here $\tilde{v}_r := \tilde{v}_r^1 + \varepsilon\tilde{v}_r^2$ so that $v_r^\varepsilon = \varepsilon V(\tilde{v}_r + \mathcal{O}(\varepsilon^2))$, $\tilde{v}_z := \tilde{v}_z^0 + \varepsilon\tilde{v}_z^1$ so that $v_z^\varepsilon = V(\tilde{v}_z + \mathcal{O}(\varepsilon^2))$, $\tilde{p} := \tilde{p}^0 + \varepsilon\tilde{p}^1$ so that $p^\varepsilon = \rho_F V^2(\tilde{p} + \mathcal{O}(\varepsilon^2))$ and $\tilde{\eta} := \tilde{\eta}^0 + \varepsilon\tilde{\eta}^1$ so that $\eta^\varepsilon = \Xi(\tilde{\eta} + \mathcal{O}(\varepsilon^2))$. The Strouhal and the Reynolds numbers are given by

$$\omega = \frac{1}{L}\sqrt{\frac{1}{\rho_F}\left(\frac{hE}{R(1-\sigma^2)} + p_{\mathrm{ref}}\right)}$$

OSCILLATION FREQUENCY OR VORTEX SHEDDING FREQUENCY

$$Sh = \frac{L\omega}{V} \quad \text{and} \quad Re = \frac{\rho_F V R^2}{\mu L}.$$

RATIO OF INERTIAL FORCES TO VISCOUS FORCES

REMARKS:

- leading-order balance of radial momentum implies hydrostatic pressure, i.e., p = p(z,t).

- leading order balance of axial momentum implies that viscous effects in the axial direction are negligible

- leading order conservation of mass implies that the axial component of the velocity is dominant of the radial velocity, i.e.,$\tilde{v}_r^0$=0, so that

$$v_r = V(\varepsilon\tilde{v}_r^1 + \varepsilon^2\tilde{v}_r^2 + \ldots) = \varepsilon V(\tilde{v}_r^1 + \varepsilon\tilde{v}_r^2 + \ldots)$$

while

$$v_z = V(\tilde{v}_z^0 + \varepsilon\,\tilde{v}_z^1 + \ldots)$$

so that

$$\frac{v_r}{v_z} = \varepsilon$$

THE ε^2 APPROX. OF THE BOUNDARY CONDITIONS IN NON-DIMENSIONAL FORM

THE LATERAL BOUNDARY CONDITIONS:

$$\tilde{p} - \tilde{p}_{\text{ref}} = \frac{1}{\rho_F V^2}\left\{\left(\frac{Eh}{(1-\sigma^2)R} + p_{\text{ref}}\right)\frac{\Xi}{R}\tilde{\eta} + \frac{h}{R}C_v\omega\frac{\Xi}{R}\frac{\partial\tilde{\eta}}{\partial\tilde{t}}\right\}$$

$$(\tilde{v}_r, \tilde{v}_z)\big|_{(1,\tilde{z},\tilde{t})} = \left(\frac{\partial\tilde{\eta}}{\partial\tilde{t}}\Big|_{(\tilde{z},\tilde{t})}, 0\right)$$

INITIAL DATA:

$$\tilde{\boldsymbol{v}}\big|_{(\tilde{r},\tilde{z},0)} = 0, \ \ \tilde{\eta}\big|_{(\tilde{z},0)} = 0$$

INLET/OUTLET BOUNDARY DATA:

$$\begin{cases} \tilde{\eta}\big|_{(z=0/L,\tilde{t})} = 0, \ \tilde{p}\big|_{(z=0/L,\tilde{t})} = \dfrac{(P_{0/L}(\tilde{t}) + p_{\text{ref}})}{\rho_F V^2}, \\ \tilde{v}_{\tilde{r}}\big|_{(1,z=0/L,\tilde{t})} = 0. \end{cases}$$

THE ε^2 APPROX. OF THE BOUNDARY CONDITIONS IN NON-DIMENSIONAL FORM

THE LATERAL BOUNDARY CONDITIONS:

$$\tilde{p} - \tilde{p}_{\text{ref}} = \frac{1}{\rho_F V^2}\left\{\left(\frac{Eh}{(1-\sigma^2)R} + p_{\text{ref}}\right)\frac{\Xi}{R}\tilde{\eta} + \frac{h}{R}C_v\omega\frac{\Xi}{R}\frac{\partial\tilde{\eta}}{\partial\tilde{t}}\right\}$$

$$(\tilde{v}_r, \tilde{v}_z)|_{(1,\tilde{z},\tilde{t})} = \left(\frac{\partial\tilde{\eta}}{\partial\tilde{t}}|_{(\tilde{z},\tilde{t})}, 0\right)$$

Dominant fluid stress: normal stress

Membrane acceleration drops out

THE ε² APPROX. OF THE BOUNDARY CONDITIONS IN NON-DIMENSIONAL FORM

THE LATERAL BOUNDARY CONDITIONS:

$$\tilde{p} - \tilde{p}_{\text{ref}} = \frac{1}{\rho_F V^2}\left\{\left(\frac{Eh}{(1-\sigma^2)R} + p_{\text{ref}}\right)\frac{\Xi}{R}\tilde{\eta} + \frac{h}{R}C_v\omega\frac{\Xi}{R}\frac{\partial\tilde{\eta}}{\partial\tilde{t}}\right\}$$

$$(\tilde{v}_r, \tilde{v}_z)|_{(1,\tilde{z},\tilde{t})} = \left(\frac{\partial\tilde{\eta}}{\partial\tilde{t}}|_{(\tilde{z},\tilde{t})}, 0\right)$$

INITIAL DATA:

$$\tilde{\boldsymbol{v}}|_{(\tilde{r},\tilde{z},0)} = 0, \quad \tilde{\eta}|_{(\tilde{z},0)} = 0$$

Initial condition for membrane velocity drops out.

INLET/OUTLET BOUNDARY DATA:

$$\begin{cases} \tilde{\eta}|_{(z=0/L,\tilde{t})} = 0, \ \tilde{p}|_{(z=0/L,\tilde{t})} = \dfrac{(P_{0/L}(\tilde{t}) + p_{\text{ref}})}{\rho_F V^2}, \\ \tilde{v}_{\tilde{r}}|_{(1,z=0/L,\tilde{t})} = 0. \end{cases}$$

THE ε^2 APPROX. OF THE FSI PROBLEM

$$\begin{aligned}
\mathrm{Sh}\frac{\partial \tilde{v}_z}{\partial \tilde{t}} + \tilde{v}_z\frac{\partial \tilde{v}_z}{\partial \tilde{z}} + \tilde{v}_r\frac{\partial \tilde{v}_z}{\partial \tilde{r}} + \frac{\partial \tilde{p}}{\partial \tilde{z}} &= \frac{1}{\mathrm{Re}}\left\{\frac{1}{\tilde{r}}\frac{\partial}{\partial \tilde{r}}\left(\tilde{r}\frac{\partial \tilde{v}_z}{\partial \tilde{r}}\right)\right\},\\
\frac{\partial}{\partial \tilde{r}}(\tilde{r}\tilde{v}_r) + \frac{\partial}{\partial \tilde{z}}(\tilde{r}\tilde{v}_z) &= 0,\\
\frac{\partial \tilde{p}}{\partial \tilde{r}} &= 0.
\end{aligned}$$

DATA:

$$\begin{cases}
\tilde{p} - \tilde{p}_{\mathrm{ref}} = \dfrac{1}{\rho_F V^2}\left\{\left(\dfrac{Eh}{(1-\sigma^2)R} + p_{\mathrm{ref}}\right)\dfrac{\Xi}{R}\tilde{\eta} + \dfrac{h}{R}C_v\omega\dfrac{\Xi}{R}\dfrac{\partial \tilde{\eta}}{\partial \tilde{t}}\right\}\\
(\tilde{v}_r, \tilde{v}_z)\big|_{(1,\tilde{z},\tilde{t})} = \left(\frac{\partial \tilde{\eta}}{\partial \tilde{t}}\big|_{(\tilde{z},\tilde{t})}, 0\right)
\end{cases}$$

$$\begin{cases}
\tilde{\eta}\big|_{(z=0/L,\tilde{t})} = 0,\ \tilde{p}\big|_{(z=0/L,\tilde{t})} = \dfrac{(P_{0/L}(\tilde{t}) + p_{\mathrm{ref}})}{\rho_F V^2},\\
\tilde{v}_{\tilde{r}}\big|_{(1,z=0/L,\tilde{t})} = 0.
\end{cases}$$

$$\tilde{\boldsymbol{v}}\big|_{(\tilde{r},\tilde{z},0)} = 0,\ \ \tilde{\eta}\big|_{(\tilde{z},0)} = 0$$

DIMENSION REDUCTION

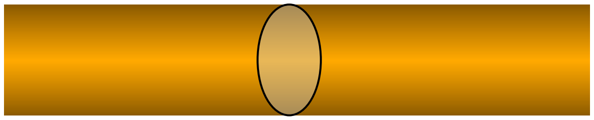

Average over the cross-section

DEFINE:

$$\tilde{A} = (1 + \tfrac{\Xi}{R}\tilde{\eta})^2 \,;\; \tilde{U} = \frac{2}{\tilde{A}} \int_0^{1+\frac{\Xi}{R}\tilde{\eta}} \tilde{v}_z \tilde{r}\, d\tilde{r} \,;\; \tilde{\alpha} = \frac{2}{\tilde{A}\tilde{U}^2} \int_0^{1+\frac{\Xi}{R}\tilde{\eta}} \tilde{v}_z^2 \tilde{r}\, d\tilde{r} \,;\quad \tilde{m} = \tilde{A}\tilde{U}$$

OBTAIN THE FOLLOWING 1D REDUCED MODEL FOR $\tilde{A}$ and $\tilde{m}$:

$$\begin{aligned} \frac{\partial \tilde{A}}{\partial \tilde{t}} + \frac{\Xi}{R}\frac{\partial \tilde{m}}{\partial \tilde{z}} &= 0, \\ Sh\frac{\partial \tilde{m}}{\partial \tilde{t}} + \frac{\partial}{\partial \tilde{z}}\left(\tilde{\alpha}\frac{\tilde{m}^2}{\tilde{A}}\right) + \tilde{A}\frac{\partial \tilde{p}}{\partial \tilde{z}} &= \frac{2}{Re}\sqrt{\tilde{A}}\left[\frac{\partial \tilde{v}_z}{\partial \tilde{r}}\right]_{\tilde{\Sigma}}. \end{aligned}$$

DIMENSION REDUCTION

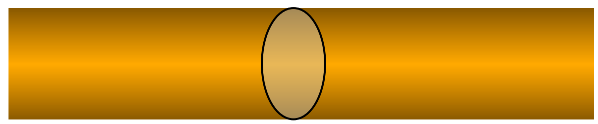

Average over the cross-section

DEFINE:

$$\tilde{A} = (1 + \tfrac{\Xi}{R}\tilde{\eta})^2 \,; \quad \tilde{U} = \frac{2}{\tilde{A}} \int_0^{1+\frac{\Xi}{R}\tilde{\eta}} \tilde{v}_z \tilde{r}\, d\tilde{r} \,; \quad \tilde{\alpha} = \frac{2}{\tilde{A}\tilde{U}^2} \int_0^{1+\frac{\Xi}{R}\tilde{\eta}} \tilde{v}_z^2 \tilde{r}\, d\tilde{r} \,; \quad \tilde{m} = \tilde{A}\tilde{U}$$

OBTAIN THE FOLLOWING 1D REDUCED MODEL FOR $\tilde{A}$ and $\tilde{m}$:

KINEMATIC COUPLING CONDITION

$$\frac{\partial \tilde{A}}{\partial \tilde{t}} + \frac{\Xi}{R}\frac{\partial \tilde{m}}{\partial \tilde{z}} = 0,$$

CONSERVATION OF MASS

$$Sh\frac{\partial \tilde{m}}{\partial \tilde{t}} + \frac{\partial}{\partial \tilde{z}}\left(\tilde{\alpha}\frac{\tilde{m}^2}{\tilde{A}}\right) + \tilde{A}\frac{\partial \tilde{p}}{\partial \tilde{z}} = \frac{2}{Re}\sqrt{\tilde{A}}\left[\frac{\partial \tilde{v}_z}{\partial \tilde{r}}\right]_{\tilde{\Sigma}}.$$

BALANCE OF RADIAL MOMENTUM

BALANCE OF AXIAL MOMENTUM

$$\begin{aligned} \frac{\partial \tilde{A}}{\partial \tilde{t}} + \frac{\Xi}{R}\frac{\partial \tilde{m}}{\partial \tilde{z}} &= 0, \\ Sh\frac{\partial \tilde{m}}{\partial \tilde{t}} + \frac{\partial}{\partial \tilde{z}}\left(\tilde{\alpha}\frac{\tilde{m}^2}{\tilde{A}}\right) + \tilde{A}\frac{\partial \tilde{p}}{\partial \tilde{z}} &= \frac{2}{Re}\sqrt{\tilde{A}}\left[\frac{\partial \tilde{v}_z}{\partial \tilde{r}}\right]_{\tilde{\Sigma}}. \end{aligned}$$

The dynamic coupling condition is used to determine the pressure p = p(A,m):

$$\tilde{p} - \tilde{p}_{\text{ref}} = \frac{1}{\rho_F V^2}\left\{\left(\frac{Eh}{(1-\sigma^2)R} + p_{\text{ref}}\right)\frac{\Xi}{R}\tilde{\eta} + \frac{h}{R}C_v\omega\frac{\Xi}{R}\frac{\partial \tilde{\eta}}{\partial \tilde{t}}\right\}$$

⇓

$$p = p_{\text{ref}} + \left(\frac{Eh}{(1-\sigma^2)R} + p_{\text{ref}}\right)\left(\sqrt{\frac{A}{A_0}} - 1\right) + \frac{hC_v}{R}\frac{\partial}{\partial t}\left(\sqrt{\frac{A}{A_0}}\right)$$

Linear, viscoelastic membrane

$$p = p_{\text{ref}} + \frac{Eh}{(1-\sigma^2)R}\left(\sqrt{\frac{A}{A_0}} - 1\right)$$

Linear, elastic membrane (Law of Laplace)

$$
\begin{cases}
\dfrac{\partial \tilde{A}}{\partial \tilde{t}} + \dfrac{\Xi}{R}\dfrac{\partial \tilde{m}}{\partial \tilde{z}} = 0, \\
Sh\dfrac{\partial \tilde{m}}{\partial \tilde{t}} + \dfrac{\partial}{\partial \tilde{z}}\left(\tilde{\alpha}\dfrac{\tilde{m}^2}{\tilde{A}}\right) + \tilde{A}\dfrac{\partial \tilde{p}}{\partial \tilde{z}} = \dfrac{2}{Re}\sqrt{\tilde{A}}\left[\dfrac{\partial \tilde{v}_z}{\partial \tilde{r}}\right]_{\tilde{\Sigma}}. \\
p = p_{\mathrm{ref}} + \dfrac{Eh}{(1-\sigma^2)R}\left(\sqrt{\dfrac{A}{A_0}} - 1\right)
\end{cases}
$$

THIS SYSTEM IS NOT CLOSED!

To close the system, the dependence of v_z on r needs to be prescribed:

$$
\tilde{v}_z(\tilde{r},\tilde{z},\tilde{t}) = \frac{\gamma+2}{\gamma}\tilde{U}(\tilde{z},\tilde{t})\left(1 - \left(\frac{\tilde{r}}{1+\frac{\Xi}{R}\tilde{\eta}(\tilde{z},\tilde{t})}\right)^{\gamma}\right)
$$

γ=2 : quadratic velocity profile (Poiseuille profile)(α=4/3)

γ=9 : “plug” velocity profile (α=1.1)

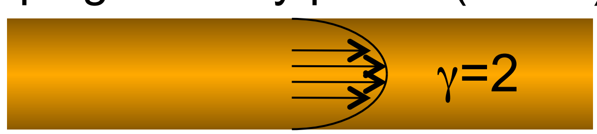

$$
\gamma = \frac{2-\alpha}{\alpha-1}
$$

R=2.5mm; E=100000Pa

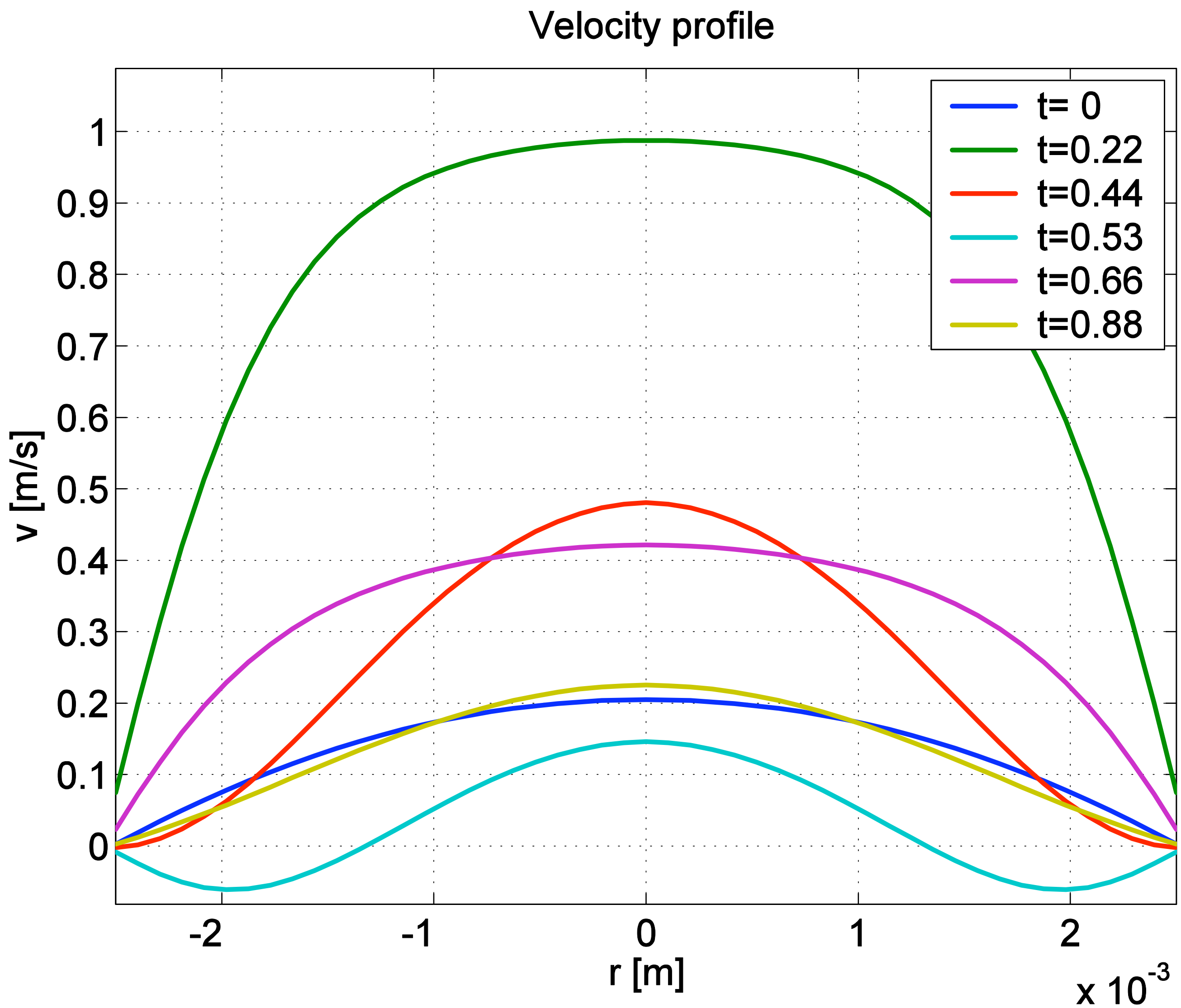

Axial velocity profile comparison between 1D and Full model

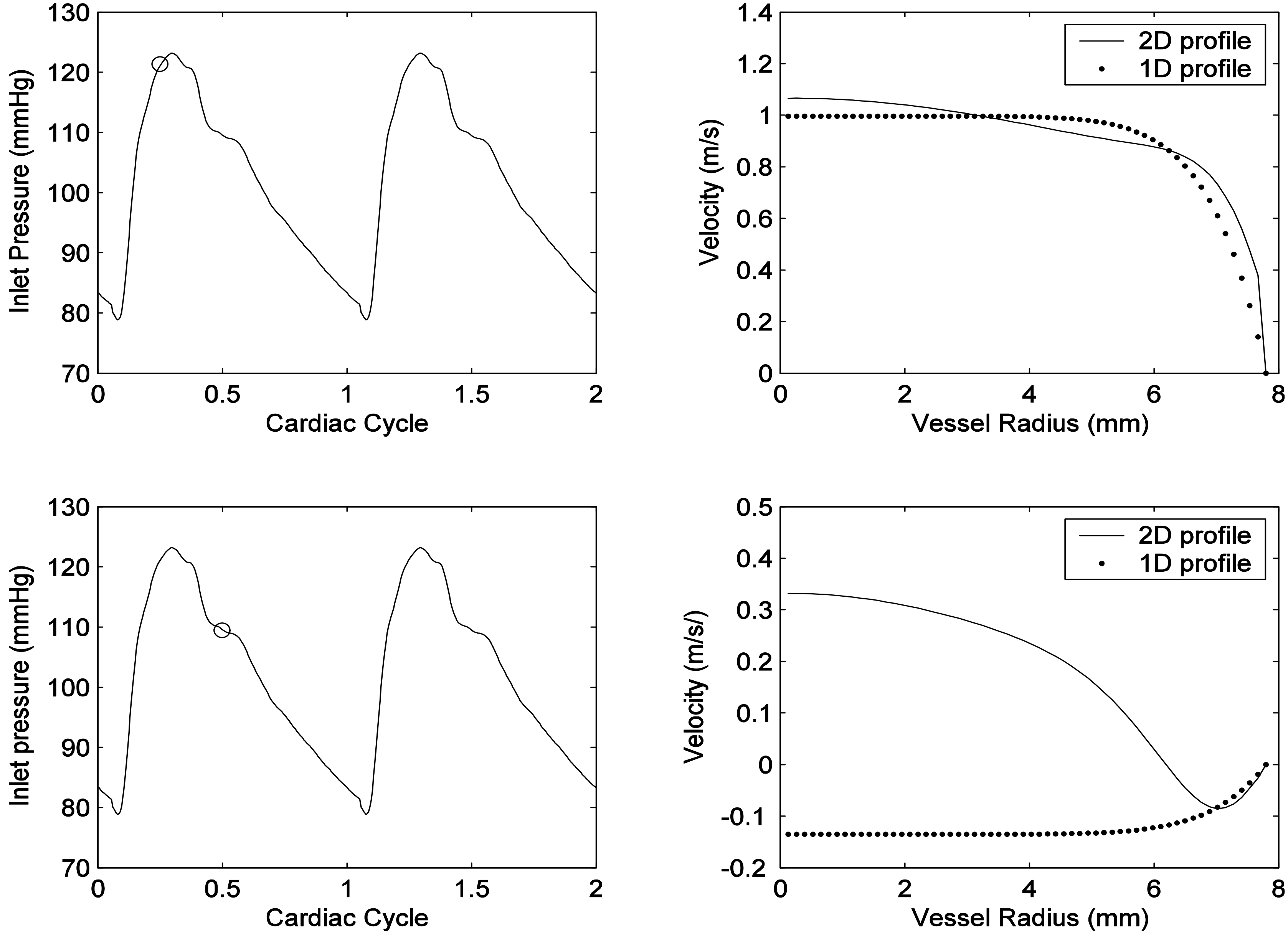

THE REDUCED 1D MODEL IN DIMENSIONAL FORM

$$\frac{\partial A}{\partial t} + \frac{\partial m}{\partial z} = 0,$$

$$\frac{\partial m}{\partial t} + \frac{\partial}{\partial z}\left(\alpha \frac{m^2}{A}\right) + \frac{A}{\rho_F}\frac{\partial p}{\partial z} = -\frac{2\mu}{\rho_F}(\gamma + 2)\frac{m}{A}.$$

$$p = p_{\mathrm{ref}} + \frac{Eh}{(1-\sigma^2)R}\left(\sqrt{\frac{A}{A_0}} - 1\right)$$

(LINEARLY ELASTIC)

Hunt and Timlake, T. Hughes, A. Quarteroni et al, A. Veneziani, A. Robertson, M. Olufsen et al, Y.C., Fung, Keener and Snyd, S. Canic et al.

THE REDUCED 1D MODEL IN DIMENSIONAL FORM

$$\frac{\partial A}{\partial t} + \frac{\partial m}{\partial z} = 0,$$

$$\frac{\partial m}{\partial t} + \frac{\partial}{\partial z}\left(\alpha \frac{m^2}{A}\right) + \frac{A}{\rho_F}\frac{\partial p}{\partial z} = -\frac{2\mu}{\rho_F}(\gamma + 2)\frac{m}{A}.$$

$$p = p_{\mathrm{ref}} + \left(\frac{Eh}{(1-\sigma^2)R} + p_{\mathrm{ref}}\right)\left(\sqrt{\frac{A}{A_0}} - 1\right) + \frac{hC_v}{R}\frac{\partial}{\partial t}\left(\sqrt{\frac{A}{A_0}}\right)$$

(LINEARLY VISCO-ELASTIC)

Hunt and Timlake, T. Hughes, A. Quarteroni et al, A. Veneziani, A. Robertson, M. Olufsen et al, Y.C., Fung, Keener and Snyd, S. Canic et al.

This reduced model holds under the following assumptions:

(1) The domain is cylindrical with small aspect ratio $\varepsilon = R_{\max}/L$.

(2) Longitudinal displacement is negligible.

(3) Radial displacement is not too large, *i.e.*, $\delta := \Xi/R \leq \varepsilon$.

(4) The reference tube radius varies slowly: $R'(z) \leq \epsilon$

(5) The Reynolds number Re is small to medium (Re $\approx$ 800).

(6) The z-derivatives of the non-dimensional quantities are $O(1)$ (not too large).

MATHEMATICAL PROPERTIES OF THE 1D MODEL

$$\frac{\partial A}{\partial t} + \frac{\partial m}{\partial z} = 0,$$

$$\frac{\partial m}{\partial t} + \frac{\partial}{\partial z}\left(\alpha \frac{m^2}{A}\right) + \frac{A}{\rho_F}\frac{\partial p}{\partial z} = -\frac{2\mu}{\rho_F}(\gamma + 2)\frac{m}{A}.$$

$$p = p_{\text{ref}} + \frac{Eh}{(1-\sigma^2)R}\left(\sqrt{\frac{A}{A_0}} - 1\right)$$

SYSTEM IN QUASILINEAR FORM:

$$\begin{pmatrix} A_t \\ m_t \end{pmatrix} + \begin{pmatrix} 0 & 1 \\ -\alpha\frac{m^2}{A^2} + \frac{1}{\rho}Ap'(A) & 2\alpha\frac{m}{A} \end{pmatrix}\begin{pmatrix} A_x \\ m_x \end{pmatrix} = \begin{pmatrix} 0 \\ -2\frac{\alpha}{\alpha-1}\nu\frac{m}{A} \end{pmatrix}$$

$$U_t + F'(U)U_x = G(U)$$

EIGENVALUES OF THE JACOBIAN F'(U):

$$\lambda = \alpha\frac{m}{A} - \frac{1}{2}\sqrt{4\alpha^2\frac{m^2}{A^2} + \frac{4}{\rho}p'(A) - 4\alpha\frac{m^2}{A^2}}, \quad \mu = \alpha\frac{m}{A} + \sqrt{4\alpha^2\frac{m^2}{A^2} + \frac{4}{\rho}p'(A) - 4\alpha\frac{m^2}{A^2}}$$

EIGENVALUES OF THE JACOBIAN F'(U):

$$\lambda = \alpha\frac{m}{A} - \frac{1}{2}\sqrt{4\alpha^2\frac{m^2}{A^2} + \frac{4}{\rho}p'(A) - 4\alpha\frac{m^2}{A^2}}, \quad \mu = \alpha\frac{m}{A} + \sqrt{4\alpha^2\frac{m^2}{A^2} + \frac{4}{\rho}p'(A) - 4\alpha\frac{m^2}{A^2}}$$

If $4\alpha^2\frac{m^2}{A^2} + \frac{4}{\rho}p'(A) - 4\alpha\frac{m^2}{A^2}$ >=0, the system would be hyperbolic.

THE SIGN OF $4\alpha^2\frac{m^2}{A^2} + \frac{4}{\rho}p'(A) - 4\alpha\frac{m^2}{A^2}$

For α=1 (plug flow): P'(A)>0 implies that the discriminant is positive

For α=4/3 (Poiseuille): P'(A) is dominant over the remaining terms because of the Youngs modulus of elasticity = O(10^5) Pa >> U=O(1)

⇨ The system is strictly hyperbolic (two real, distinct eigenvalues)

CONSEQUENCES

- The system is nonlinear and hyperbolic. This implies that solutions can exhibit shock waves in A, and/or m.

-Shock waves can be interpreted as sharp pressure/velocity wave fronts. Those are not physiologically observed in healthy humans. Sharp pressure waves can be heard through a stethoscope in patients with aortic insufficiency.

- Mathematical analysis of shock wave formation in this model* shows that for the inlet and outlet pressure data that corresponds to healthy humans, the first time the shock waves form for this model is 3 meters away from the heart!

- Mathematical analysis and numerical simulation also showed that for patients with aortic insufficiency, the shock wave generated by this model occurs within 15 cm away from the heart.

*Canic , S. and E. H. Kim. Mathematical Analysis of the Quasilinear Effects in a Hyperbolic Model of Blood Flow through Compliant Axisymmetric Vessels, *Mathematical Methods in Applied Sciences, 26 (14) (2003), 1161-1186.*

1D Model: Shock Formation

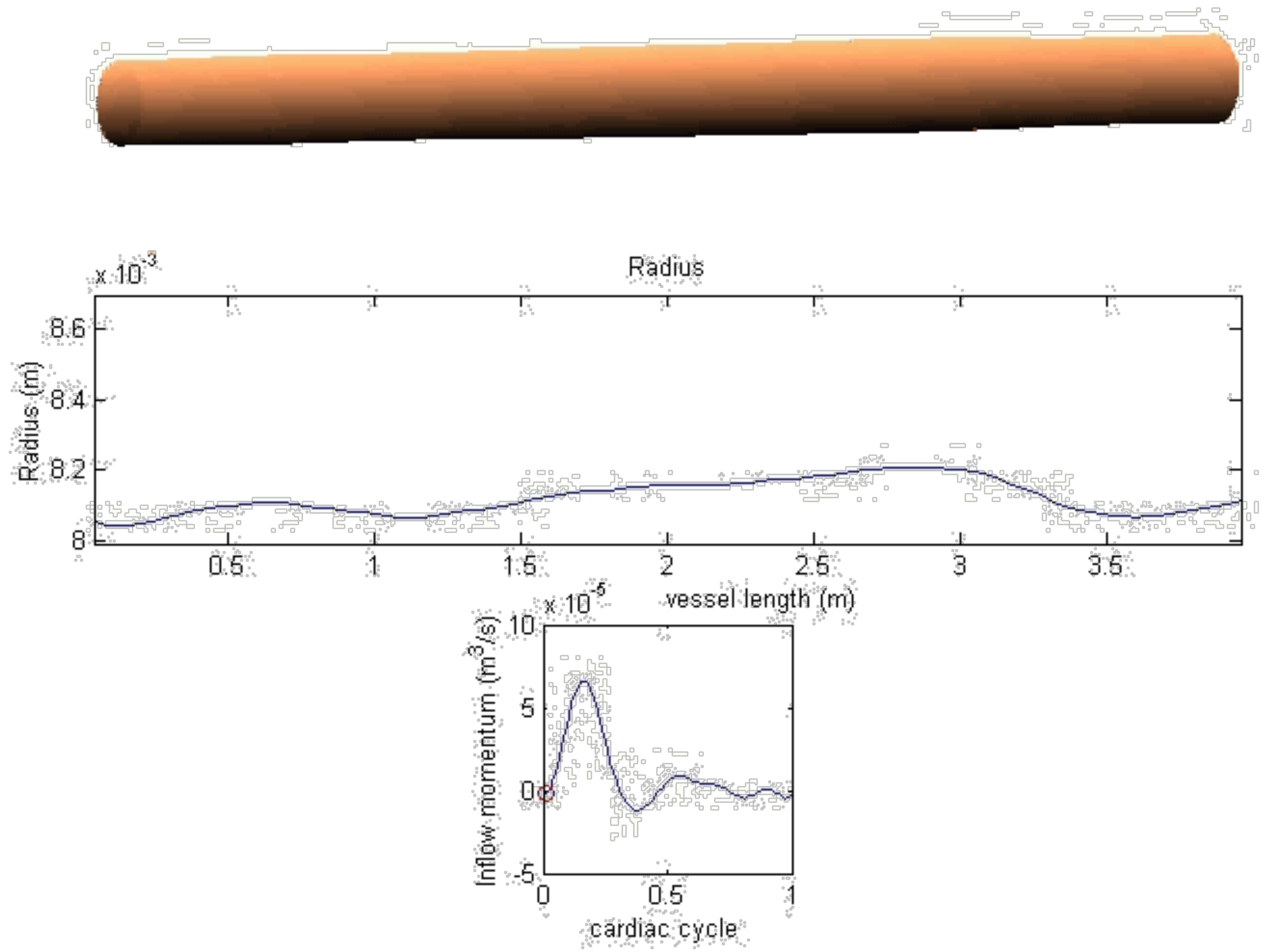

CONSEQUENCES

• Boundary conditions: the structure of characteristics determines which boundary conditions give rise to a well-defined problem.

-The eigenvalues have opposite signs. This implies that we have two families of characteristics: one with positive slope, and one with negative slope.

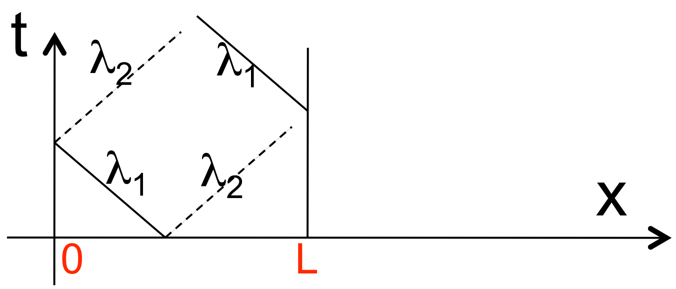

-This means that 2 pieces of boundary data need to be prescribed: one at the left boundary, and one at the right boundary. So, a well-defined problem would have, say, pressure prescribed at both ends (displacement), or flow rate at both ends, or a combination of pressure and flow rate at each end (Riemann invariants).

Canic , S. and E. H. Kim. Mathematical Analysis of the Quasilinear Effects in a Hyperbolic Model of Blood Flow through Compliant Axisymmetric Vessels, *Mathematical Methods in Applied Sciences, 26 (14) (2003), 1161-1186.*

CONSEQUENCES

- Hyperbolicity implies that traveling waves will reflect from the outlet and inlet of the tube if Dirichlet data are prescribed.

  - These reflected waves contaminate the physiological flow.

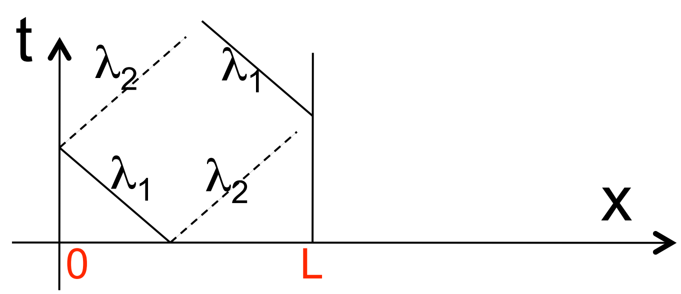

- Prescribing “transparent” outlet boundary conditions can minimize the presence of spurious reflected waves.

A REDUCED MODEL WITHOUT AN AD-HOC CLOSURE

Canic & Mikelic et al.

By using homogenization theory and energy estimates one obtains*:

- an approximation to the zero-th order in terms of v_z^0 and η^0 where

$$v_z = v_z^0 + \varepsilon\, v_z^1 + O(\varepsilon^2),\ \eta = \eta^0 + \varepsilon\, \eta^1 + O(\varepsilon^2)$$

- an ε-correction in terms of v_z^1 and η^1.

Homogenization provided the correct scaling that enabled the derivation
Of a close model that approximates the original problem to the ε^2-accuracy.

The 0^{th} –order solution plus the ε-correction solution satisfy the original problem to the ε^2 accuracy*.

Canic and Mikelic. Effective equations modeling the flow of a viscous incompressible fluid through a long elastic tube arising in the study of blood flow through small arteries. SIAM Journal on Applied Dynamical Systems 2(3) (2003) 431-463.

Canic , S. A. Mikelic, and D. Lamponi, and J. Tambaca. Self-Consistent Effective Equations Modeling Blood Flow in Medium-to-Large Compliant Arteries. *SIAM J. Multiscale Analysis and Simulation 3(3) (2005) 559-596.*

Canic, C.J. Hartley, D. Rosenstrauch, J. Tambaca, G. guidoboni, A. Mikelic. Blood Flow in Compliant Arteries: An Effective Viscoelastic Reduced Model, Numerics and Experimental Validation. Annals of Biomedical Engineering. 34 (2006), pp.`575 - 592.

THE REDUCED EQUATIONS

$\varepsilon = \frac{R}{L} << 1$, Re moderate

<u>0th-order approximation:</u> $v_r^0 = 0$ and (v_z^0, η^0) satisfy

$$(R+\eta^0)\frac{\partial \eta^0}{\partial t} + \frac{\partial}{\partial z}\int_0^{R+\eta^0} 2 r v_z^0 \, dr = 0$$

nonlinear transport

$$\rho \frac{\partial v_z^0}{\partial t} - \mu \frac{1}{r}\frac{\partial}{\partial r}\left(r \frac{\partial v_z^0}{\partial r}\right) = -\frac{\partial p^0}{\partial z}$$

degenerate diffusion

$$\tilde{p}^0 = C\eta^0 + D\frac{\partial \eta^0}{\partial t}$$

viscoelastic membrane

NOTE: nonlinearity due to the fluid-structure coupling dominates the nonlinearity of fluid advection.

Biot (1956), Mikelic (2002)
Sanchez-Palencia (1980)
Camassa (2002)
Canic et al. (2005)(2006)

$$where \quad C = \frac{hE}{R^2(1-\sigma^2)}$$

INITIAL and BOUNDARY DATA

$$v_z^0(r=0) - bounded, \; v_z^0(r = R+\eta^0) = 0, \; v_z^0(t=0) = 0$$

$$\eta^0(z=0) = \frac{P_0(t)}{C}, \; \eta^0(z=L) = \frac{P_L(t)}{C}, \; \eta^0(t=0) = 0$$

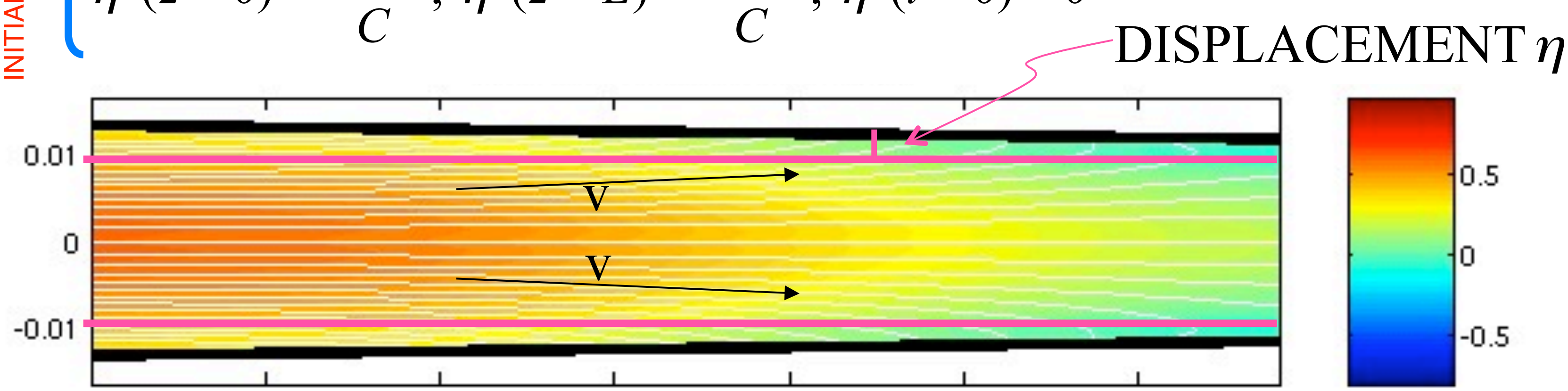

THE REDUCED EQUATIONS

$\varepsilon = \frac{R}{L} << 1$, Re moderate

The ε-correction: correction for the velocity: $v_r^1(r,z,t)$ and $v_z^1(r,z,t)$

1. Recover:

$$r v_r^1(r,z,t) = (R+\eta^0)\frac{\partial \eta^0}{\partial t} + \int_r^{R+\eta^0} \frac{\partial v_z^0}{\partial z}(\xi,z,t)\,\xi\,d\xi$$

2. Solve linear fixed-boundary problem:

$$\frac{\partial v_z^1}{\partial t} - \nu\frac{1}{r}\frac{\partial}{\partial r}\left(r\frac{\partial v_z^1}{\partial r}\right) = -S_{v_z^1}(r,z,t)$$

$$v_z^1(0,z,t) \text{ bounded}, \; v_z^1(R+\eta^0(z,t),z,t) = 0$$

$$v_z^1(r,0,t) = v_z^1(r,L,t) = 0 \quad \text{and} \quad v_z^1(r,z,0) = 0$$

where

$$S_{v_z^1}(r,z,t) = v_r^1\frac{\partial v_z^0}{\partial r} + v_z^0\frac{\partial v_z^0}{\partial z}.$$

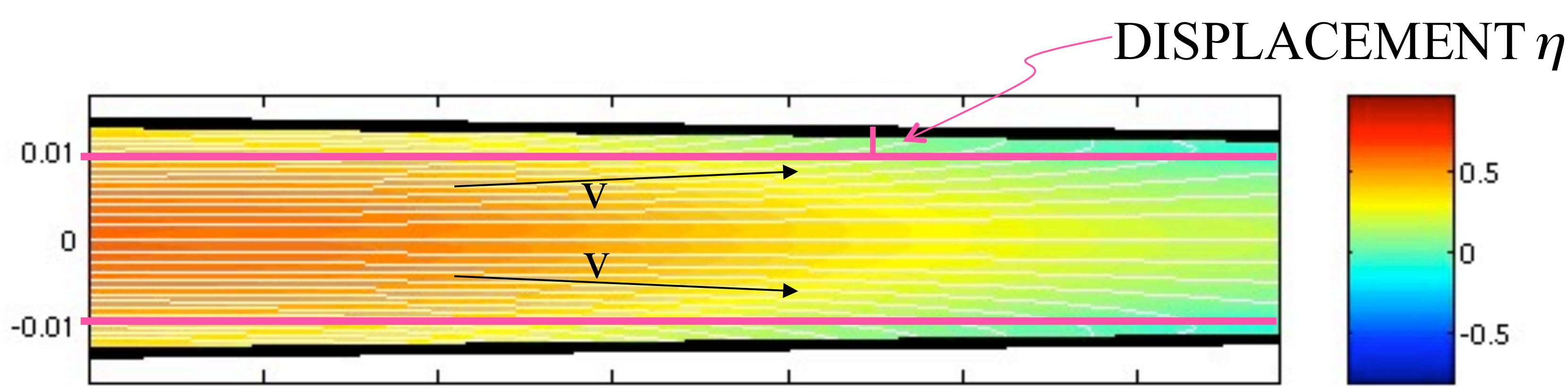

THE LEADING-ORDER APPROXIMATION

$$(R+\eta^0)\frac{\partial \eta^0}{\partial t} + \frac{\partial}{\partial z}\int_0^{R+\eta^0} 2rv_z^0\,dr = 0$$ nonlinear transport

$$\rho\frac{\partial v_z^0}{\partial t} - \mu\frac{1}{r}\frac{\partial}{\partial r}\left(r\frac{\partial v_z^0}{\partial r}\right) = -\frac{\partial p^0}{\partial z}$$ degenerate diffusion

$$\tilde{p}^0 = C\eta^0 + D\frac{\partial \eta^0}{\partial t}$$ viscoelastic membrane

$$\begin{cases} v_z^0(r=0)-bounded,\; v_z^0(r=R+\eta^0)=0,\; v_z^0(t=0)=0 \\ \eta^0(z=0)=\dfrac{P_0(t)}{C},\; \eta^0(z=L)=\dfrac{P_L(t)}{C},\; \eta^0(t=0)=0 \end{cases}$$

- NONLINEAR MOVING BOUNDARY PROBLEM
- 2 SPATIAL DIMENSIONS (r,z) and TIME t
- BUT, THE DIMENSIONS ARE “SPLIT” SO THAT NUMERICALLY AND ANALYTICALLY, 1D TECHNIQUES APPLY!
- THIS IS WHY WE WILL SAY THAT THIS MODEL IS 1.5 D

NUMERICAL SIMULATION

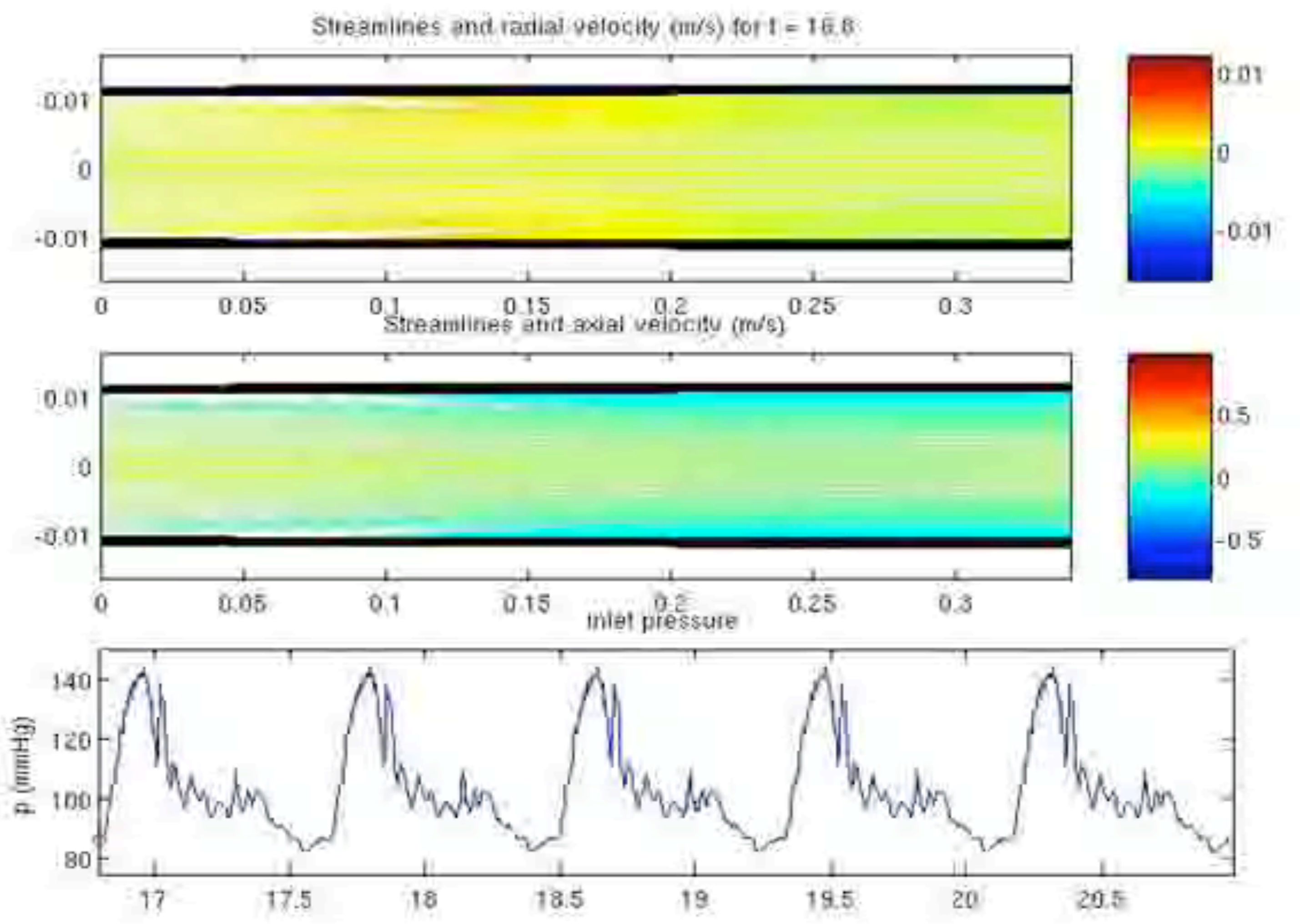

EXPERIMENTAL VALIDATION

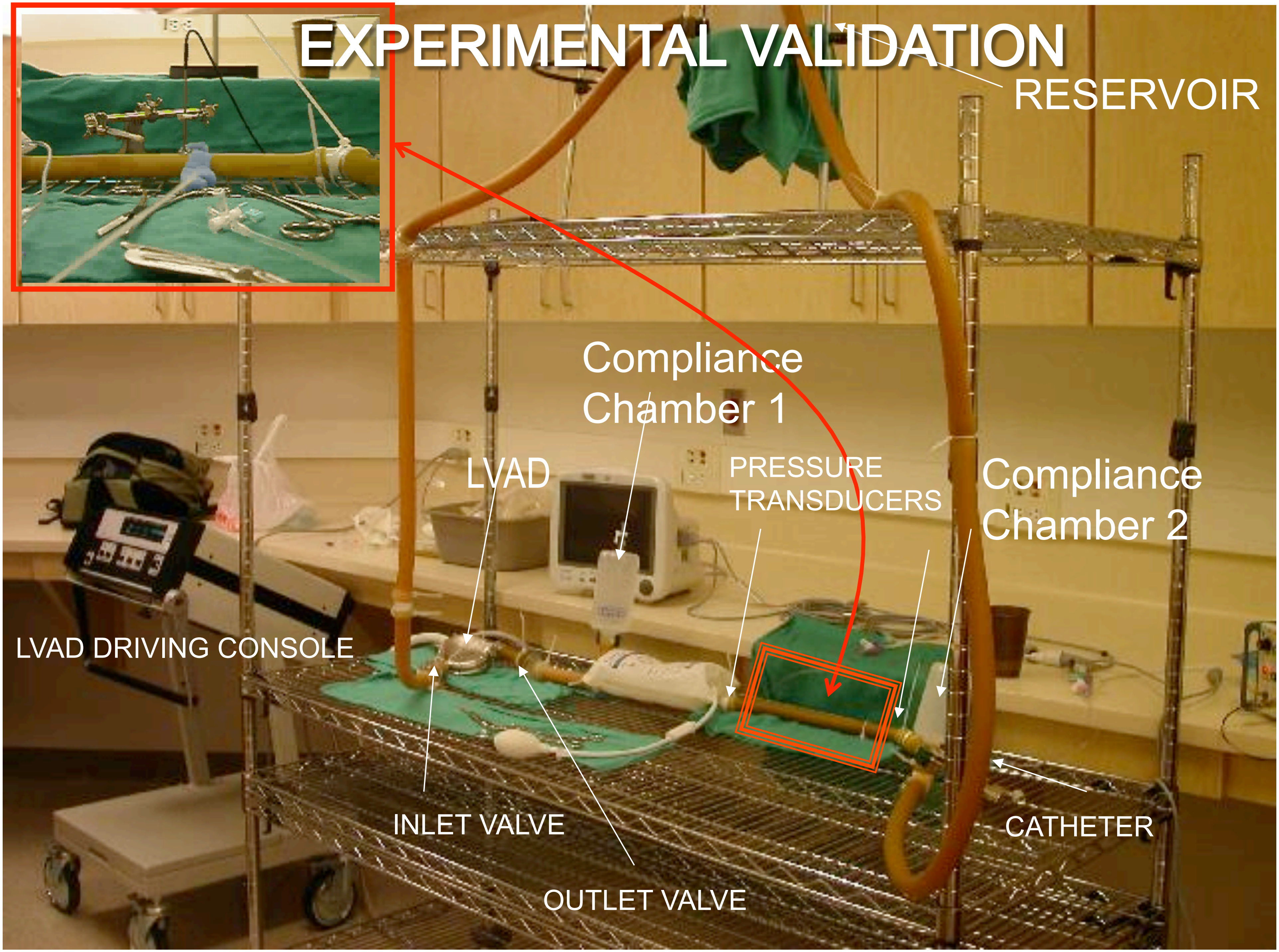

•Recreate conditions in a healthy human abdominal aorta.

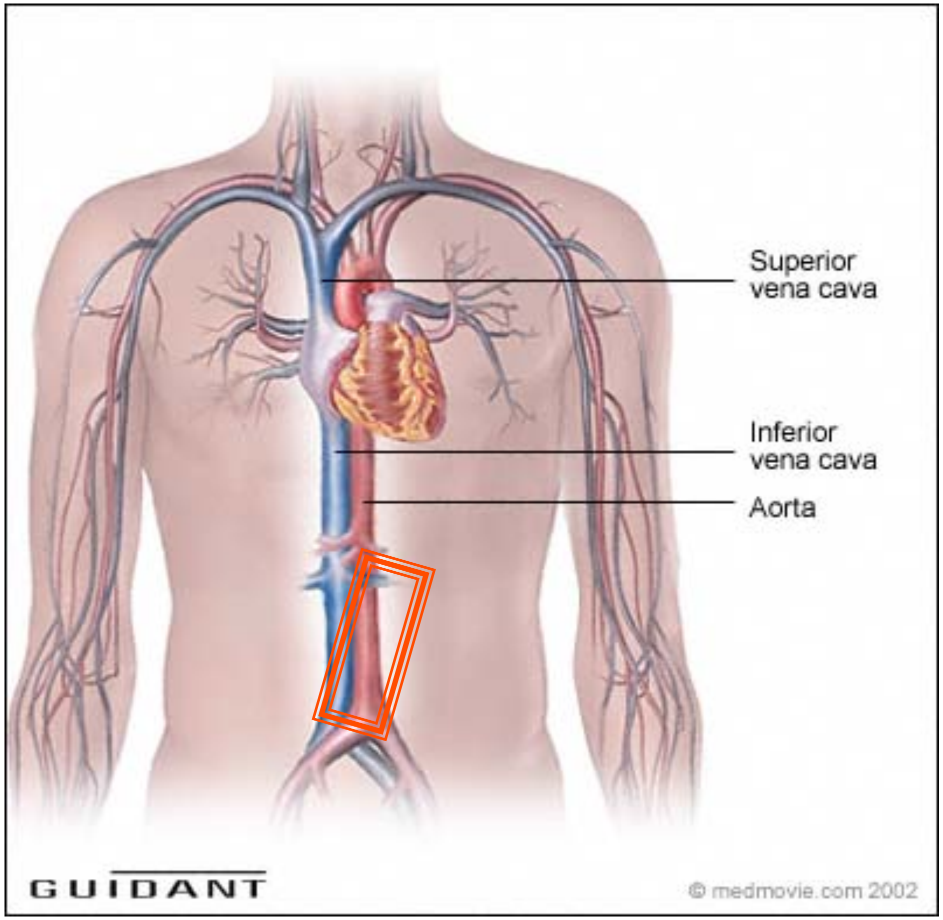

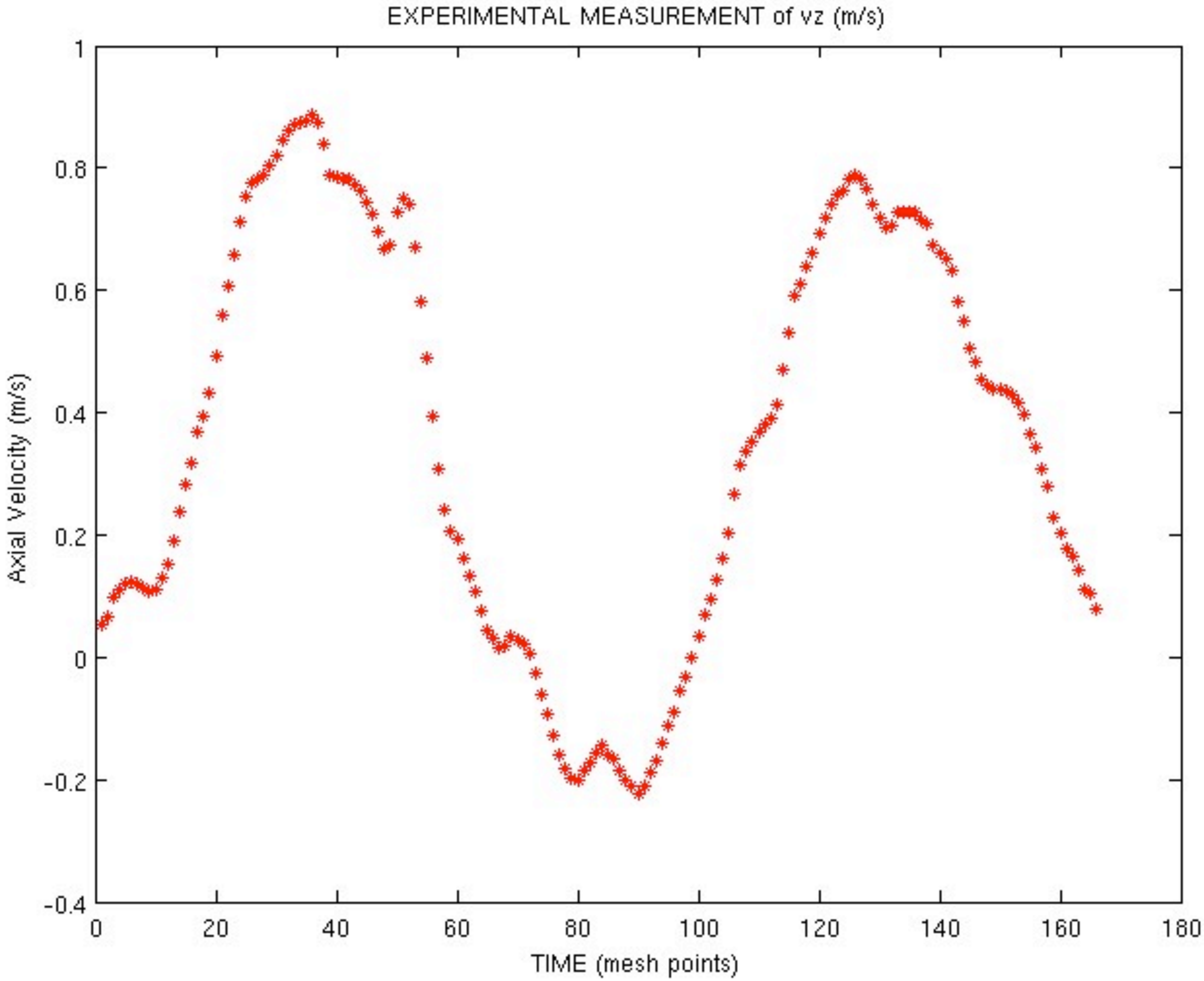

EXPERIMENTAL MEASUREMENT of vz (m/s)
Axial Velocity (m/s)
TIME (mesh points)
1
0.8
0.6
0.4
0.2
0
-0.2
-0.4
0
20
40
60
80
100
120
140
160
180

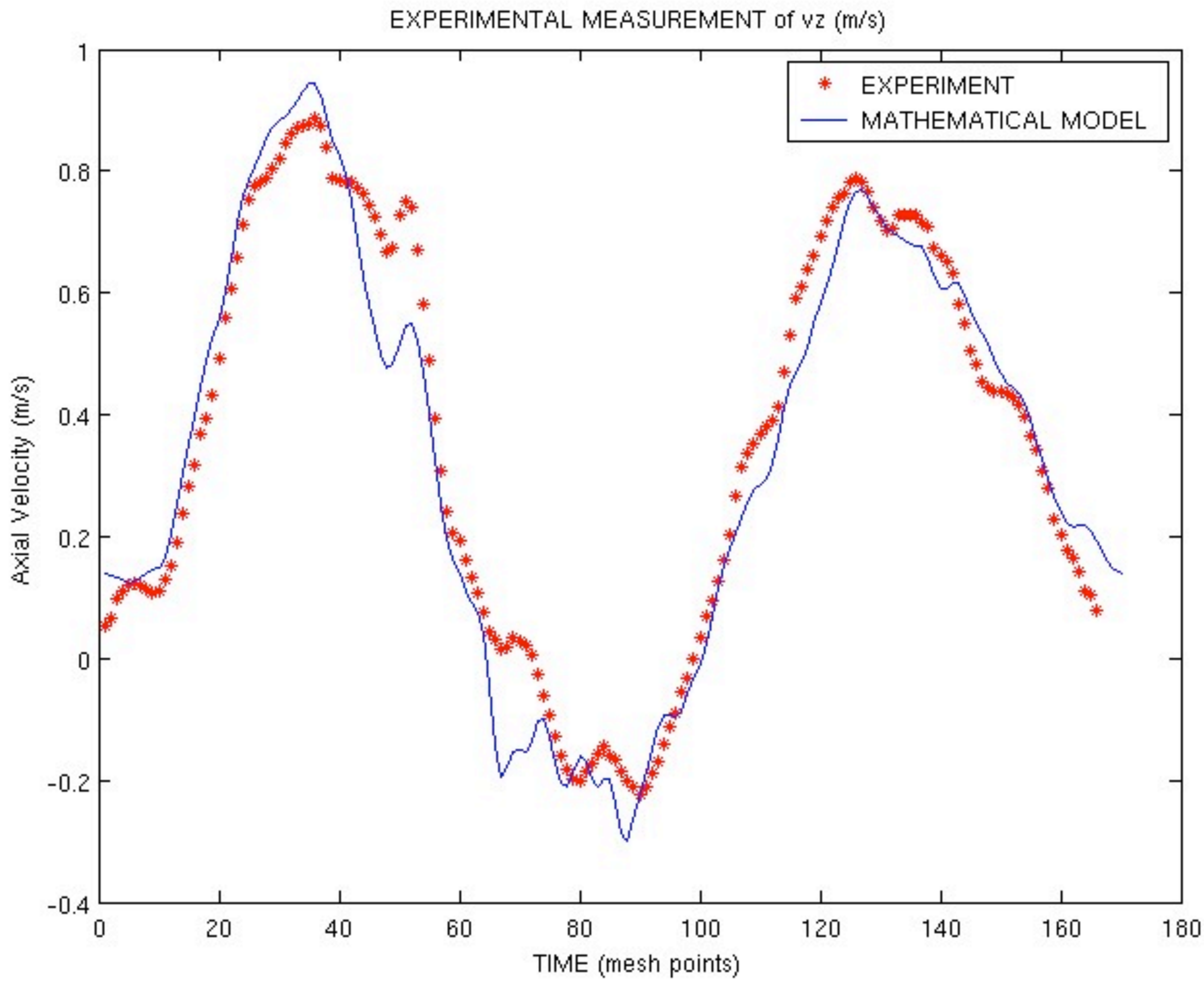
EXPERIMENTAL MEASUREMENT of vz (m/s)
EXPERIMENT
MATHEMATICAL MODEL
Axial Velocity (m/s)
TIME (mesh points)
1
0.8
0.6
0.4
0.2
0
-0.2
-0.4
0
20
40
60
80
100
120
140
160
180

COMPARISON WITH EXPERIMENTS

(viscoelastic model)

Measured pressure-diameter response (Armetano et al.*):

Numerical simulation using the reduced (Biot) model

(human femoral artery)

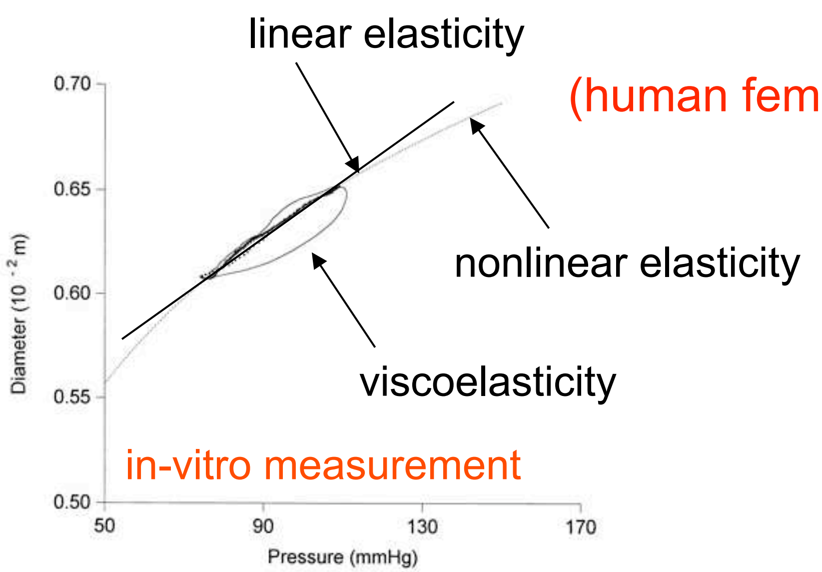

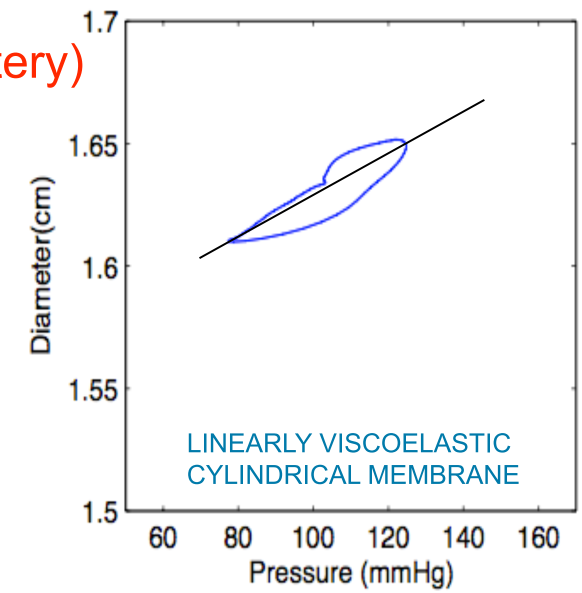

[1] SIAM J Multiscale Modeling and Simulation 3(3) 2005.
[2] Annals of Biomedical Engineering Vol. 34, 2006.
[3] SIAM J Applied Mathematics 67(1) 2006.

coming soon: user-friendly software posted on www.math.uh.edu/~canic (Tambaca&Kosor)

*[1] Armentano R.L., J.G. Barra, J. Levenson, A. Simon, R.H. Pichel. Arterial wall mechanics in conscious dogs: assessment of viscous,inertial,and elastic moduli to characterize aortic wall behavior. Circ. Res. 76: 1995.

* [2] Armentano R.L., J.L. Megnien, A. Simon, F. Bellenfant, J.G. Barra, J. Levenson. Effects of hypertension on viscoelasticity of carotid and femoral arteries in humans. Hypertension 26:48--54, 1995.

EXISTENCE OF A UNIQUE MILD SOLUTION

THEOREM: Assumptions: Initial data for displacement (pressure) η^0 *in* $H^1(0,L)$
Boundary data for displacement (pressure) η_0, η_L *in* $H^1(0,T)$
Initial data for velocity v_z *in* $H^1{}_{0,0}(\Omega)$

Then, for the inlet and outlet pressure data close to the reference pressure p_{ref}*, and for the initial data close the reference cylinder of radius R and initial axial velocity close to 0, there exists exactly one (mild) solution to the Biot FSI problem.*

Kim, Canic, Guidoboni. Comm. Pure and Appl. Analysis 9 (4) 839-865 (2010)

S. Canic, A. Mikelic, G. Guidoboni. "Existence of a Unique Solution to a Nonlinear Moving-Boundary Problem of Mixed type Arising in Modeling Blood Flow". IMA Mathematics And its Application, Volume 153: pp 235-256 (2011)

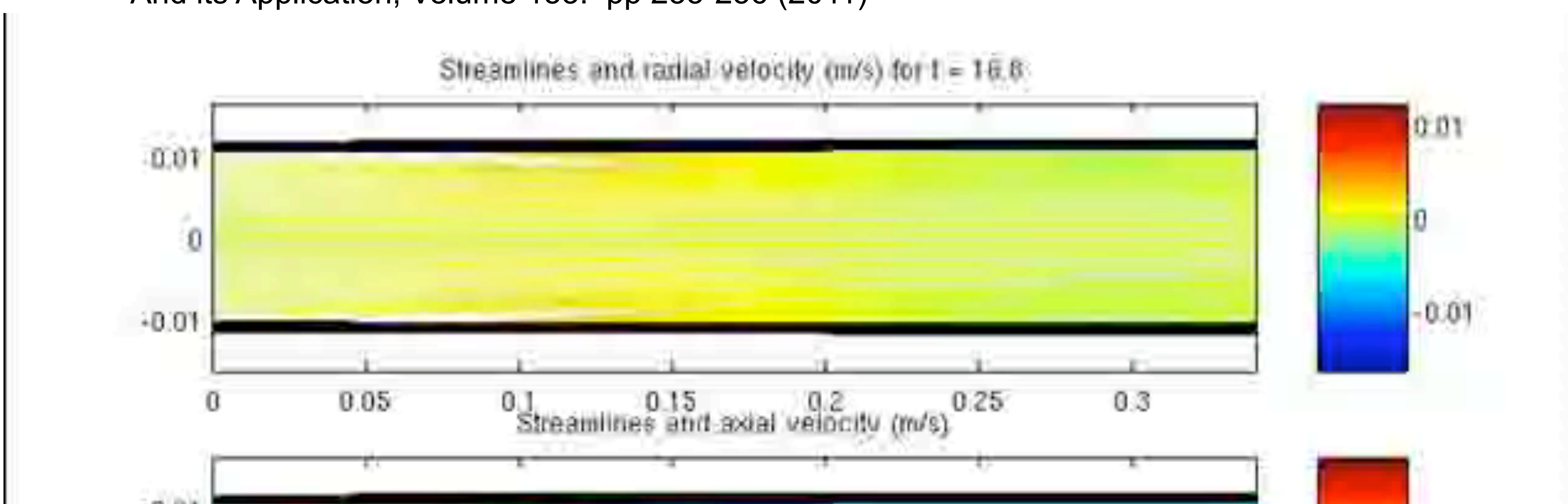

PROOF (MAIN STEPS)

1. MAP ONTO FIXED DOMAIN (ADDITIONAL NONLINEARITY IN PDEs)

2. IMPLICIT FUNCTION THEOREM (HILDEBRANDT AND GRAVES):

Assumptions:

1. Λ,X,Z – Banach spaces
2. F: Λ x X $\rightarrow$ Z defined on an open neighborhood $U(\lambda_0,x_0)$ and $F(\lambda_0,x_0) = 0$
3. F_x exists as a Frechet derivative on $U(\lambda_0,x_0)$ and $F_x(\lambda_0,x_0) : X \rightarrow Z$ bijective
4. F and F_x continuous at (λ_0,x_0)

Then:

1. There exist $\delta_0>0$ and $\delta>0$ such that for every λ in Λ such that $||\lambda-\lambda_0||<\delta_0$ there is exactly one x in X for which $||x-x_0||<\delta$ and $F(\lambda,x) = 0$.
2. If F is continuous in a neighborhood of (λ_0,x_0) then x is continuous in a neighborhood of λ_0.

MAPPING F

Mapping F:

$$F : \underbrace{((\gamma^0, v_z^0, \gamma_0, \gamma_L)}_{\lambda}, \underbrace{(\gamma, v_z))}_{X} := \underbrace{\frac{\partial v_z}{\partial t} - C_1 \frac{1}{\gamma^2} \Delta_r v_z - \frac{r}{\gamma} \frac{\partial \gamma}{\partial t} \frac{\partial v_z}{\partial r} + C_2 \frac{\partial \gamma}{\partial z} + C_3 \frac{\partial^2 \gamma}{\partial z \partial t}}_{\text{left hand-side of balance of momentum}},$$

where:

$$\underbrace{\frac{\partial \gamma}{\partial t} + 2 < v_z > \frac{\partial \gamma}{\partial z} + \gamma \frac{\partial < v_z >}{\partial z} = 0}_{\text{CONSTRAINT: conservation of mass (linear in } \gamma)} \qquad (\gamma = \gamma(v_z))$$

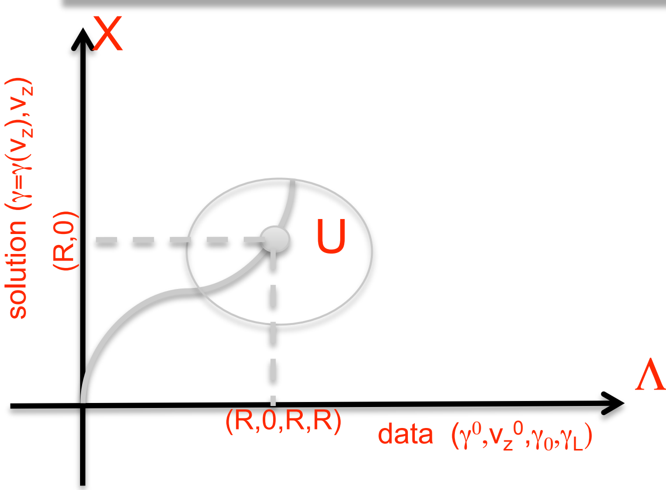

$$F : U((R,0,R,R),((R,0)) \subset \Lambda \times X \rightarrow Z,$$

FRECHET DERIVATIVE AT (λ_0, x_0)

$$F_x((R,0,R,R),(R,0))(\eta,w_z) := \frac{\partial w_z}{\partial t} - C_1\frac{1}{R^2}\Delta_r w_z + C_2\frac{\partial \eta}{\partial z} + C_3\frac{\partial^2\eta}{\partial z\partial t}$$

where $$2\frac{\partial \eta}{\partial t} + R\frac{\partial}{\partial z} < w_z >= 0,$$

$$\begin{cases} \eta(0,t)=0,\ \eta(1,t)=0,\ \eta(z,0)=0, \\ w_z(1,z,t)=0, w_z(r,z,0)=0,\ w_z(0,z,t)-bounded. \end{cases}$$

THEOREM: *Frechet derivative at (λ_0, v_0) is a bijective mapping from X to Z.*

PROOF (MAIN STEPS): existence of a unique (mild) solution to

$$\frac{\partial \eta}{\partial t} + R\frac{\partial}{\partial z} < w_z >= 0,$$
$$\frac{\partial w_z}{\partial t} - \frac{C_1}{R^2}\Delta_r\, w_z + C_2\frac{\partial \eta}{\partial z} + C_3\frac{\partial^2\eta}{\partial z\partial t} = f(r,z,t).$$

EXISTENCE OF A UNIQUE (MILD) SOLUTION TO:

$$\frac{\partial \eta}{\partial t} + R\frac{\partial}{\partial z} < w_z >= 0,$$
$$\frac{\partial w_z}{\partial t} - \frac{C_1}{R^2}\, \Delta_r\, w_z + C_2\frac{\partial \eta}{\partial z} + C_3\frac{\partial^2 \eta}{\partial z \partial t} = f(r,z,t),$$

with

$$\begin{cases} \eta(0,t) = \eta_0(t),\ \eta(1,t) = \eta_L(t),\ \eta(z,0) = \eta^0(z) \\ w_z(1,z,t) = 0,\ w_z(0,z,t) - \text{bounded},\ w_z(r,z,0) = w_z^0(r,z). \end{cases}$$

MAIN STEPS:

1. Existence of a unique WEAK solution
   - 1a. Galerkin approximations
   - 1b. Uniform energy estimates (nontrivial due to mixed hyper-deg. parab. type)
   - 1c. Compactness: weak convergence (to solution)
   - 1d. Uniqueness
2. Higher regularity (energy estimates) to get to mild solution

WEAK SOLUTION

$$\overline{\eta} \in \Gamma = H^1(0,T : L^2(0,1)),$$

$$w_z \in V = \{w \in L^2(0,T : H^1_{0,0}(\Omega,r)) : \frac{\partial w}{\partial t} \in L^2(0,T : H^{-1}_{0,0}(\Omega,r))\}.$$

$$H^1_{0,0}(\Omega,r) = \Big\{w \in L^2(\Omega,r) : \frac{\partial w}{\partial r} \in L^2(\Omega,r),\ \int_0^1 w\ rdr \in H^1(0,1),$$
$$w|_{r=1} = 0,\ |\ w|_{r=0}\ | < +\infty\Big\}.$$

$$\int_0^1 \frac{\partial \bar{\eta}}{\partial t}\varphi\ dz - R\int_0^1 < w_z > \frac{\partial \varphi}{\partial z}\ dz = -\int_0^1 g_1\varphi\ dz \qquad \forall \varphi \in H^1_0(0,L)$$

$$\int_\Omega \frac{\partial w_z}{\partial t}\xi\ rdrdz + \frac{C_1}{R^2}\int_\Omega \frac{\partial w_z}{\partial r}\frac{\partial \xi}{\partial r}\ rdrdz - C_2\int_0^1 \bar{\eta}\ \frac{\partial}{\partial z} < \xi > \ dz$$
$$-C_3\int_0^1 \frac{\partial \bar{\eta}}{\partial t}\ \frac{\partial}{\partial z} < \xi > \ dz = \int_0^1 f\varphi\ dz - \int_0^1 g_2\varphi\ dz,\ a.e.\ 0 \le t \le T,\ \forall w_z \in H^1_{0,0}(\Omega,r)$$

with

$$\bar{\eta}(z,0) = \bar{\eta}^0(z), \quad w_z(r,z,0) = w_z^0(r,z)$$ (both in L^2)

THEOREM: *Assume that the initial data* $\bar{\eta}^0$ *and* w_z^0 *satisfy* $\bar{\eta}^0 \in L^2(0,1)$ *and* $w_z^0 \in L^2(\Omega, r)$ *and that the boundary data* $\eta_0(t)$ *and* $\eta_L(t)$ *satisfy* $\eta_0, \eta_1 \in H^1(0,T)$. *Then there exists a unique weak solution* $(\bar{\eta}, w_z) \in \Gamma \times V$

THEOREM: *(Improved Regularity: Part I) Suppose that the boundary data* $\eta_1, \eta_0 \in H^2(0,T)$ *and the initial data* $\bar{\eta}^0 \in L^2(0,1)$, $w_z^0 \in H^1_{0,0}(\Omega, r)$. *Then the weak solution* $(\bar{\eta}, w_z) \in \Gamma \times V$ *belongs to*

$$\frac{\partial \bar{\eta}}{\partial t} \in L^\infty(0,T : L^2(0,1)), \ \frac{\partial w_z}{\partial r} \in L^\infty(0,T : L^2(\Omega, r)), \ \frac{\partial w_z}{\partial t} \in L^2(0,T : L^2(\Omega, r)).$$

Moreover, the following estimate holds

$$\sup_{0 \le t \le T} \left[\frac{C_3}{R} \left\| \frac{\partial \bar{\eta}}{\partial t} \right\|^2_{L^2(0,1)} + \frac{2C_1}{R^2} \left\| \frac{\partial w_z}{\partial r} \right\|^2_{L^2(\Omega,r)} \right] + 2 \int_0^T \left\| \frac{\partial w_z}{\partial t} \right\|^2_{L^2(\Omega,r)} ds$$
$$\le C \left(\|f\|^2_{L^2(0,T:L^2(\Omega,r))} + \|\eta_1 - \eta_0\|^2_{H^2(0,T)} + \|\eta_0\|^2_{H^2(0,T)} + \|\bar{\eta}^0\|^2_{L^2(0,1)} + \|w_z^0\|^2_{H^1_{0,0}(\Omega,r)} \right).$$

where C *depends on* $1/R, C_2, C_3, T$.

THEOREM: *(Improved regularity: Part II) Assume, in addition to the assumptions of Theorem II-4.9, that the initial data $\bar{\eta}^0 \in H^1(0,1)$. Then the weak solution $\bar{\eta}$ satisfies $\bar{\eta} \in H^1(0,T;H^1(0,1))$. Furthermore, the following estimate holds:*

$$\sup_{0\le t\le T} \frac{C_2 C_3}{12}\left\|\frac{\partial\bar{\eta}}{\partial z}\right\|^2_{L^2(0,1)} + \frac{C_3^2}{12}\left\|\frac{\partial^2\bar{\eta}}{\partial t\partial z}\right\|^2_{L^2(0,T:L^2(0,1))} \le C\Big(\|f\|^2_{L^2(0,T:L^2(\Omega,r))} + \|\eta_1-\eta_0\|^2_{H^2(0,T)} + \|\eta_0\|^2_{H^2(0,T)} + \|\bar{\eta}^0\|^2_{H^1(0,1)} + \|w_z^0\|^2_{H^1_{0,0}(\Omega)}\Big),$$

where C depends on $1/R, C_2, C_3, T$. This implies that, in fact,

$$\frac{\partial^2 < w_z >}{\partial z^2} \in L^2(0,T:L^2(0,1)), \quad \Delta_r w_z \in L^2(0,T:L^2(\Omega,r)).$$

⇒ EXISTENCE OF A UNIQUE MILD SOLUTION TO LINEARIZATION THUS, $F_X(\lambda_0,x_0)$ IS BIJECTIVE.

+ CONTINUITY OF F and F_x at (λ_0,x_0) $\xrightarrow{\text{IFT}}$ EXISTENCE FOR NONLINEAR PROLEM

BACK TO CARDIOVASCULAR NETWORKS

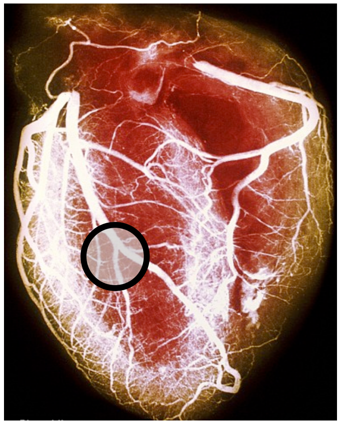

SIMPLE NETWORK
(3 arteries)

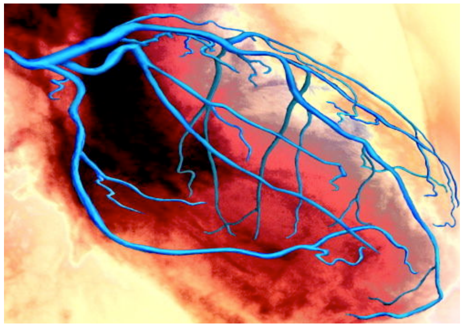

1. GEOMETRY: describing how individual components, such as individual vessels, comprise a global network of arteries.

2. PHYSICS: derivation of models describing the physical properties of each individual network component (single artery) <u>1D MODEL</u>

3. COUPLING CONDITIONS: describing the physics of how individual network components interact with each other at network's vertices.

CARDIOVASCULAR NETWORKS

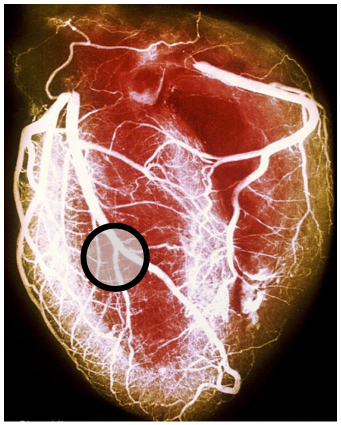

SIMPLE NETWORK
(3 arteries)

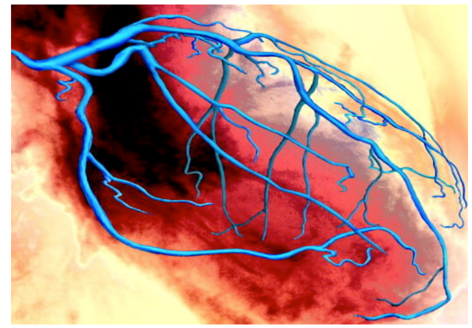

1. ✓ GEOMETRY: describing how individual components, such as individual vessels, comprise a global network of arteries.

2. PHYSICS: derivation of models describing the physical properties of each individual network component (single artery)

3. COUPLING CONDITIONS: describing the physics of how individual network components interact with each other at network's vertices.

CARDIOVASCULAR NETWORKS

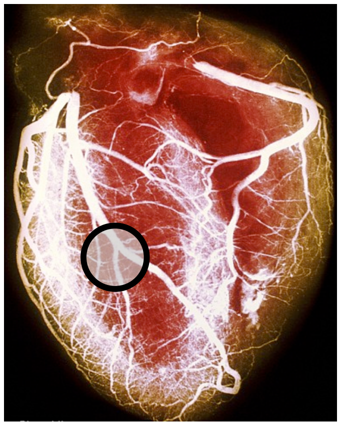

SIMPLE NETWORK
(3 arteries)

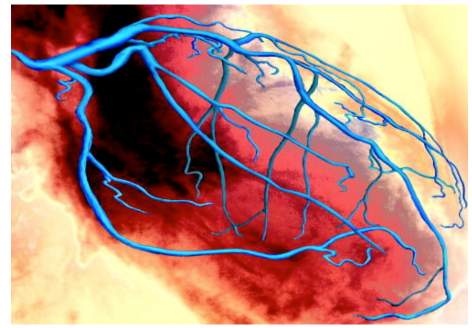

1. ✓ GEOMETRY: describing how individual components, such as individual vessels, comprise a global network of arteries.

2. ✓ PHYSICS: derivation of models describing the physical properties of each individual network component (single artery)

3. COUPLING CONDITIONS: describing the physics of how individual network components interact with each other at network's vertices.

COUPLING CONDITIONS (FOR 1D MODEL)
(i.e., PHYSICS OF THE COUPLING)

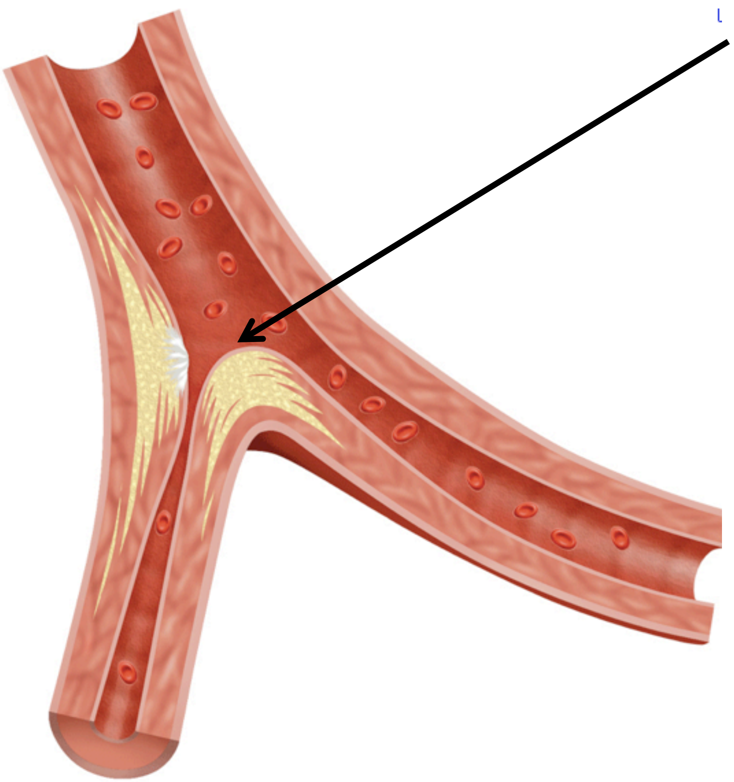

TWO CONDITIONS ARE PHYSICALLY REASONABLE:

COUPLING CONDITIONS (FOR 1D MODEL)
(i.e., PHYSICS OF THE COUPLING)

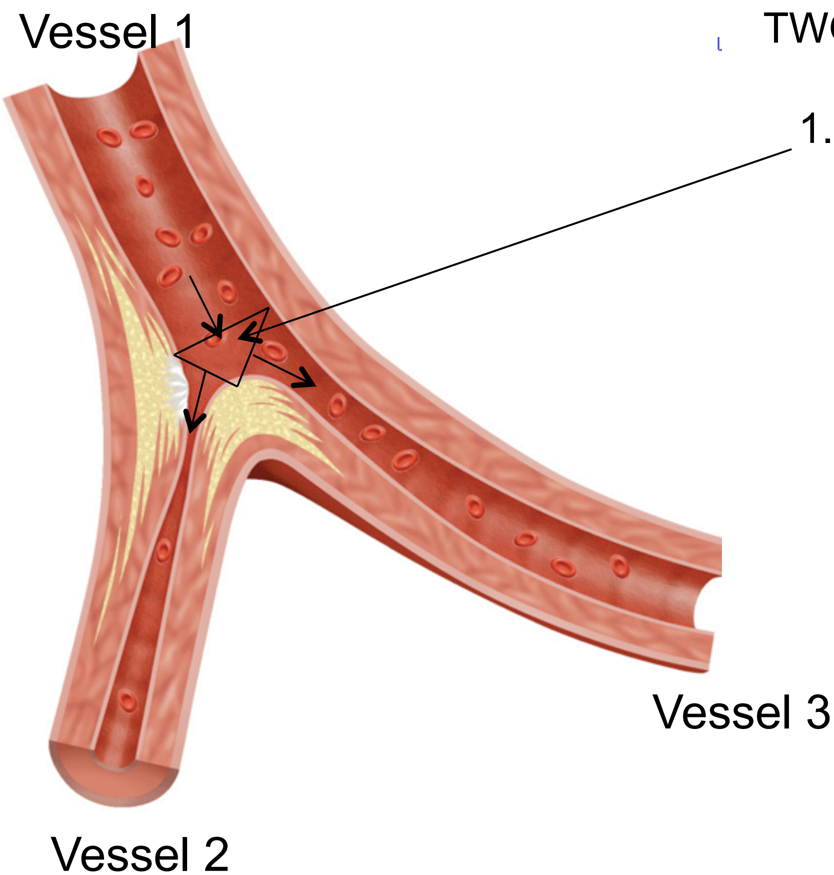

TWO CONDITIONS ARE PHYSICALLY REASONABLE:

1. CONTINUITY OF PRESSURE

$$p_1 = p_2 = p_3$$

COUPLING CONDITIONS (FOR 1D MODEL)
(i.e., PHYSICS OF THE COUPLING)

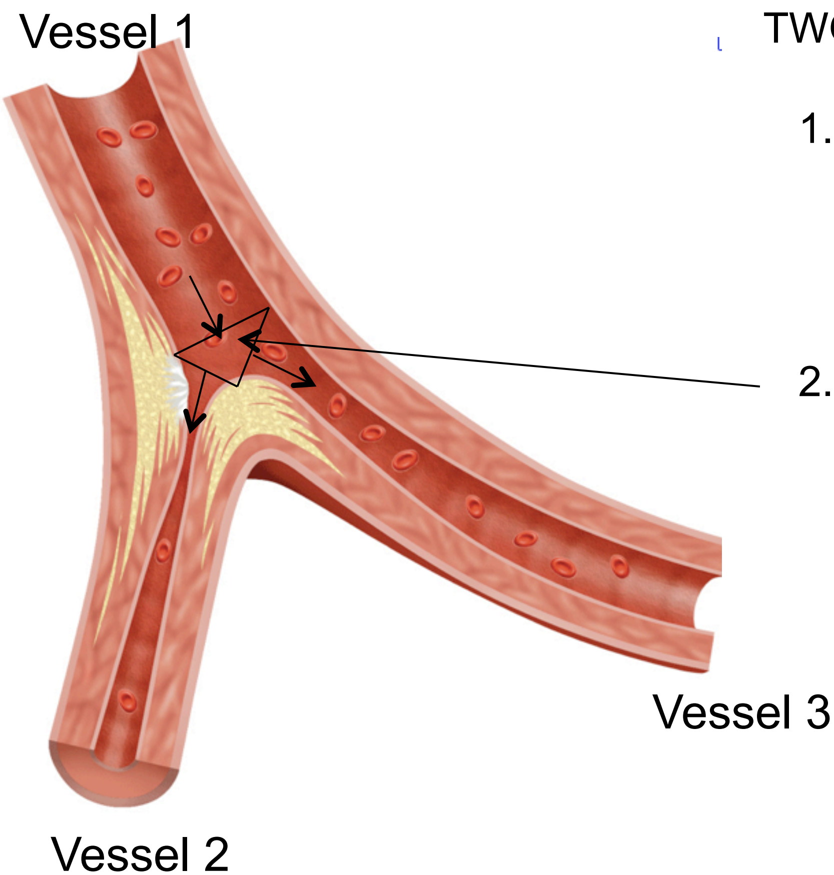

TWO CONDITIONS ARE PHYSICALLY REASONABLE:

1. CONTINUITY OF PRESSURE

$$p_1 = p_2 = p_3$$

2. CONSERVATION OF MASS

$$m_1 = m_2 + m_3$$

(m is the flow rate)

These conditions lead to a network problem, similar to that one for the nonlinear wave equation.

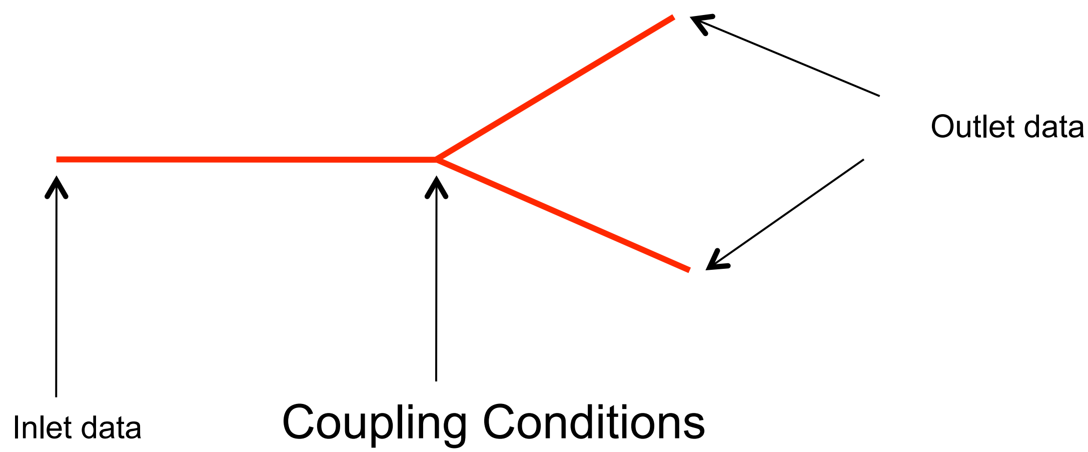

General existence result is open. Smooth solutions can be studied using Riemann Invariants. Numerical results can be obtained using different approaches (Finite Difference Scheme, Finite Element Method).

References:

Canic , S. and E. H. Kim. Mathematical Analysis of the Quasilinear Effects in a Hyperbolic Model of Blood Flow through Compliant Axisymmetric Vessels, *Mathematical Methods in Applied Sciences, 26 (14) (2003), 1161-1186*

Canic , S. and A. Mikelic. Effective equations modeling the flow of a viscous incompressible fluid through a long elastic tube arising in the study of blood flow through small arteries. SIAM Journal on Applied Dynamical Systems 2(3) (2003) 431-463*.*.

Canic , S. A. Mikelic, and D. Lamponi, and J. Tambaca. Self-Consistent Effective Equations Modeling Blood Flow in Medium-to-Large Compliant Arteries. *SIAM J. Multiscale Analysis and Simulation 3(3) (2005) 559-596.*

S. Canic, J. Tambaca, G. Guidoboni, A. Mikelic, C.J. Hartley, D. Rosenstrauch. Modeling viscoelastic behavior of arterial walls and their interaction with pulsatile blood flow. SIAM J Applied Mathematics. SIAM J. Appl. Math., Volume 67 Issue 1 (2006) Pages 164-193.

T. Li and S. Canic. Critical Thresholds in a Quasilinear Hyperbolic Model of Blood Flow. Networks and Heterogeneous Media 4(3) 527-536 (2009)

A Mikelic, G. Guidoboni, S. Canic. Fluid-Structure Interaction in a Pre-Stressed Tube with Thick Elastic Walls I: The Stationary Stokes Problem. Networks and Heterogeneous Media Vol. 2(3) 2007 397-423.

S. Canic, C.J. Hartley, D. Rosenstrauch, J. Tambaca, G. Guidoboni, A. Mikelic. Blood Flow in Compliant Arteries: An Effective Viscoelastic Reduced Model, Numerics and Experimental Validation. Annals of Biomedical Engineering. 34 (2006), pp.`575 - 592.

S. Canic, A. Mikelic, G. Guidoboni. "Existence of a Unique Solution to a Nonlinear Moving-Boundary Problem of Mixed type Arising in Modeling Blood Flow". IMA Volume 153: Nonlinear Conservation Laws and Applications edited by Alberto Bressan, Gui-Qiang Chen, Marta Lewicka, and Dehua Wang, pp 235-256 (2011)

G. Guidoboni, R. Glowinski, N. Cavallini, S. Canic. Stable loosely-coupled-type algorithm for fluid-structure interaction in blood flow. Journal of Computational Physics Vol. 228, Issue 18 6916-6937 (2009).

Existence and well-posedness for fluid-solid interaction:

D. Coutand and S. Shkoller. *On the motion of an elastic solid inside of an incompressible viscous fluid.* Archive for rational mechanics and analysis, Vol. **176**, pp. 25–102, 2005.

D. Coutand and S. Shkoller. *On the interaction between quasilinear elastodynamics and the Navier-Stokes equations* Archive for Rational Mechanics and Analysis, Vol. **179**, pp. 303–352, 2006.

A. Chambolle, B. Desjardins, M. Esteban, and C. Grandmont. *Existence of weak solutions for an unsteady fluid-plate interaction problem.* J Math. Fluid Mech. **7** (2005), pp. 368–404.

B. Desjardin, M.J. Esteban, C. Grandmont, and P. Le Tallec. *Weak solutions for a fluid-elastic structure interaction model.* Revista Mathem'atica complutense, Vol. XIV, num. 2, 523–538, 2001.

B. da Veiga. *On the existence of strong solutions to a coupled fluid-structure evolution problem.* Journal of Mathematical Fluid Mechanics, Vol. **6**, pp. 1422–6928 (Print), pp. 1422–6952 (Online), 2004.

G. P. GALDI. *On the Steady Self-Propelled Motion of a Body in a Viscous Incompressible Fluid.* Arch. Rational Mech. Anal 148 (1), 53-88 (1999)

KUKAVICA, I., TUFFAHA, A., ZIANE, M. (2010). *Strong solutions to a fluid structure interaction system*. Advances in Differential Equations. Vol. 15 (3-4), pp. 231-254.

KUKAVICA, I., ZIANE, M., TUFFAHA, A. (2009). *Strong solutions to a nonlinear fluid structure interaction system*. Journal of Differential Equations. Vol. 247, pp. 1452-1478.

Largest Medical Center in the World

Employees: 93,500

Volunteers: 12,000

Academic institutions: 21
Hospitals: 14
Medical Schools: 3
Nursing Schools: 6

Surgeries: 153,000
Daily visitors: 160,000

Area: 1000+ acres (size of the inner Chicago loop)

Annual patient visits: 6 million
Babies delivered: 28,000

University of Houston, MD Anderson Library

THANKS:

- The National Science Foundation
- The National Institutes of Health (joint with NSF: NIGMS)
- Roderick Duncan MacDonald Research Grant at St. Luke's Episcopal Hospital, Houston
- Texas Higher Education Board (ATP Mathematics) 2006 and 2010
- Kent Elastomer Products Inc.
- UH GEAR grant and UH TLCC grant
- Medtronic Inc.